Dielectric measurements by voltage step methods

Laverick, Elizabeth

DIELECTRIC MEASUREMENTS

BY

VOLTAGE STEP METHODS

ACKNOWLEDGEMENT.

The author gratefully acknowledges the kind assistance of all who have contributed in any way towards the progress of this work.

Thanks are due to the members of the Department for their kind co-operation, to the Department of Scientific and Industrial Research and the Council of Durham Colleges whose financial assistance made the research programme possible, to the General Electric Co.Ltd., and to James, A.Jobling and Co.Ltd., who readily supplied glass samples for test.

Finally, the author would particularly like to mention her supervisor, Dr.W.A.Prowse, whose sympathy and understanding, constant assistance and encouragement, greatly lightened the burden of the work.

Elizabeth Laverick.

Department of Physics,
The University Science Laboratories,
South Road,
Durham City.

15 March 1950.

CONTENTS.

LIST OF DIAGRAMS.

LIST OF TABLES.

I. INTRODUCTION.

In general, the electrical properties of a dielectric are described by one quantity, the permittivity. This quantity is, for most materials, independent of the strength of the applied field for moderate field strengths but dependent on temperature, and, in the case of sinusoidal fields, dependent on frequency also. The variation of permittivity with frequency, and the absorption of energy involved, gave rise to the concept of a complex permittivity,

$$\epsilon = \epsilon_1 + i\epsilon_2$$

where ϵ_1 and ϵ_2 depend on frequency, and ϵ_2 is proportional to the dielectric loss.

The properties of a dielectric are often measured using alternating current in terms of an equivalent network of linear circuit elements. The values of the equivalent network components are dependent on frequency and in order to examine the properties of the dielectric over a range of frequencies, it is necessary to measure those values at a series of discrete frequencies within the required frequency range.

To envisage the properties of a given circuit element, there are advantages in thinking in terms of

a voltage step, however. For example, in an inductive circuit upon applying a voltage step, the initial rate of rise of current in the circuit is determined entirely by the inductance. On the other hand, upon applying a current step to a capacitive circuit, the capacitance alone determines the rate of rise of voltage across the circuit. Early experiments with dielectric media were based on similar conceptions. A D.C. field or voltage step was applied to a condenser containing the dielectric under investigation, and, either the current flowing into the condenser, or the total charge on the condenser was measured as a function of time. The results were explained in terms of three component currents, forming the total current flowing into the condenser: namely the normal charging current, representing the instantaneous charging of the condenser, the normal conduction current resulting from conduction across the dielectric, and the anomalous charging current, or absorption current, resulting from the readjustment of charges in the dielectric.

The methods then available however, were not suitable for studying variations which occurred within, say, 10^{-2} seconds of the application of the field. Today, the advent of the electronic circuit makes the rapid switch on and off of the applied field possible, and the repeated application of a voltage step in the

form of rectangular pulses or square waves, can be achieved. Also, the use of the cathode ray oscillograph enables the results to be displayed, and makes possible the study of events occurring immediately upon the application of the field to the dielectric.

The use of bridge methods in alternating current measurements, particularly on dielectric properties, is well known, and such methods have been developed to a high point of precision. The application of bridge methods in pulse measurements is however less well known.[1] Yet it would appear that a combination of a bridge circuit and voltage steps makes it possible in the comparison of two circuits to cancel out factors which are precisely similar in the two circuits, and to indicate differences only, selected according to the time at which these differences arise. Hence the possibility arises of displaying and measuring the electrical characteristics of actual materials which can often be represented approximately by a network of linear circuit elements.

Bridge balance, using pulses, requires the balance of the Fourier components of the pulse[2] in both phase and amplitude. This forms the advantage, as well as the difficulty of pulse work, in that a pulse investigation of a system provides a means of indicating

in a single test, information equivalent to the phase shift and amplitude response over a range of frequencies.[3] But there is also the disadvantage that the development of the apparatus, the experimental procedure, and the analysis of the results demand an approach which differs considerably from that adopted in alternating current measurements.

The present work is a study of the possibilities of using the pulsed bridge for

1) the measurement of networks approximating to a condenser filled with natural dielectric,

2) the examination of some dielectrics by the methods thus developed.

II. A THEORETICAL APPROACH TO THE PROBLEM.

It is proposed in the first instance to study the flow of charge as a function of time in a network of linear circuit elements approximating to a condenser filled with natural dielectric, to which a voltage step has been applied. In particular, it is proposed to use a pulsed bridge for the purpose, and, by comparing such a network with some suitable circuit element, (e.g., a 'pure' capacitance, representing a condenser filled with non-lossy dielectric), to obtain an indication of the differences between the two circuits which arise at specific times.

Upon applying an electric field to a dielectric, the charging process in the dielectric is not instantaneous due to the slow response of the displaced charges in the dielectric. The variation of charge with time is probably of the form shown, APT, in Fig.1).

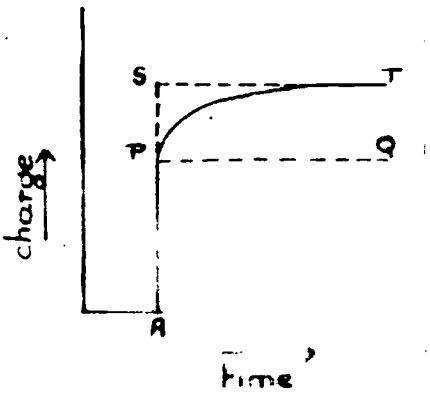

Fig.1). Charge-time variation in dielectric.

Whether there is a discontinuity at P as indicated in the diagram is to be regarded as uncertain. Any such discontinuity implies that the polarisation of the dielectric may be divided into two components:- an instantaneous component arising from the displacement of electrons and atoms within the molecule, and a non-instantaneous component arising, among other possibilities, from the rotation of polar molecules. On this basis, a possible network of linear circuit elements approximating to a condenser filled with natural dielectric may be built up. The instantaneous processes are represented by a pure capacitance, C_1', in parallel with a large resistance, R_p', (cf. Fig. 2).

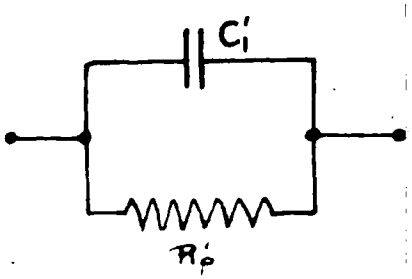

Fig. 2). Network representing the instantaneous polarisation processes occurring in a dielectric.

Upon the application of an electric field, the capacitance charges up instantaneously to its full value. The ensuing leakage of charge across the parallel resistance could be considered as a representation of the displacement of electrons and atoms within the molecules of the dielectric,

loading to a surface charge which compensates some of the charge on the condenser plates. Similarly, the non-instantaneous component of the polarisation of the dielectric could be thought of in terms of a small capacitance, C_j', and series resistance, R_j, in parallel with the main capacitance, C_i', (cf. Fig.3).

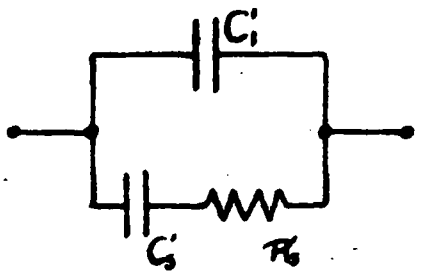

Fig.3). Network representing the non-instantaneous polarisation processes occurring in a dielectric.

Upon the application of an electric field, the capacitance C_i' charges instantaneously to its full value. The charging process is then completed at a rate determined by the time constant $C_j'R_j'$. This gradual completion of charging could represent the rotation of the polar molecules towards alignment in the direction of the applied field.

A combination of these two networks is a possible approximation to a condenser filled with natural dielectric, (cf. Fig.4).

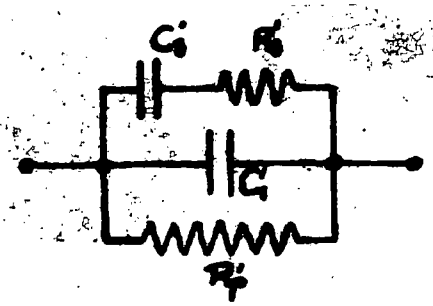

Fig.4). Network representing a condenser filled with natural dielectric.

A diagrammatic representation of a bridge for the comparison of such a network with, say, a capacitance, is shown in Fig.5). D is a difference indicator.

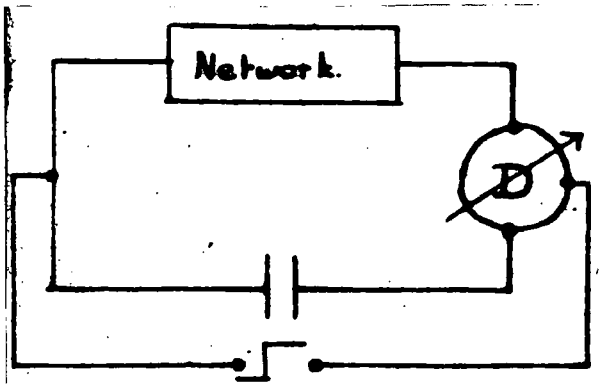

Fig.5). Bridge circuit for the comparison of network with capacitance.

Suppose the characteristic charge-time curve for the network is represented by APT in Fig.1), and let the capacitance apply through the indicating system a charge cancelling APQ. Then the difference indicator will indicate a charge-time variation as shown in Fig.6), and the corresponding current-time, and rate of change

of current-time variations can then be deduced.

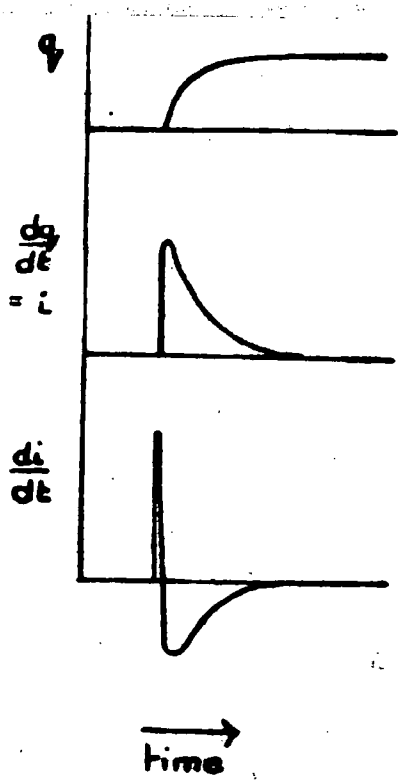

Fig.6). Variation of charge, current, and rate of change of current with time, under conditions stated above(see P.8).

Alternatively, if the capacitance is adjusted to apply a charge AST in opposition to APT,(cf.Fig.1), the difference indication will be of the form shown in Fig.7). Again, the current-time, and rate of change of current time variations can be deduced, ~~also~~.

In order to study these waveforms in practice, it is necessary to choose a bridge whose ratio arms (which form the difference indicator in the diagrammatic representation) are suited to the nature of the work involved.

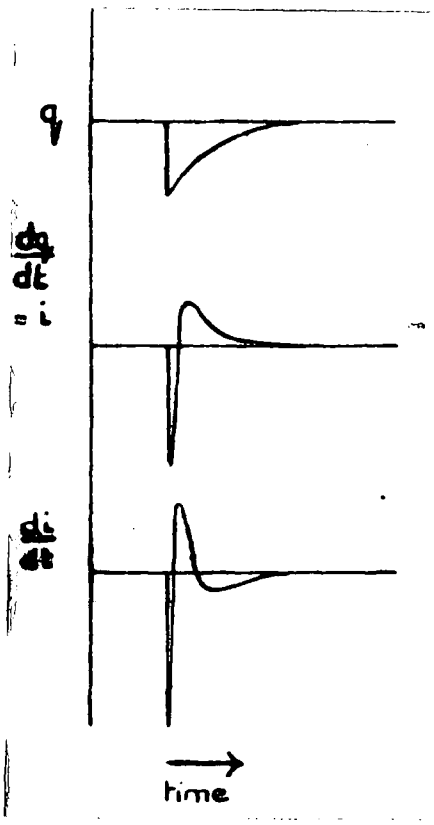

Fig.7). Variation of charge, current, and rate of change of current with time, under conditions stated above(see P.9).

The following conditions must be fulfilled by the bridge:-

1). The form of the ratio arms must not interfere with the performance of the voltage-step source.

2). The properties of the indicating system must be clearly defined, and must permit of amplification.

3). The screening and balance of the bridge circuit must be complete over the range of frequencies incorporated in the applied voltage step.

Some possible forms of bridge circuit are shown in (Fig.8).

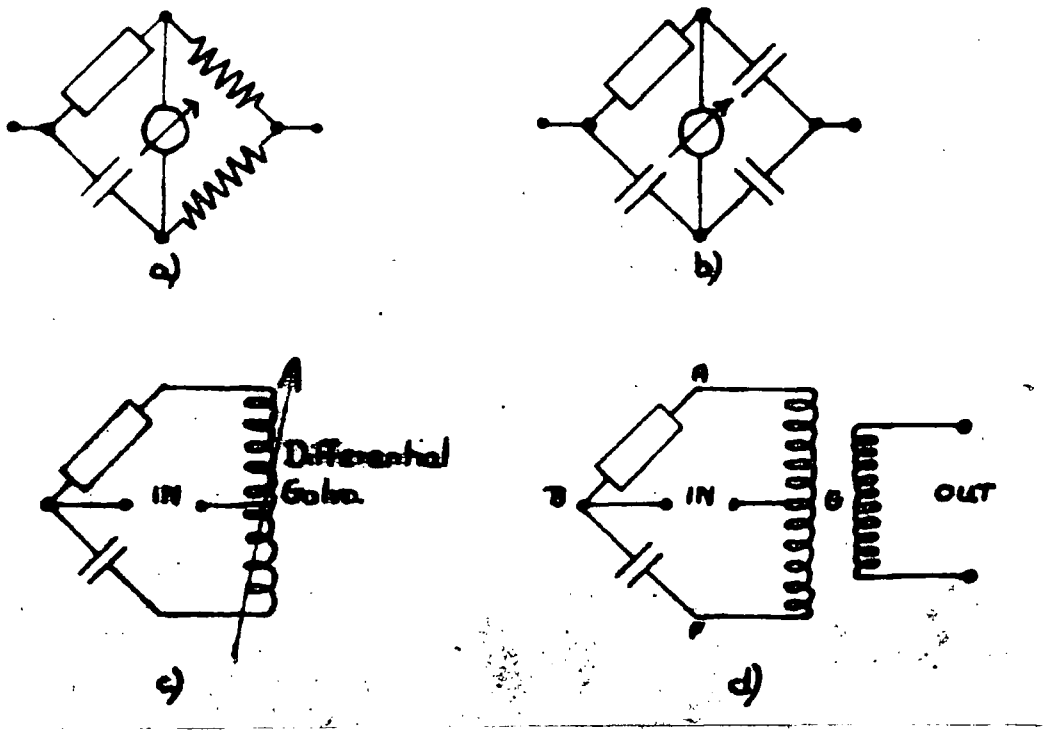

Fig.8). Possible forms of bridge circuit:-
a). The resistive ratio arm bridge.
b). The capacitive ratio arm bridge.
c). The differential galvanometer bridge.
d). The differential transformer bridge.

The use of the resistive ratio arm bridge,(Fig.8a), is eliminated by the fact that the ratio arms interfere with the performance of the voltage-step source. This disadvantage can only be overcome by the use of large resistors, in which case the bridge is unable to respond to rapid events which may occur, and the system loses its sensitivity.

The capacitive ratio arm bridge,(Fig.8b), presents

special difficulties with respect to the second condition that the indicating system must permit of amplification. From a consideration of the circuit,(cf.Fig.9), it can be seen that the anode and cathode resistors involved in the amplification stage constitute an auxiliary bridge. This would require preliminary balancing, and such a balance would depend partly on the properties of the valves concerned. These are liable to change with time, and from valve to valve, hence this circuit presents serious problems.

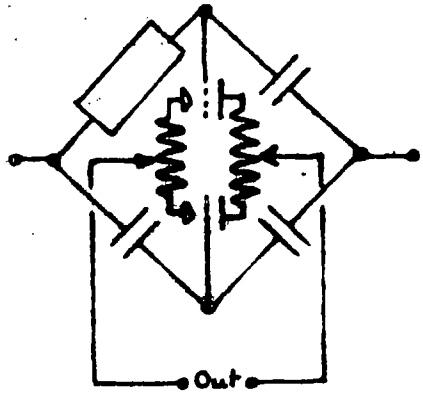

Fig.9). Capacitive bridge with amplification stage.

The third condition, regarding completeness of screening and balance over a range of frequencies practically necessitates a bridge of simple design with 1:1 ratio arms. In this respect, circuit 8c), using a differential galvanometer is quite satisfactory. However, the response time of the indicating system in this case is too slow to permit observation of events occurring immediately upon the application

of the voltage step to the bridge.

The differential transformer bridge,(Fig.8c), on the other hand,overcomes this difficulty, meets all the requirements laid down above, and possesses special possibilities. This bridge has equal inductive ratio arms wound in opposition on a toroidal dust core[4], the two arms being tightly coupled to one another. The output is taken by way of the secondary winding which is placed symmetrically with respect to the two primary windings. With regard to the requirements laid down above, provided the leakage inductance of the differential transformer primary windings is small, the bridge ratio arms do not affect the performance of the voltage-step source[5]. The indicating system is provided by the secondary of the differential transformer. Its properties are therefore clearly defined, and amplification of the bridge output can be achieved without affecting the bridge itself. At balance, the time constants of the two branches of the bridge are equal, and for capacitive bridge arms the time constants are zero. Hence, in the differential transformer bridge, the growth of charge is limited only by the components under comparison, whereas in most bridges it is limited also by the ratio arms themselves, (cf.Fig.10). One advantage of the differential transformer bridge, therefore, is its ability to display rapid events

occurring immediately upon the application of the bridge input.

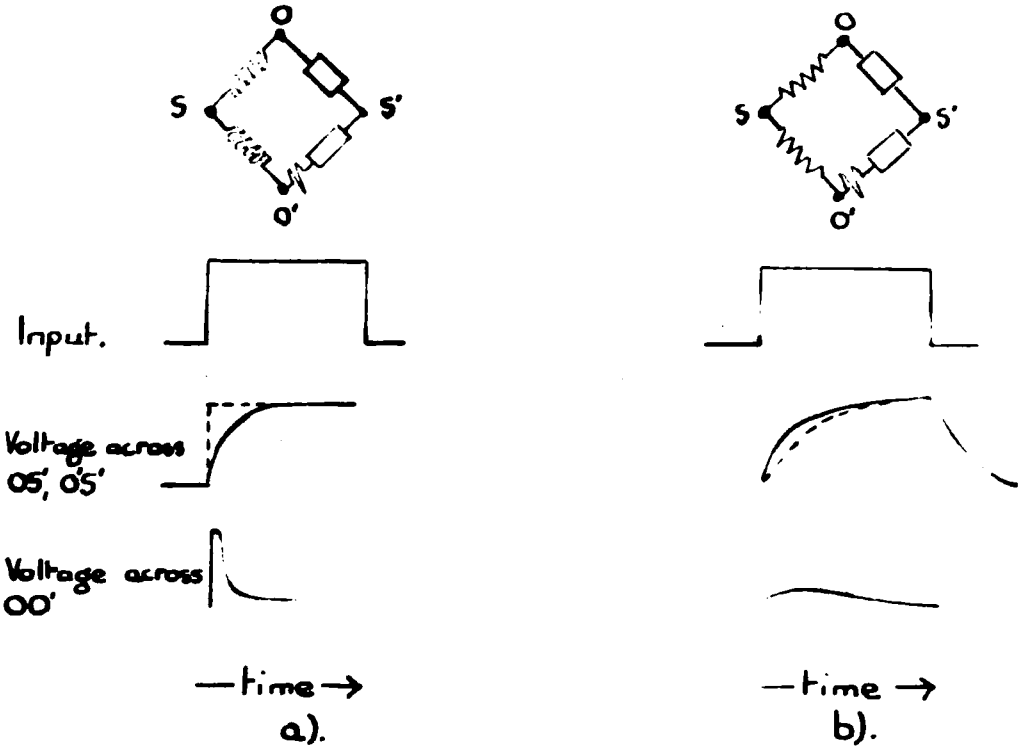

Fig.10). A comparison of the responses to an applied pulse, of:-
a), the differential transformer bridge,
b), a resistive ratio arm bridge.

In general, there are two types of strays in bridges, namely, strays to earth, and strays due to cross-coupling[6]. These can be represented by Z_A, Z_B, Z_C, and Z_D, and Z_1, Z_2, Z_3, Z_4, Z_5, and Z_6, respectively, as shown in Fig.11). By means of suitable screening, and the choice of a suitable reference point in the circuit as earth, it is often possible to arrange that some of these strays be reduced to a negligible amount, and the rest compensated for.

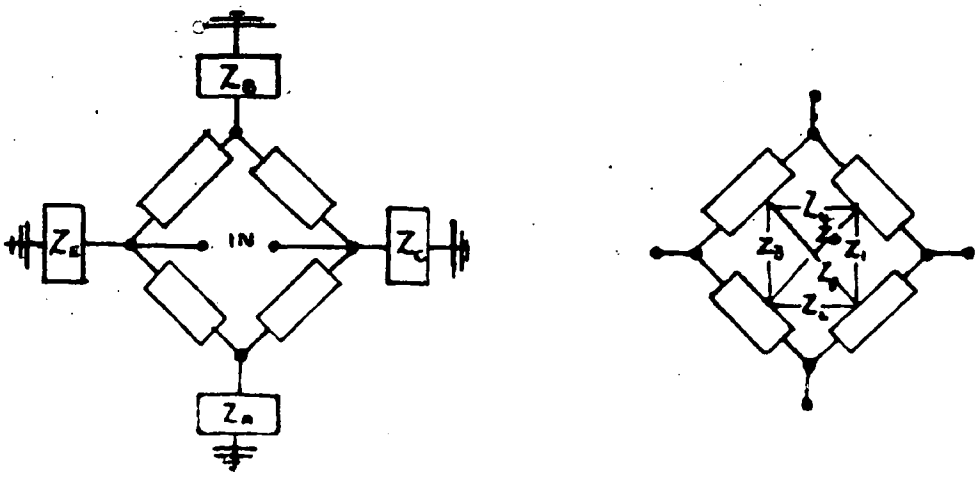

Fig.11). Representation of strays in bridges:-
a).Strays to earth.
b).Strays due to cross-coupling.

In the case of the differential transformer bridge, if the symmetry of the ratio arms is to be retained, there are two possible earth points, namely, the junction of the ratio arms, C, and the junction of the comparison and measuring arms of the bridge,E, (cf.Fig.12).

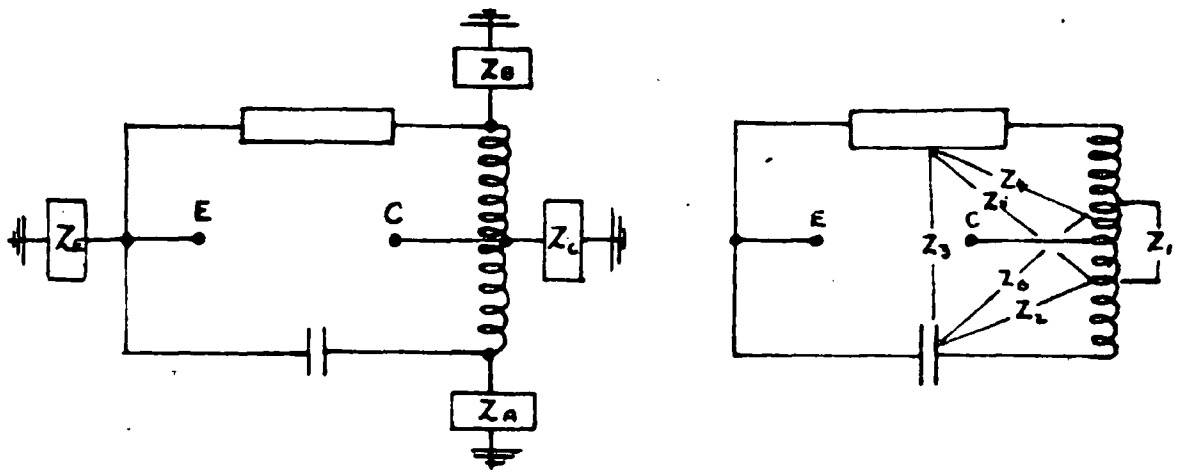

Fig.12). Representation of strays in the differential transformer bridge:-
a) Strays to earth,
b) Strays due to cross-coupling.
'C' and 'E' are possible earth points.

Considering first the strays to earth:- at balance, the currents through the two primary windings are equal and opposite. The voltage drop across the primaries is effectively zero, assuming the effects of leakage inductance and resistance to be negligible. Then if C is the earth point, Z_A, Z_B, and Z_C are practically eliminated. Z_E is effectively in parallel with the bridge source, and, provided it is small, has negligible effect on the performance of the source. If, on the other hand, E is made the earth point, Z_A and Z_B act in parallel with the network in the comparison arm and the capacitance in the measuring arm of the bridge respectively. These can be included in the calibration of those arms, provided Z_A and Z_B are independent of frequency. Z_E is eliminated, and Z_C acts in parallel with the bridge source, and , provided it is small, has negligible effect on the performance of that source. Thus without the use of special earthing devices, such as the Wagner arm, a bridge is obtained which is relatively unaffected by strays to earth at all except the highest frequencies.

Of the strays due to cross-coupling, Z_2, Z_3, Z_4, Z_5, and Z_6 can be reduced to negligible amounts by suitable layout of the apparatus. Z_1, representing the electrostatic coupling between the inductive ratio arms, depends on the design of those arms, and must be kept small.

The differential transformer bridge has been used

in alternating current work to measure impedance, resistance coupling, capacitance, phase displacement and power [7]. Little work has been published on it recently however [8].

From a consideration of the differential transformer bridge with voltage step input, it is possible to deduce the characteristic features of the charge-time variations and hence the current and rate of change of current waveforms for various networks in the comparison arm of the bridge. In general, upon the application of a voltage step to the bridge, the large inductance of the differential transformer primary windings imposes initially the condition of equal growths of current in the two bridge arms. This is followed by a relatively slow adjustment to the final steady condition controlled by the flux in the core.

Consider the following simple networks, assuming a variable capacitance in the measuring arm of the bridge.

1). Pure capacitance (cf.Fig.13).

When $C_1 = C_1'$, the flux through the primary windings cancels out, and the output is zero. When $C_1 < C_1'$, the rates of growth of charge in the circuit are instantaneous until C_1 is fully charged, whereupon the charge in C_1' increases gradually to its full value, the rate of increase being controlled by the natural frequency of the ring circuit, ABFG. The variation of $\Delta q = (q' - q)$, $\Delta i = \frac{d}{dt}(\Delta q)$, and $\frac{d}{dt}(\Delta i)$,

with time under these conditions is shown in Fig.13).

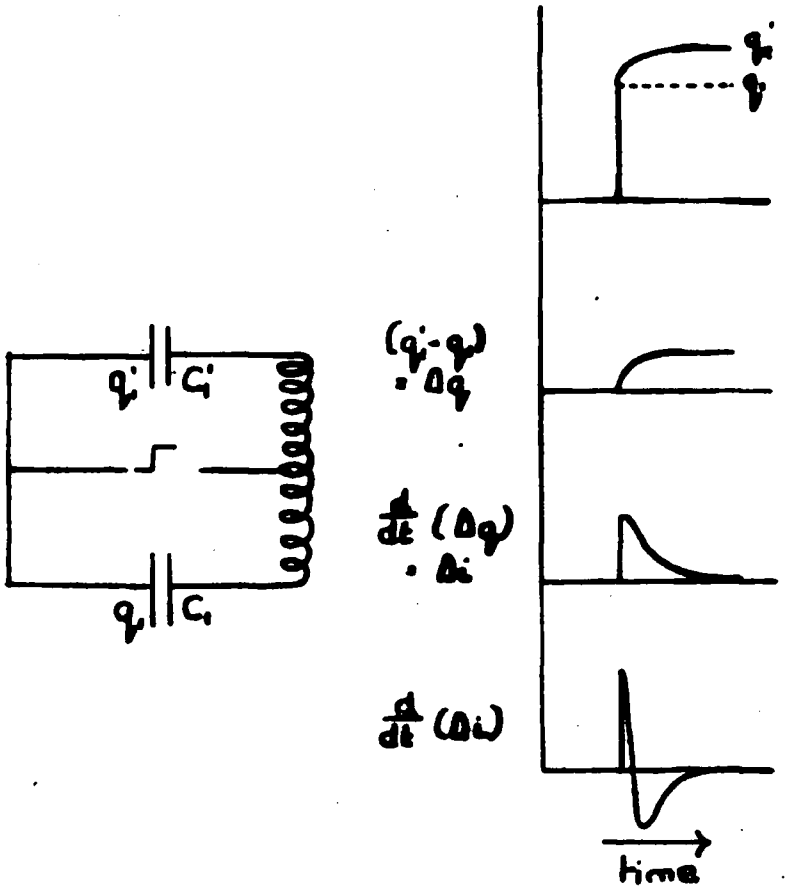

Fig.13). Variation of charge, current, and rate of change of current with time for pure capacitance in comparison arm of bridge.

2). Capacitance and series resistance in parallel with a capacitance, (cf.Fig.14).

When $C_1 = C_1' + C_1''$, the charging process is instantaneous until C_1' has acquired a charge VC_1', (where V= magnitude of applied potential). Thereupon C_1'' charges at a rate determined by the time constant $C_1''R_1''$, and a sensibly equal current flows in the C_1--branch, since the large

inductance of the primary windings imposes a condition of equal currents in the two arms. The currents are not precisely equal, the difference, which is small compared with the original charging current, being such as to produce an inductive back e.m.f. restraining the flow of current in the lower branch to that in the upper branch. This restraint is produced by the changing magnetic field, hence an e.m.f. of precisely similar form appears across the secondary terminals.

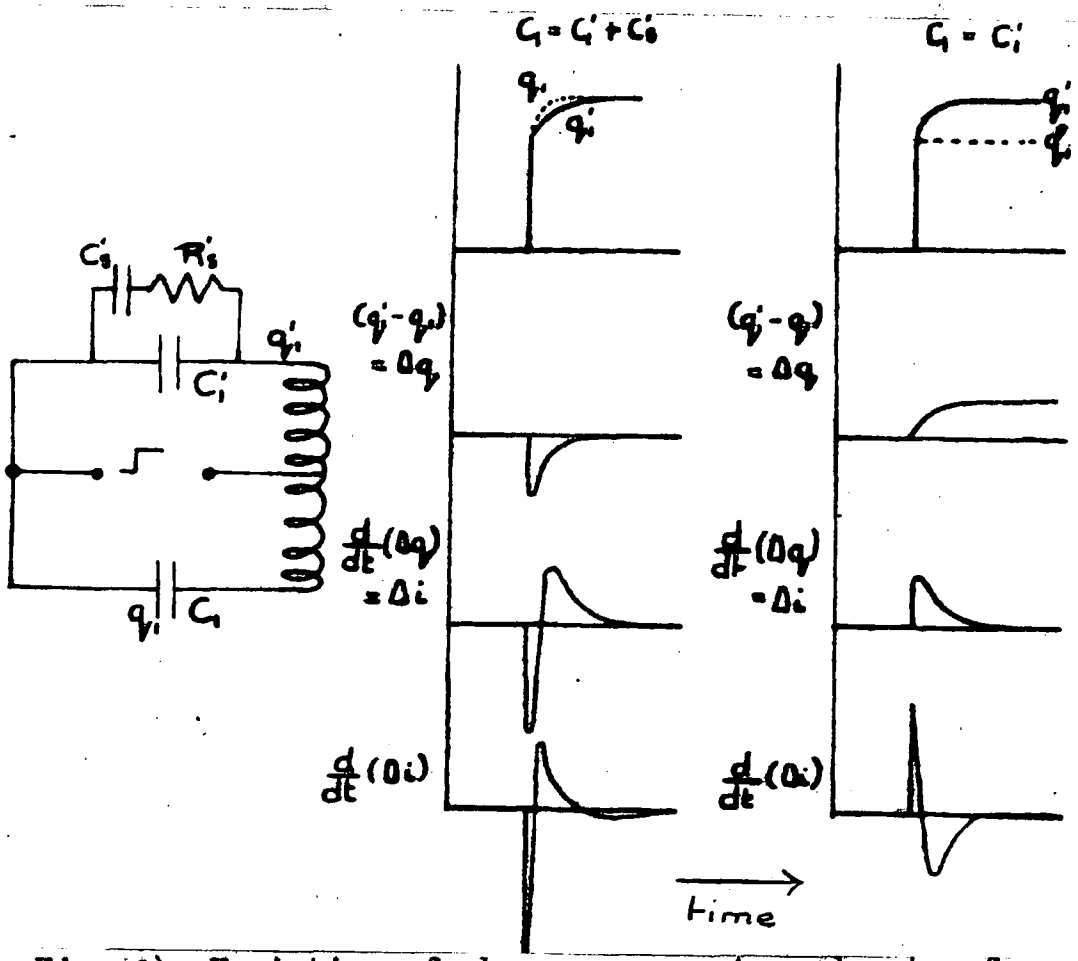

Fig.14). Variation of charge, current, and rate of change of current with time for a network of capacitance and series resistance in parallel with a capacitance.

When $C_1 = C_1'$, however, C_1 and C_1' charge to their full value instantaneously, whereupon C_1' shares its charge with C_2' by way of R_2'. This results in a readjustment of the charge in the two arms, which, depending as it does on the properties of the 'ring' circuit ABFG, is relatively slow, (cf. Fig. 14b).

3). Capacitance and parallel resistance, (cf. Fig. 15).

In this case, when $C_1 = C_1'$ the two arms charge instantaneously until C_1 and C_1' are fully charged. Thereupon the charge flowing in the C_1' arm increases slowly at a rate governed by the parallel resistance and the primary inductance.

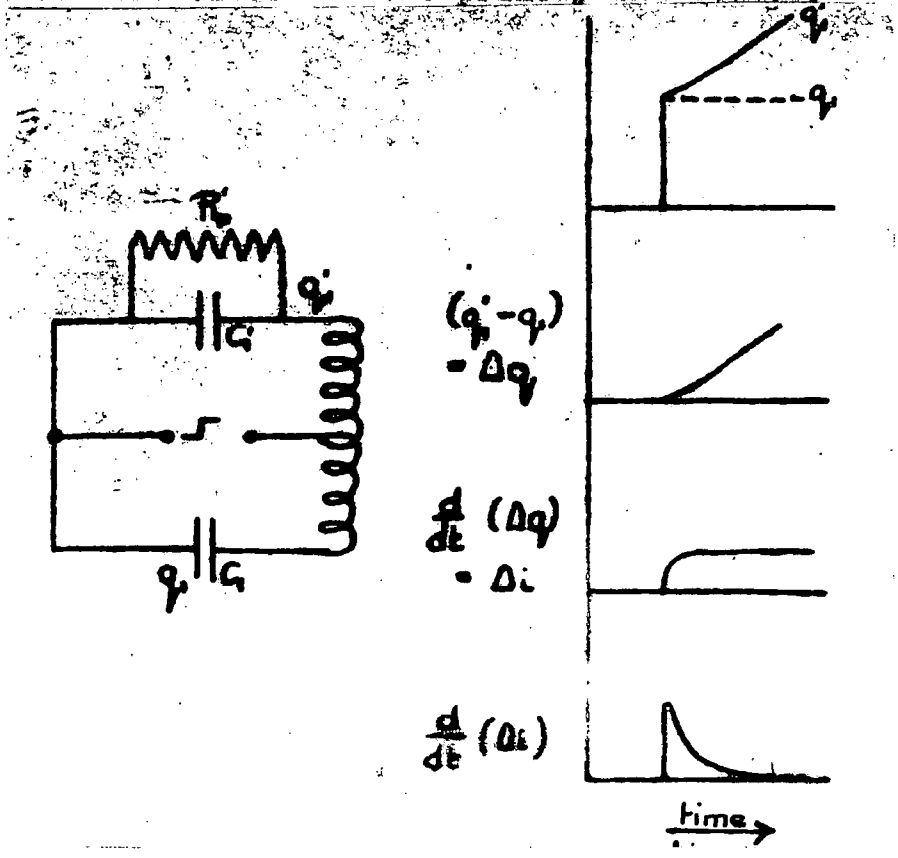

Fig. 15). Variation of charge, current, and rate of change of current with time for a network of capacitance and parallel resistance.

The 'ring' circuit, ABFC, forms an oscillatory circuit. Any unbalance of the bridge arms would therefore be expected to result in a damped oscillation whose frequency is the natural frequency of the ring circuit. A damping resistor of suitable value across the differential transformer secondary should damp out this unwanted oscillation.

III. THE APPARATUS.

1). The differential transformer bridge.

In the design of the differential transformer bridge the following factors must be considered:-

i). The transformer primary windings must be exactly similar with equal mutual inductances with respect to the common secondary.

ii). The leakage inductance and resistance of the primary windings must be a minimum.

iii). The coupling between primary and secondary must be entirely magnetic, and in no degree electrostatic.

iv). Errors due to strays must be eliminated as far as possible by th use of screening and a symmetrical arrangement of the apparatus.

In particular, for use of the bridge with pulses, the conditions indicated above must apply over a range of frequencies corresponding to the frequency components contained in the applied pulse. Also, the instrument itself must be capable of responding over that frequency range.

The differential transformer, (cf. Fig.16), developed for this work consisted of two primary coils of 150 turns each, wound with twin wire on a toroidal dust core[4]. This method of winding inevitably introduces considerable electrostatic

coupling between the two coils, but this disadvantage is offset by the fact that tight coupling between the two primary windings is ensured, the primary coils are practically identical, and magnetic leakages are reduced to a minimum. The secondary of 450 turns was wound on a copper former, and covered by a copper strip, thus screening it electrostatically from the primary windings. To avoid forming a short-circuited turn round the primary, the copper former for the secondary was made up of two sections insulated from one another. The transformer as a whole was shielded from external influences by an earthed screen.

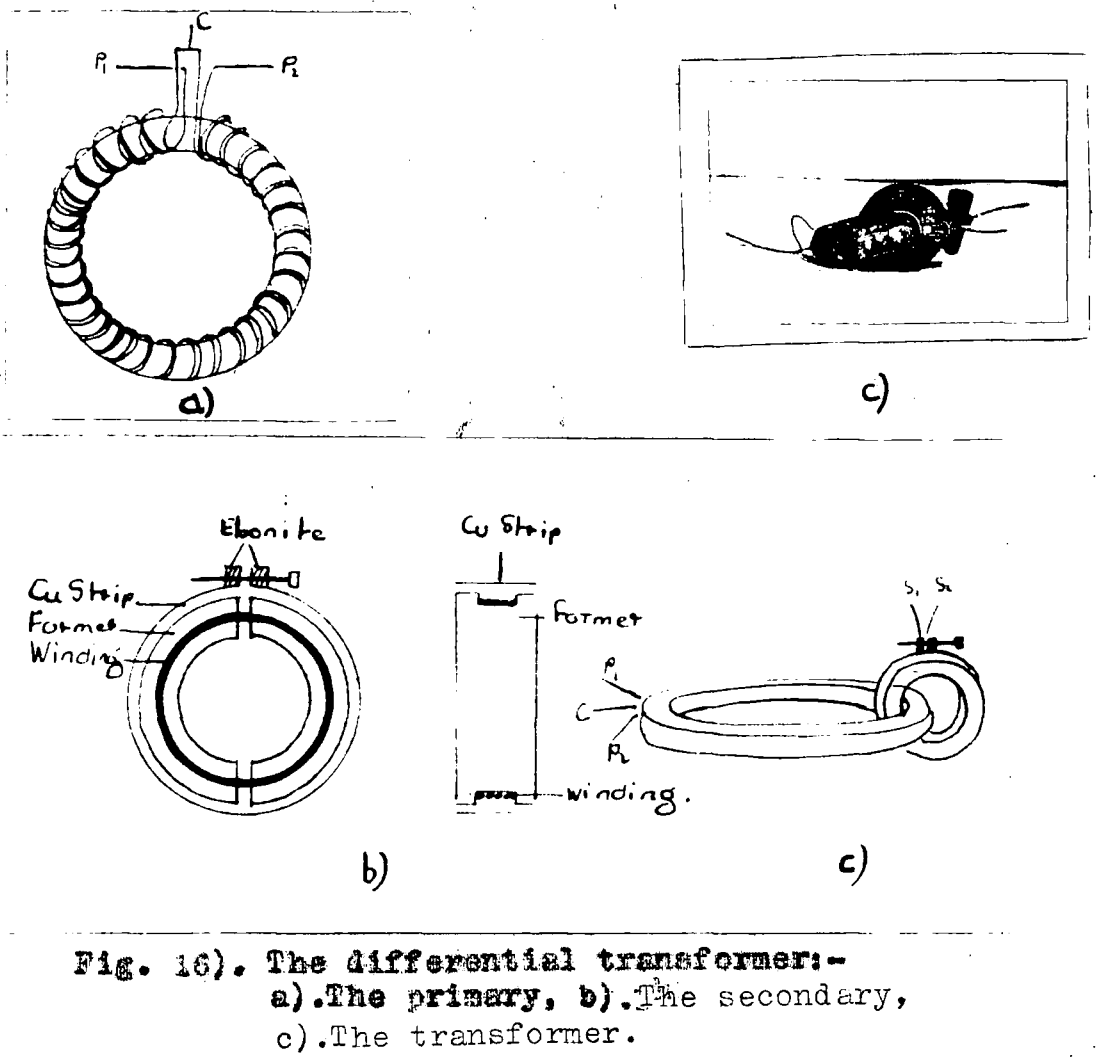

Fig. 16). The differential transformer:-
a).The primary, b).The secondary,
c).The transformer.

Measurement of the self-inductance of the differential transformer primary.

Several attempts were made to measure the self-inductance of the differential transformer primary. Resonance methods were not sufficiently sensitive with the apparatus available. The following method was finally adopted. A sinusoidal input of known frequency was applied across a variable resistance in series with the differential transformer primary(two windings in series). The differential transformer secondary was on open circuit. Using a valve-voltmeter, the voltages developed across the inductance and resistance respectively were compared, and the resistance varied until those voltages were equal. Then,(cf.Fig.17),

$$wL = R,$$

$$L = \frac{R}{w},$$

where w = applied frequency in radians/sec.
Hence L, the inductance of the differential transformer primary was obtained.

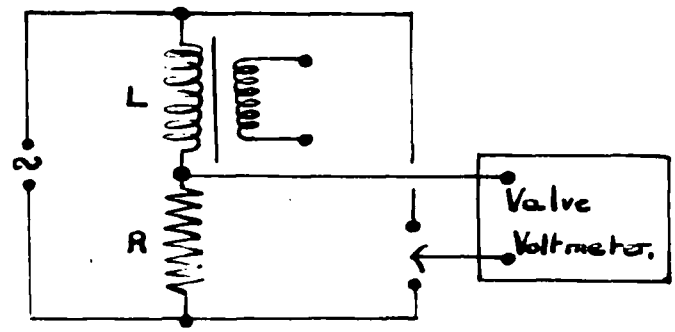

Fig.17). Circuit for determination of inductance of differential transformer primary.

Measurements were made at three frequencies in the audio-frequency range, and an average taken of the results, (cf.Table I).

Frequency in (cycles/sec.).	R in ohms.	L in Henries.	
0.5×10^3	0.62 K.	0.20	
1.0×10^3	1.40 K.	0.22	0.22
2.0×10^3	3.05 K.	0.24	

Table I. Measurements of self-inductance of differential transformer primary.

From these measurements it was concluded that the inductance of the differential transformer primary was approximately 0.22 Henries (secondary open-circuited). Assuming perfect coupling between the two primaries, the self-inductance of each primary winding was therefore 0.055 Henries.

The bridge arms, were developed with a view to studying the electrical networks, and combinations of these networks which were discussed theoretically in the preceeding chapter. Low-loss leads connected the ends of the primary windings to the bridge arms, which consist basically of two screened 0 to 50 $\mu\mu$F variable air condensers. These were used as

a fine adjustment in all capacitance measurements and will henceforth be referred to as "measuring" condensers. With this arrangement any zero errors in the measuring condensers were automatically balanced out. Facilities were provided for adding the electrical networks in parallel with the measuring condensers as required.

Network elements. For the large capacitive network elements, 30 to 300$\mu\mu$F Sullivan standard variable air condensers were used, whilst for the smaller values, 0 to 10$\mu\mu$F and 0 to 50$\mu\mu$F variable air condensers were mounted and screened. High stability Dubilier resistors were used for the series resistance elements covering ranges:-

From 1K to 10K in approximately 1K steps.
10K to 100K in " 10K " .
100K to 500K in " 100K " .

[Symbols:- K = Kilohms M = Megohms].

Any value between 1K and 610K could thus be obtained to within the nearest 1K. The parallel resistance elements were formed by several 1M Erie resistors connected in series. All network elements were fitted with small metal plugs, to plug in and out of sockets suitably arranged on a low loss base.

Calibrations:- All capacitive components of the bridge were calibrated under actual working conditions, the main sources of error in the differential transformer bridge such as ratio error are being eliminated.

The capacitance to be calibrated was connected in the comparison arm of the bridge, and using A.C. input to the bridge calibrated in terms of the 30 to 300μμF Sullivan standard condensers. It was estimated experimentally that the error of dial setting of the component under calibration was limited mainly by the accuracy of the standard used and was $\pm\frac{1}{2}$μμF (cf. Fig 18 and Table 11.)

The series resistance components were calibrated independently of the bridge, by the usual Post Office Box method. The maximum error was estimated experimently to be less than 0·1%.

The parallel resistance components were not calibrated independently, their value being far from critical in the measurements undertaken. The tolerance of the parallel resistance components was specified as ± 20%.

Differential transformer bridge tests.

It has been shown (cf. previous chapter) that the choice of a suitable reference point in the bridge circuit as earth, could simplify the system as regards the effects of strays in the system. Two possible earth points in the differential transformer bridge were discussed, namely, the junction of the ratio arms, and the junction of the measuring and comparison arms. Although the former earth point gives one the advantage of working with the whole of the differential transformer

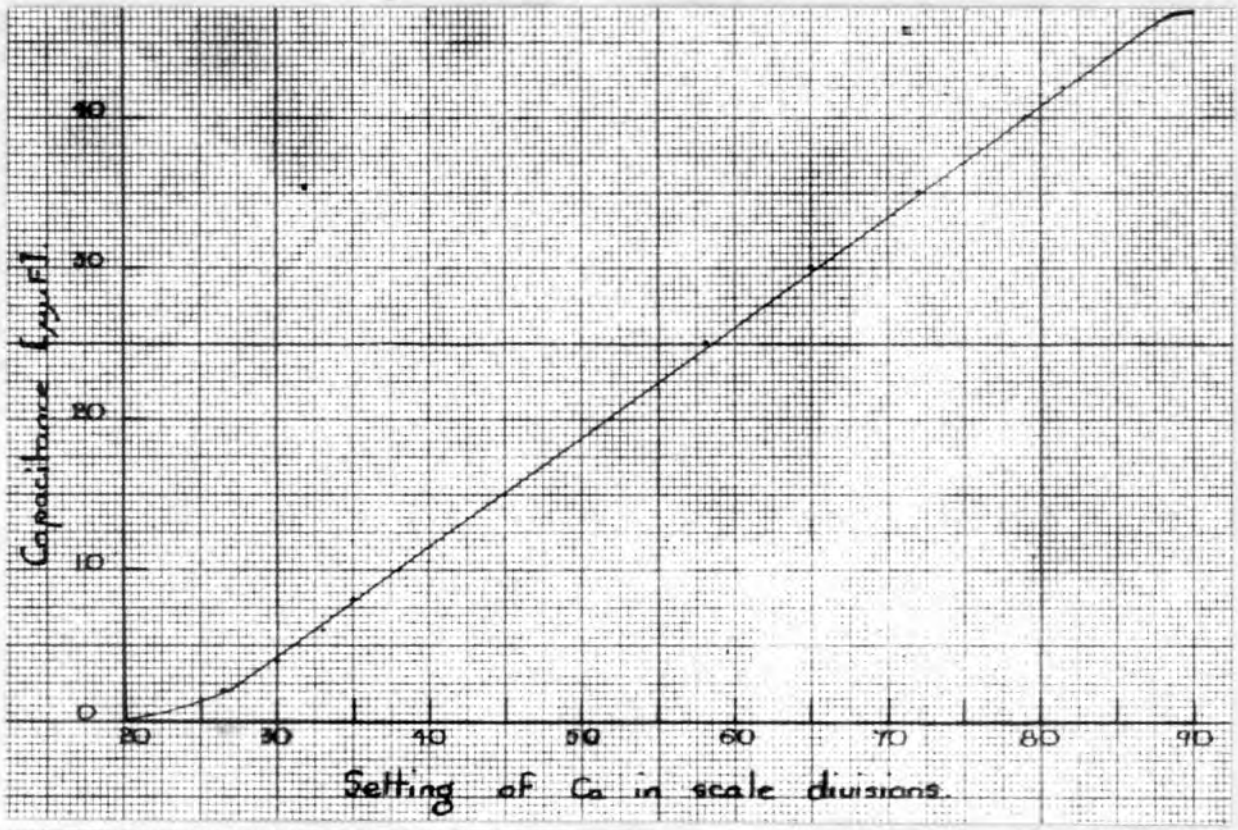

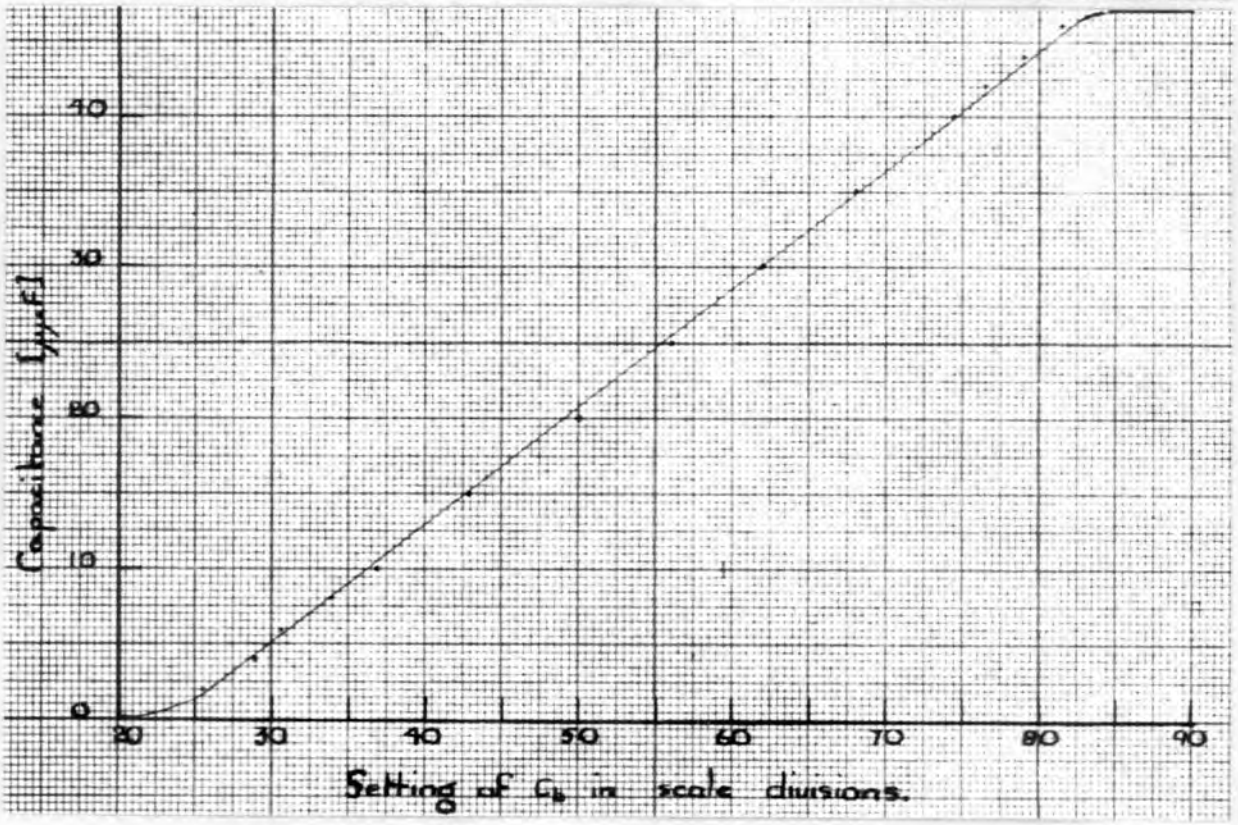

Fig. 18) Calibration curves for measuring condensers, a) and b)

primary practically at earth potential, on approaching balance, it was decided to choose the latter, (the junction of the comparison and measuring arms). This choice allowed the absolute determination of and compensation for strays in the networks under investigation. This can be seen from a consideration of the bridge circuit with, for example, pure capacitive arms.

~~In general~~ The capacitance components were screened, the moving plates of each condenser being connected to the screens to eliminate the variations of strays with the position of the moving plates. Hence, if the junction of the ratio arms was earthed, two possibilities arose. The screens could either be connected to the positive input, (cf. Fig. 19a), in which case the bridge arm capacitances and the bridge source would be shunted by small fixed stray capacitances; or on the other hand, the screens could be connected to the end of the primary windings, (cf. Fig. 19b). Then, apart from the small stray capacitances across the bridge arms capacitances would be introduced in shunt with the primary windings.

Table II. Accuracy of calibration of capacitive components.

Applied Frequ.(c/s)	Repetitive setting of capacitance($\mu\mu$F)	Average value($\mu\mu$F)	Maximum error($\mu\mu$F)
950	26.0 26.5 27.0 26.5 27.0 26.5 26.5 26.5 26.0 26.5	26.5	0.5

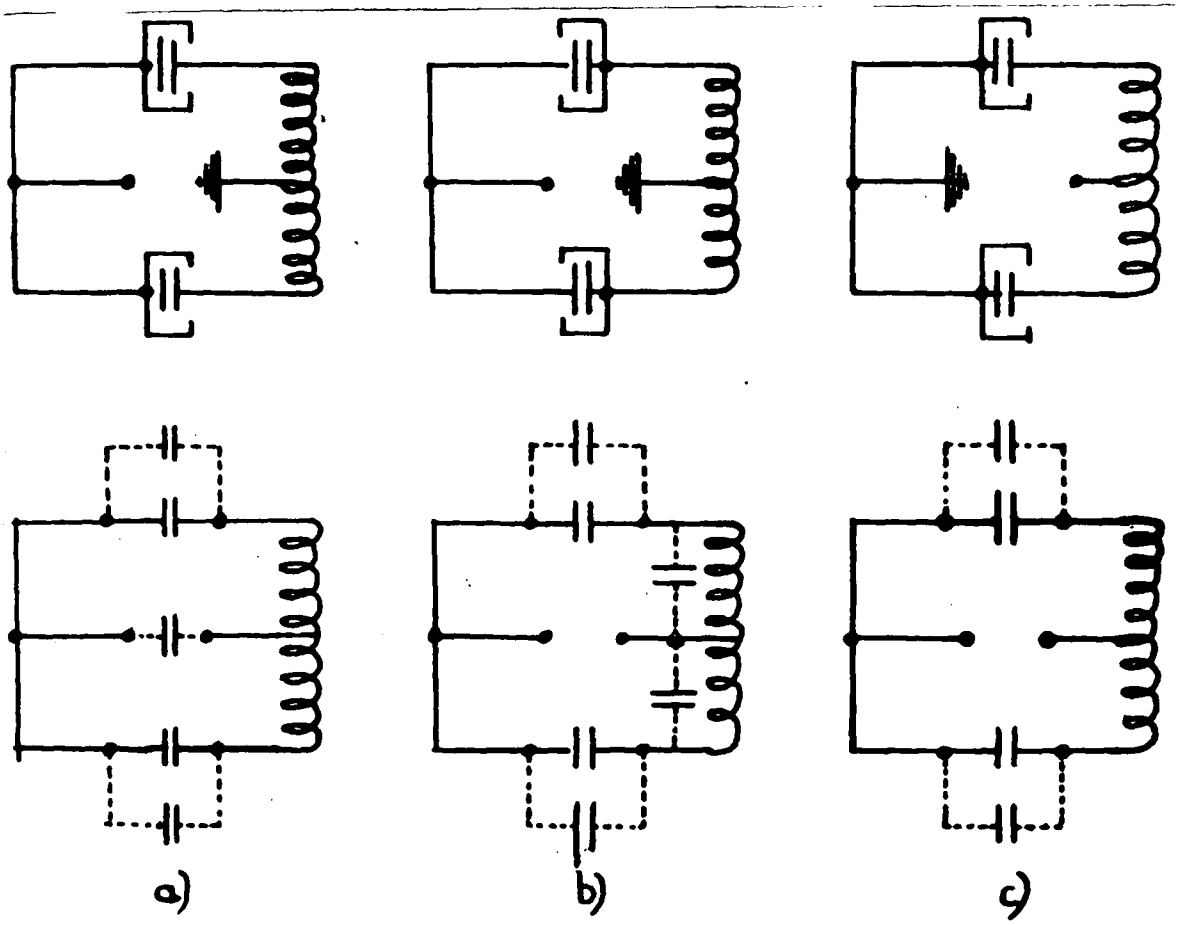

Fig.(9). Strays in the differential transformer bridge.

The former earthing system is acceptable provided that the magnitudes involved are small. The latter however, destroys the simplicity of the bridge ratio arms system. If, on the other hand, the junction of the measuring and comparison arms were earthed, the screens of the capacitive components could be connected direct to earth, resulting in the introduction of small fixed capacitances in shunt with those arms. Hence, either of the earthing systems a) or c) could be used. At the beginning of this work it was decided to earth the junction

of the comparison and measuring arms of the bridge.

With more complicated arms, such as the series resistance capacitance network, stray capacitances could be compensated for quite simply with the earthing system chosen. There were two possible arrangements; the resistance could be placed between the capacitance and earth, or between the capacitance and the primary winding,(cf.Fig.20a and b).

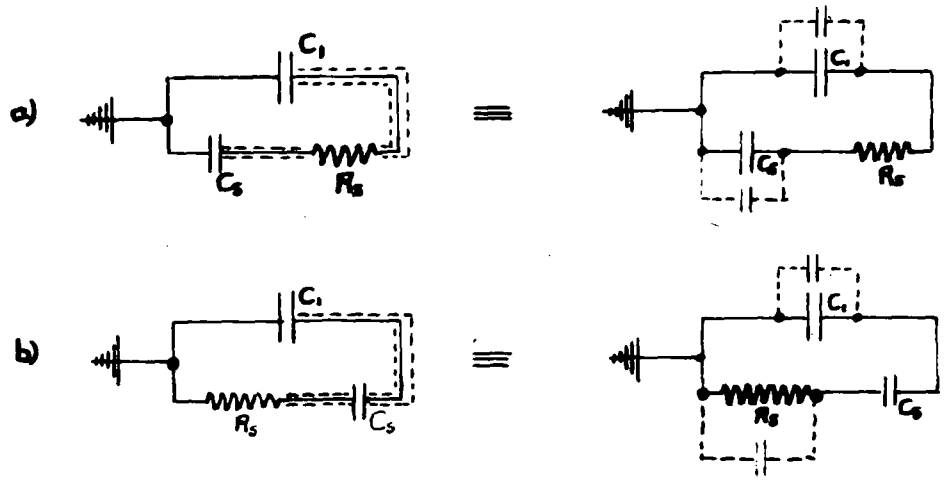

Fig.20). Effect of strays:- a) C_s on earth side of R_s,
b) C_s on positive side of R_s.

The latter was satisfactory in that it introduced stray capacitances in shunt with the capacitive components only, whereas the former arrangement introduced stray capacitances across the resistive components also. These could not be compensated for in the calibration of the bridge arms.

By suitable arrangement of the bridge arms as indicated above, and by the use of short screened leads and shielded capacitances, it was possible to fix all strays in the bridge arms to earth, reduce their effects to a minimum by symmetrical layout of the bridge arms, and to compensate for the remaining strays in the calibration of the bridge arm components.

In order to investigate and reduce possible sources of error due to strays in the differential transformer itself, tests were carried out to estimate the total order of error involved, and the relative importance of the errors due to strays to earth and cross-coupling effects. The stray impedances involved in the bridge circuit were almost purely capacitive from the nature and layout of the bridge.

The following tests were made:-

i) With the bridge arms opencircuited, and a square-wave applied to the bridge, the output from across the differential transformer secondary was observed on a cathode-ray oscillograph. Theoretically this should be zero, but due to the presence of strays to earth and cross-coupling effects, the output was appreciable, (cf. Fig. 21a).

ii) With the bridge arms short-circuited the test was repeated. Under these conditions strays to earth are relatively

ineffective, and the unbalance indicated by the bridge arms was evidence of the assymmetry of the primary windings and the cross-coupling between those windings,(cf.Fig.21b).

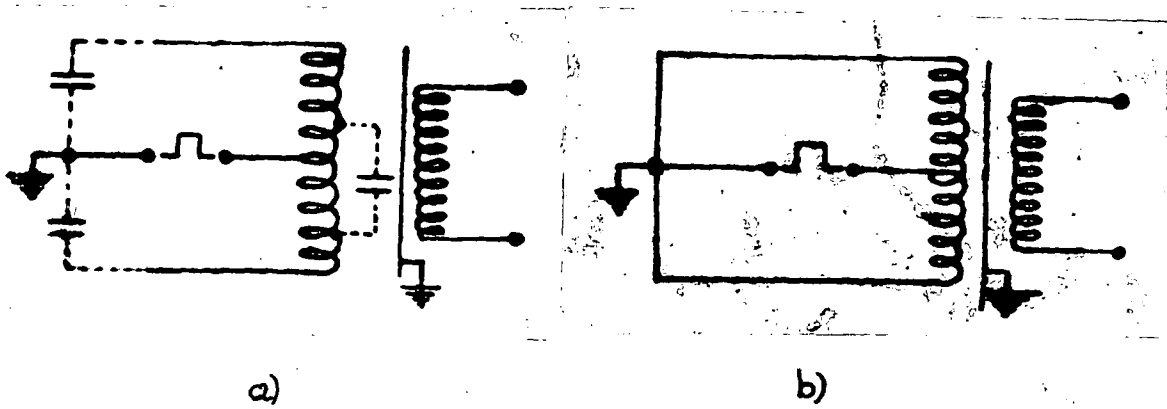

Fig.21). Strays in the differential transformer bridge:-
a) bridge arms open-circuited,
b) bridge arms short-circuited.

iii) The above tests indicated the presence of both earth and cross-coupling strays. In order to test the relative effects of the two types of strays, and reduce those effects to a minimum, observations were made on the bridge output with pure capacitive bridge arms, (cf.Fig.22).

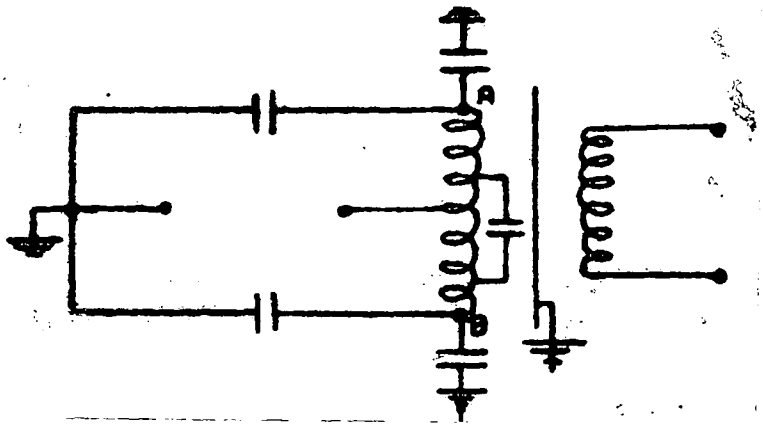

Fig.22). Strays in the differential transformer bridge with pure capacitive arms.

By reversing the bridge arms at points A and B, it was possible to isolate and measure the effects of assymmetrical strays to earth. Since these strays were in parallel with the bridge arms, on reversing the arms any assymmetry of those strays will be revealed by an apparent change of balance point of the bridge arms.

In practice, it was observed that upon reversing the bridge arms as described above, the apparent balance point changed by 5$\mu\mu$F. This was comparatively unaffected by adding a few turns to either of the primary windings. It was concluded that the effect was entirely due to assymmetry, and of the order of $\pm$ 2.5 $\mu\mu$F. In order to compensate for this effect two 0 to 5$\mu\mu$F trimming condensers were connected from the ends of the primary windings, A and B, to earth, (cf. Fig.23)

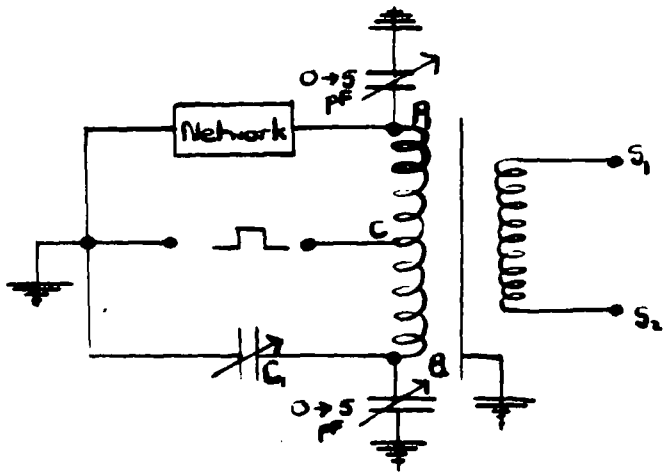

Fig.23). Differential transformer bridge showing 0 to 5$\mu\mu$F compensating condensers from A and B to earth.

These condensers were adjusted so that on reversing the bridge arms at A andB , there was no change of balance point of the bridge.

With pure capacitive bridge arms, the output should be zero at balance. This was unattainable in practice, but the bridge output obtained under those conditions was an indication of the uncompensated strays in the bridge. It was observed that this output was affected by the disposition of the transformer leads within the transformer shield, and the position of the differential transformer secondary with respect to the primary. These were varied until the best approximation to a straight line output was obtained, (cf.Fig24 Under these conditions it was assumed that the effect of strays in the differential transformer bridge was reduced to a negligible amount.

Fig.24). Output waveform for equal capacitive bridge arms.

It was later observed that reversing the input to the bridge, and making the junction of the ratio arms the earth

point did not affect the resultant waveform at balance for pure capacitive arms. This again supported our conclusion that the effects of strays in the circuit were negligible, and illustrated the comparative simplicity of the differential transformer bridge with regard to screening and elimination of strays.

As mentioned in the previous chapter, it was necessary to damp the differential transformer bridge in order to avoid unwanted oscillation . In practice, two damping resistors were required:- 8K across the differential transformer primary, and 10K across the differential transformer secondary The effect of these damping resistors on the bridge output for pure capacitive arms is shown in Fig.25).

a) b) c)

Fig.25). Bridge output waveform for pure capacitive bridge arms:- a) no damping,
b) 8K across the primary,
c) 10K across the secondary.

2). The bridge source.

A study of the response of electrical networks to an applied pulse by the bridge method indicated above demanded a source of square-waves whose vertical edge and corners were extremely sharp. Also, for the purposes of this investigation, it was convenient to be able to regulate both the repetition frequency and amplitude of the input pulse. A square-wave source fulfilling these requirements was supplied by F.H.Ritson, of the Department of Electrical Engineering, Kings College, Newcastle-upon-Tyne. It covered a range of repetition frequencies from 350 cycles/second to 2 Kilocycles/second, and an amplitude range from 0 to 50 volts. The circuit is shown in Fig.26).

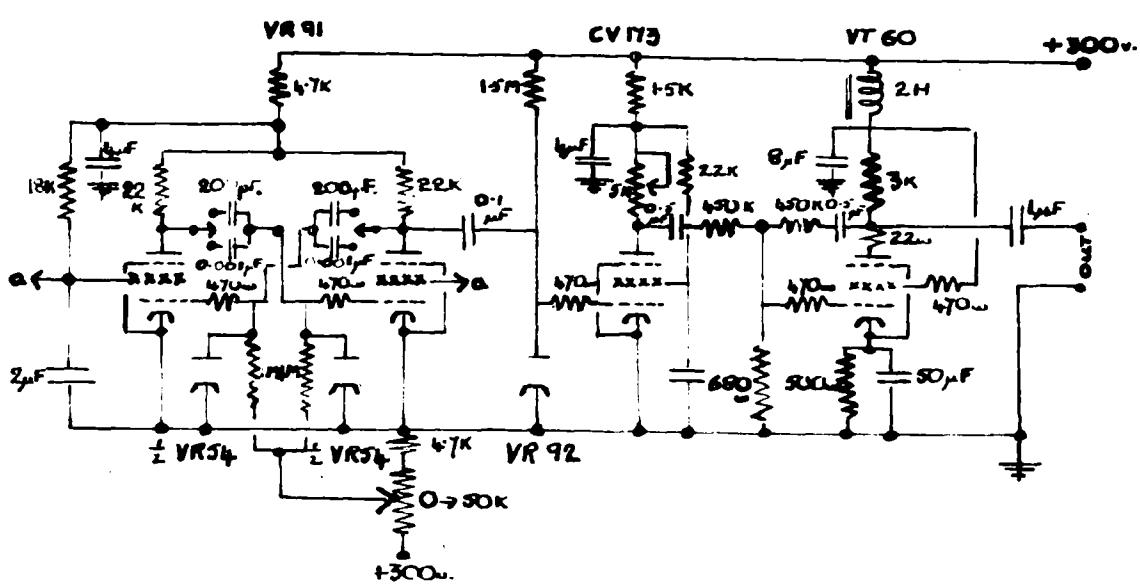

Fig.26). Square-wave generator circuit.

The action of the circuit is as follows:- the output from the multivibrator, the lower level of which is regulated by the action of the double-diodes, is applied to the grid of the following stage, which acts as a 'squaring'device. The output is taken by way of a See-saw amplifier to the bridge.

A convenient reference point in these measurements is the point at which the impedance moduli of the two bridge arms are equal. In order to obtain this point, a sinusoidal wave of variable frequency was applied to the bridge. For this purpose a Beat-frequency oscillator was used. By means of a two-way switch in the input lead to the bridge it was arranged that either the square-wave or the sinusoidal input could be applied to the bridge as required. The two sources and the bridge were connected to a common earth,(cf.Fig.27).

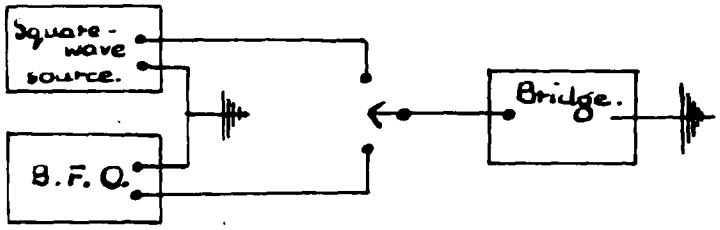

Fig. 27). Switching system to bridge input terminals.

3). The bridge indicating system.

In order to attain a sensitivity sufficient for practical purposes it was necessary to incorporate into the indicating system a stage of amplification. A bridge output amplifier was developed, the output from which was applied either to a cathode-ray tube for the study of the output waveform, or to an auxiliary circuit (to be described later) to indicate the current flowing in the differential transformer secondary.

i). The bridge output amplifier. This amplifier was designed to meet the special requirements resulting from the use of square-waves. If the applied pulse is considered to be made up of a range of individual component sinusoids with a definite phase relation between them, then the amplifier must not only amplify each component without distortion, but it must also preserve the correct phase relation between the components. It was estimated that the square-wave used involved frequency components ranging from the repetition frequency (360 cycles/second, minimum) to approximately 2 Mega-cycles/second. It is required that the gain of the amplifier should be constant over that range of frequencies.

The most suitable type of amplifier to meet these require ments is the resistance-capacitance coupled amplifier. A three stage resistance-capacitance coupled amplifier was therefore designed to cover the frequency range indicated(cf.Fig. 28).

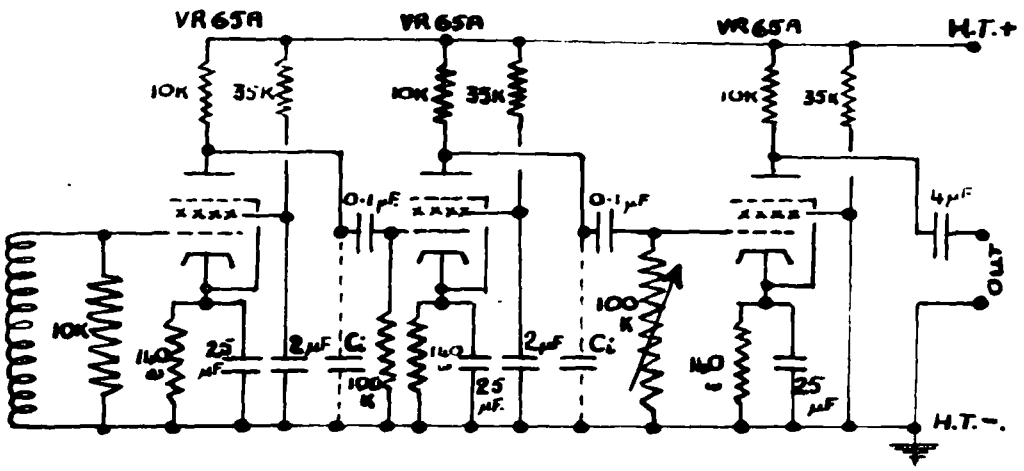

Fig.28). Bridge output amplifier.

Details regarding the actual design of the amplifier are given in Appendix I. An amplification control was provided in the form of a variable grid resistor to the third stage. The estimated maximum amplification at intermediate frequencies was 729 [cf. App. I].

The performance of the amplifier was influenced considerably by the layout and earthing of the circuit. Undue coupling between stages gave rise to multivibration. To eliminate this the circuit was arranged so as to reduce inter-lead and inter-stage capacitance coupling to a minimum, and the leads were kept as short as possible, thus reducing stray capacitances to earth. The inputs to the separate stages were applied by way of screened leads

to the grids of the corresponding valves, and the corresponding earth points were placed as near to the valves on the chassis as possible, thus avoiding unwanted effects due to earth currents.

To test the frequency response of the amplifier over the desired frequency range,(350 cycles/second to 2 Megacycles/second), the square-wave was applied direct to the amplifier, and the output and input waveforms compared on a cathode-ray oscillograph. Provided the amplifier valves are not working to saturation level, any inability of the amplifier to respond to the higher frequency components of the pulse would be exemplified in the rounding of the corners of the square-wave.There being no visual evidence of such distortion it was concluded that the frequency response of the amplifier was satisfactory forthe purposes of this research.

With the circuit described so far, the bridge output waveform represented the variation of rate of change of current with time. Reference has already been made to the waveforms of current and charge as well as rate of change of current,(cf.Ch.II). These waveforms were obtained in practice by incorporating two possible stages of integration in the bridge output amplifier circuit. These are indicated by dotted lines in the diagram,(cf.Fig.28).

ii). Indicating circuits. The cathode-ray tube was used for

studying the response of networks and of dielectrics to an applied pulse was an American Sylvania tube, type 3BP1. This tube had the advantages of sharp focussing and satisfactory brilliance and was very suitable for photographic purposes, and for making direct observations of the waveform.

To facilitate observation the time-base was derived by way of a capacitance-resistance circuit from the bridge input. It was thus synchronised automatically with the amplified bridge output which was applied to the Y-plates of the tube. By means of a reversing switch, the C-R circuit could function as either an integrating or a differentiating circuit, (cf. Fig.29) In this way either the beginning or the end of the trace could be examined in detail, and the time-base could be expanded or contracted as required by variation of the integrating/differentiating condenser, C_1.

All measurements carried out in this research were made using the integrated form of the time-base.

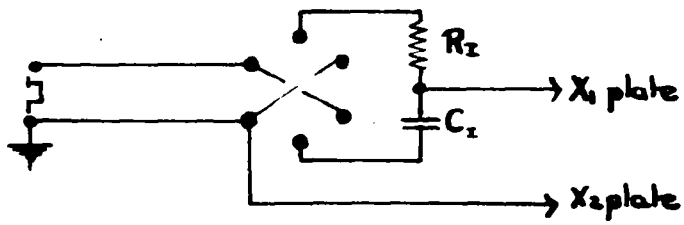

Fig.29). Switch system for C.R.O. time_base.

In order to calibrate the time-base for a given setting of C_1 a circuit was developed whereby the pulse edge of the bridge input initiated a decaying oscillation of known frequency, $w = 2\pi n = \frac{1}{(LC)^{\frac{1}{2}}}$, (cf. Fig. 39). Applying this to the Y-plates of the cathode-ray tube the horizontal sweep was divided into intervals, each interval representing $\frac{10^6}{2n}$ seconds. A permanent calibration was made on a piece of Perspex for a given setting of C_1, the repetition frequency of the applied pulse being 2 Kilocycles/second, and its amplitude a maximum. The calibration was used to check the order of time constants involved in any waveform.

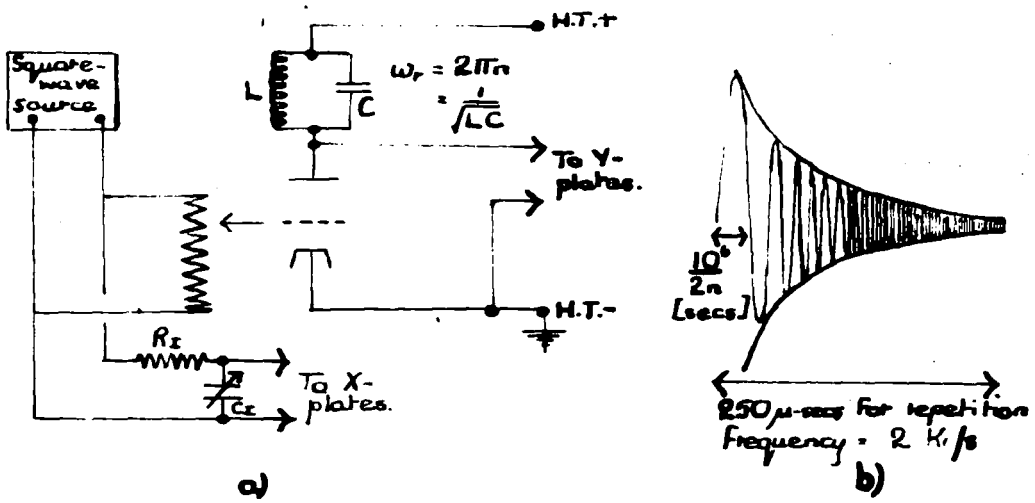

Fig. 30. Calibration of C.R.O. sweep:-
a) Circuit used,
b) Calibration waveform on C.R.O.

The possibility of suppressing the return track of the electron beam was considered. In practice, it was found that this rendered observation and measurements on the waveforms

more difficult.

An initial study of the bridge output waveforms for various simple electrical networks clearly indicated that it was not possible to judge accurately the point of balance of the bridge arms,(defined by equal impedance moduli in the bridge arms)at the repetition frequency of the square-wave), from a visual observation of the waveforms. This definition necessarily involved minimum current through the differential transformer secondary, and this provided the means of obtaining the balance point precisely. What was required was some sort of ballistic system to measure the total current round the circuit over a period of time which was large compared with the time constant associated with the bridge output. The outcome of this was the development of a ballistic indicator consisting of a tuned circuit,(L= ·16Henries,C = $1/\mu$ F) in parallel with a CV101 crystal detector and a micro-ammeter, (cf. Fig.31).

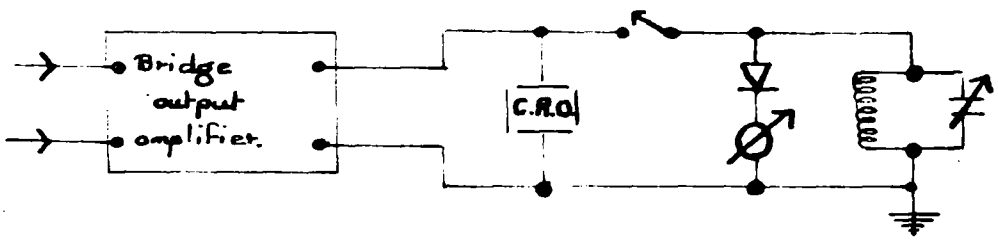

Fig.31. Ballistic indicating circuit.

Applying a sinusoidal input to the bridge the amplified bridge output could be applied by means of a switch across this indicating circuit, and a measure of the current through the differential transformer secondary obtained in terms of the micro-ammeter reading. When the total capacitances in the two bridge arms were equal, the micro-ammeter registered zero deflection. Tests showed that the bridge balance indication obtained by these means, could be adjusted to within $\pm$ 1.5 $\mu\mu$F, and that the balance point so obtained was independent of applied frequency in the audio-frequency range, for networks involving comparatively small resistive elements, (cf. Table III). When comparatively large resistances were involved the associated time constants became comparable with the time of response of the indicating circuit itself, and it was necessary to readjust the ballistic balance after compensating for the large resistive components. This will be described in more ~~detail later~~.

R = 500K.

TABLE III.

Frequency:-	410c/s.	[illegible] c/s.	24.5 660c/s.	[illegible] c/s.	[illegible] c/s.
Capacitance:- ($\mu\mu$F).	24.5	25.3	24.5	24.0	24.0
	24.5	26.5	24.5	[illegible]	24.0
	26.0	24.5	25.5	24.5	24.5
	24.0	24.0	25.5	25.5	24.5
	26.3	25.0	24.0	24.0	24.0
	25.0	25.5	25.0	25.5	24.5
	24.0	[illegible]	26.0		
	25.0	25.5			
	[illegible]	24.7			
Average Cap ($\mu\mu$F)	[illegible]		24.6	24.7	24.3
Maximum error ($\mu\mu$F)	1.6	1.2	1.1	1.3	0.3

[see Record Book Feb. 4th 1947].

4). <u>The design of the apparatus as a whole.</u>

The design of the apparatus as a whole was based on the necessity of avoiding inductive and capacitive coupling between the various sections of the apparatus. Such coupling may be direct between the sections, or by way of the connecting leads. To avoid direct coupling the apparatus was arranged so that input and output stages were removed from one another as far as possible. This was achieved by distributing the an apparatus as shown in Fig.32.

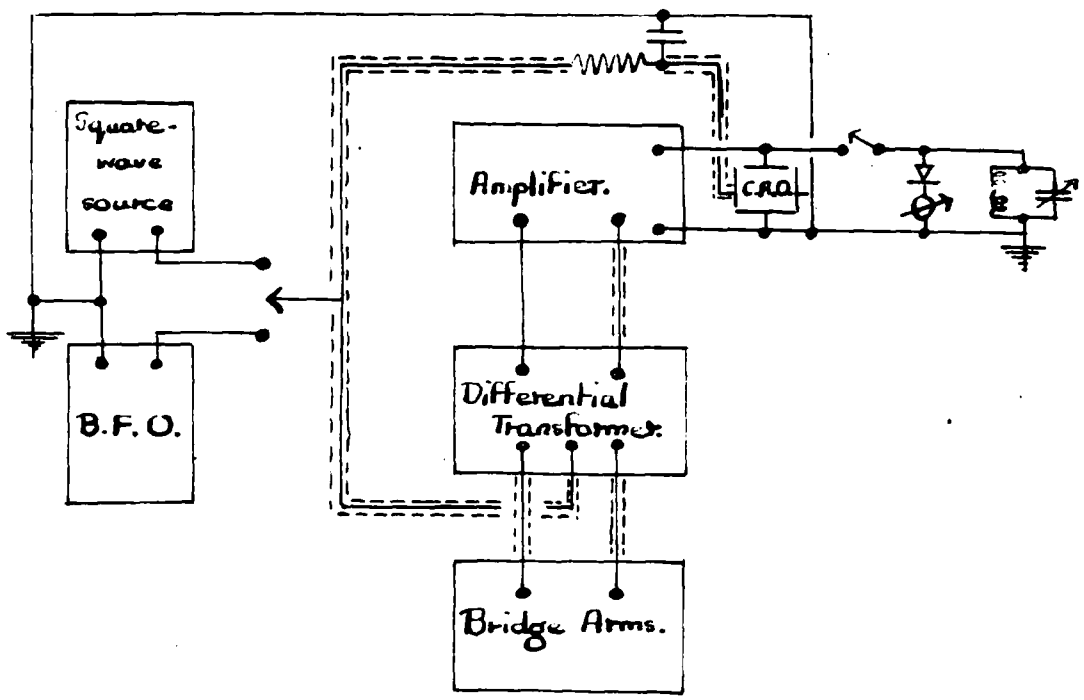

Fig.32). Experimental layout of the apparatus.

To eliminate effects arising from the connecting leads all leads between the sections were screened, the screens being connected to earth. The earth point for the complete system was the H.T.-^{ve} point, a true earth proving unsatisfactory. Each section of the apparatus was earthed independently to the H.T. -^{ve}.

9).

IV. THE MATHEMATICAL THEORY OF THE CIRCUIT.

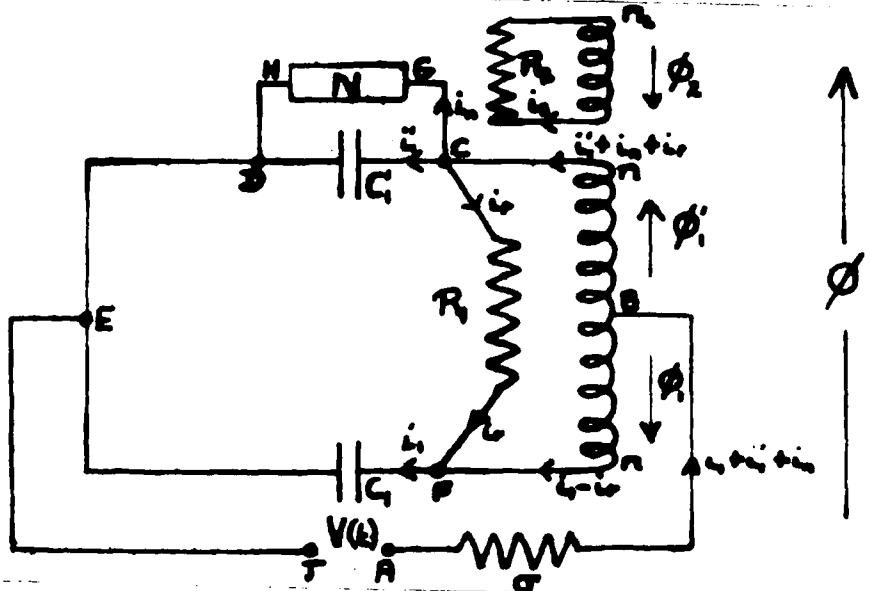

Fig.33). General circuit of differential ~~bridge~~. transformer bridge.

1). The general circuit of the differential transformer bridge as used in this work is shown in Fig.33). N represents the network under investigation. σ represents the impedance of the square-wave generator.

Consider the flux in the transformer. Let ϕ_1, ϕ_1', and ϕ_2 be the fluxes due to the two primaries and the secondary of the differential transformer respectively. Consider the case when $\phi_1' > \phi_1$. Then, by Lenz's law, ϕ_2 is in opposition to the resultant of ϕ_1' and ϕ_1. Hence, ϕ_1, ϕ_1' and ϕ_2 have the directions indicated in Fig.33). If ϕ_1' is considered positive, ϕ and ϕ_2 must therefore be negative.

Total flux in the core, $\phi = \phi_1 + \phi_1' + \phi_2$

But, $\phi_1 = -n(i_1 - i_r)$,

$\phi_1' = +n(i_1' + i_n + i_r)$

$\phi_2 = -n_2 i_2$

where n = flux per unit current in each primary coil, and is proportional to the number of turns in each primary coil, and n_2 = flux per unit current in secondary coil, and is proportional to the number of turns in the secondary coil.

$$\therefore \phi = -n(i_1 - i_r) + n(i_1' + i_n + i_r) - n_2 i_2 \qquad \text{1.1)}$$

But, from circuit BCFB,

$$i_r R_1 = -2n \frac{d\phi}{dt},$$

$$i_r = -\frac{2n}{R_1} \frac{d\phi}{dt}.$$

Also, from circuit of differential transformer secondary,

$$-i_2 R_2 = -n_2 \frac{d\phi}{dt},$$

$$i_2 = +\frac{n_2}{R_2} \frac{d\phi}{dt}.$$

Substituting for i_r and i_2 in 1.1),

$$\phi = n(i_1' + i_n - i_1) - \frac{4n^2}{R_1} \frac{d\phi}{dt} - \frac{n_2^2}{R_2} \frac{d\phi}{dt},$$

$$K \frac{d\phi}{dt} + \phi - n(i_1' + i_n - i_1) = 0 \qquad \text{1.2).}$$

where $K = \frac{4n^2}{R_1} + \frac{n_2^2}{R_2}$.

From circuit AEFEJA,

$$V(t) = \sigma\left[i_1 + i_{m_1} + i_4\right] - n\frac{d\phi}{dt} + \frac{q_1}{C_1}$$

$$V(t) = -n\frac{d\phi}{dt} + \frac{q_1}{C_1} + \sigma\left[\frac{dq_1}{dt} + \frac{dq_2}{dt} + \frac{dq_4}{dt}\right] \qquad \text{1.3)}$$

From circuit ABCDEJA,

$$V(t) = \sigma\left[i_4 + i_{m_2} + i_3\right] + n\frac{d\phi}{dt} + \frac{q_2}{C_2}$$

$$V(t) = +n\frac{d\phi}{dt} + \frac{q_2}{C_2} + \sigma\left[\frac{dq_2}{dt} + \frac{dq_3}{dt} + \frac{dq_4}{dt}\right] \qquad \text{1.4)}$$

From circuit CGHDC,

$$\frac{q_3}{C_3} = f\left[q_3, Z_3\right] \qquad \text{1.5)}$$

where $f[q_3, Z_3]$ = voltage developed across the network, N. This is a function of the charge flowing ~~across~~ through the network, and the properties of the network.

The bridge output voltage from across the differential transformer secondary, at any instant, is proportional to the rate of change of flux, $(\frac{d\phi}{dt})$, at that instant. The output waveform therefore represents the variation of $\frac{d\phi}{dt}$ with time. The four differential equations of the circuit, (1.2), 1.3), 1.4) and 1.5) contain four unknowns, q_1, q_2, q_3 and ϕ, (remembering that $\frac{dq}{dt} = i$). It is thus possible to eliminate q_1, q_2 and q_3, and solve the equations for ϕ. Hence $\frac{d\phi}{dt}$ may be obtained as a function of time in terms of the circuit constants, for any network, N, of known properties.

2). Capacitance in comparison arm of bridge, (N = open circuit, $i_n = 0$), (cf. Fig. 34).

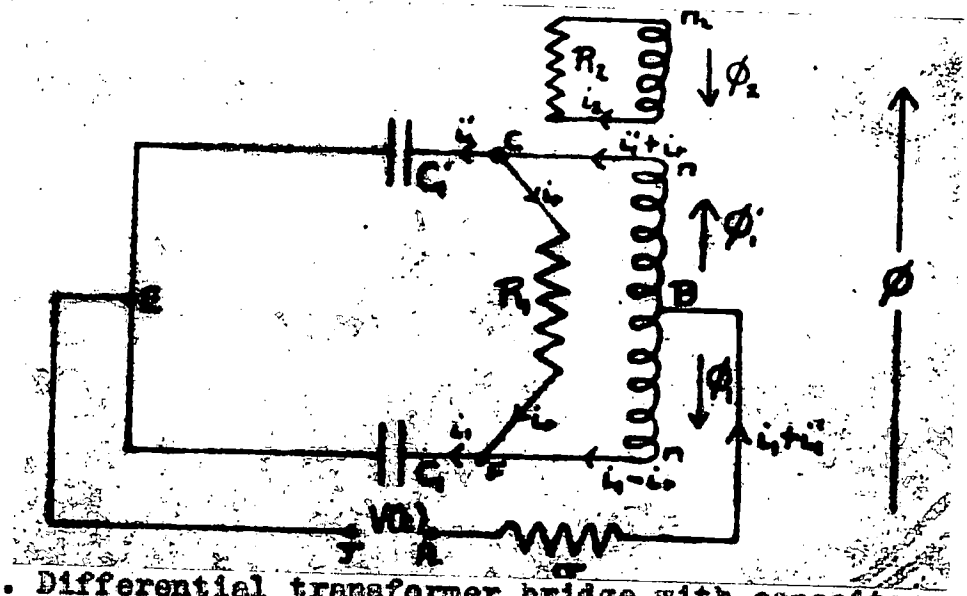

Fig.34). Differential transformer bridge with capacitance in comparison arm.

The differential equations of the circuit become:-

$$K\frac{d\phi}{dt} + \phi - n\left(\frac{dq_1'}{dt} - \frac{dq_1}{dt}\right) = 0 \qquad \text{2.1)}$$

$$-n\frac{d\phi}{dt} + \frac{q_1}{C_1} + \sigma\left(\frac{dq_1'}{dt} + \frac{dq_1}{dt}\right) = V(t) \qquad \text{2.2)}$$

$$+n\frac{d\phi}{dt} + \frac{q_1'}{C_1} + \sigma\left(\frac{dq_1'}{dt} + \frac{dq_1}{dt}\right) = V(t) \qquad \text{2.3)}$$

Boundary conditions:-

$V(t) = 0$ For $t < 0$, $V(t) = V$ for $t \geq 0$,

For $t \leq 0$, $q_1 = 0$, $q_1' = 0$, $\phi = 0$.

For $t > 0$, $q_1 = q_1$, $q_1' = q_1'$, $\phi = \phi$.

Using the Laplace Transform, the subsidiary equations become:-

$$\bar{\phi}\,[pK+1] + np\bar{q}_1 - np\bar{q}_2 = 0 \qquad \text{2.4)}$$

$$-np\bar{\phi} + \bar{q}_1\left(\frac{1}{C_1} + \sigma p\right) + \sigma p\bar{q}_2 = \frac{V}{p} \qquad \text{2.5)}$$

$$+np\bar{\phi} + \bar{q}_1 \cdot \sigma p + \bar{q}_2\left(\frac{1}{C_2} + \sigma p\right) = \frac{V}{p} \qquad \text{2.6)}$$

(The bar above a quantity indicates that we are dealing with the Laplace Transform of that quantity, e.g., $\bar{\phi} = \int_0^\infty e^{-pt}\,.\,dt$). [where p = large positive number]

Solving for $\bar{\phi}$:-

$$\bar{\phi} = \frac{V}{p\Delta}\begin{vmatrix} np & -np & 0 \\ \sigma p + \frac{1}{C_1} & \sigma p & 1 \\ \sigma p & \sigma p + \frac{1}{C_2} & 1 \end{vmatrix}$$

where $$\Delta = \begin{vmatrix} pK+1 & +np & -np \\ -np & \sigma p + \frac{1}{C_1} & \sigma p \\ +np & \sigma p & \sigma p + \frac{1}{C_2} \end{vmatrix}$$

$$\therefore \bar{\phi} = \frac{Vn}{\Delta}\left(\frac{1}{C_1} - \frac{1}{C_2}\right) \qquad \text{2.7)}$$

$$\Delta = (\rho K + 1)\left\{(\sigma\rho + \frac{1}{C_1})(\sigma\rho + \frac{1}{C_1'}) - \sigma^2\rho^2\right\} + n\rho\left\{4n\sigma\rho^2 + \frac{2\sigma\rho}{C_1'} + \frac{n\rho}{C_1}\right\}$$

$$= \frac{1}{C_1 C_1'}\left\{n^2\rho^2(C_1+C_1') + \rho K + 1\right\}\left\{1 + \sigma\rho\cdot\frac{4C_1C_1'}{C_1+C_1'}\right\}$$

when $(C_1 - C_1')$ becomes small.

$$\Delta = 4n^2\sigma\left[\rho^2 + \rho\cdot\frac{K}{n^2(C_1+C_1')} + \frac{1}{n^2(C_1+C_1')}\right]\left[\rho + \frac{C_1+C_1'}{4\sigma C_1 C_1'}\right]$$

$$= 4n^2\sigma\left[\rho - \alpha\right]\left[\rho - \beta\right]\left[\rho + \frac{C_1+C_1'}{4\sigma C_1 C_1'}\right]$$

where α and β are roots of the equation,

$$\rho^2 + \rho\cdot\frac{K}{n^2(C_1+C_1')} + \frac{1}{n^2(C_1+C_1')}.$$

When $K^2 < 4n^2(C_1+C_1')$, α and β are imaginary. This indicates that the system will oscillate.

Condition for damping is given by:-

$$K = \frac{4n^2}{R_1} + \frac{n^2}{R_2} \geq 2n\sqrt{C_1+C_1'}$$

Consider the simplest case when damping just occurs.

Then $$K = 2n\sqrt{C_1+C_1'}$$

and

$$\alpha = \beta = \frac{-K}{2n^2(C_1+C_1')}$$

$$= \frac{-1}{n\sqrt{C_1+C_1'}}$$

$$\Delta = 4n^2\sigma\left[p + \frac{1}{n\sqrt{C_1+C_1'}}\right]^2\left[p + \frac{C_1+C_1'}{4\sigma C_1 C_1'}\right]$$

From 2.7), $$\bar{\phi} = \frac{V[C_1 - C_1']}{4n\sigma C_1 C_1'\left[p + \frac{1}{n\sqrt{C_1+C_1'}}\right]^2\left[p + \frac{C_1+C_1'}{4\sigma C_1 C_1'}\right]}$$

$$\bar{\phi}' = \frac{d\bar{\phi}}{dt} = p\bar{\phi}$$

$$= \frac{V[C_1 - C_1']\ p}{4n\sigma C_1 C_1'\left[p + \frac{1}{n\sqrt{C_1+C_1'}}\right]^2\left[p + \frac{C_1+C_1'}{4\sigma C_1 C_1'}\right]} \qquad \text{2.8)}$$

$n\sqrt{C_1+C_1'} = \sqrt{L(C_1+C_1')}$, where L = effective inductance of each primary coil of the differential transformer. The quantity $n\sqrt{C_1+C_1'}$ has the dimensions of time and is equal to the natural periodic time of a circuit consisting of the inductance L in series with the capacitances C_1 and C_1' in parallel. $\frac{4\sigma C_1 C_1'}{C_1+C_1'}$ also has the dimensions of time, and is equal to the time constant of a circuit consisting of a resistance 4σ in series with the capacitances C_1 and C_1'.

Let $n\sqrt{C_1+C_1'} = T_n$ and $\frac{4\sigma C_1 C_1'}{C_1+C_1'} = T_\sigma$

Then, $$\frac{V_n(C_1 - C_1')}{T_n^2 T_\sigma}\ \frac{p}{\left[p + \frac{1}{T_n}\right]^2\left[p + \frac{1}{T_\sigma}\right]} \qquad \text{2.9)}$$

By Heaviside's Expansion Theorem:-

$$\phi' = \frac{V_n(C_1' - C_1)}{T_n^2 T_\sigma}\left\{\left|\frac{d}{dp}\left[\frac{p}{p + \frac{1}{T_\sigma}}\right]\right|_{p=-\frac{1}{T_n}} e^{-t/T_n} + \left|\frac{p}{p + \frac{1}{T_\sigma}}\right|_{p=-\frac{1}{T_n}} t e^{-t/T_n} + \left|\frac{p}{(p + \frac{1}{T_n})^2}\right|_{p=-\frac{1}{T_\sigma}} e^{-t/T_\sigma}\right\}$$

$$\phi' = \frac{V_n (C_1' - C_1)}{T_n'^2 (T_n - T_\sigma)^2} \left\{ \left[T_n' - t(T_n - T_\sigma) \right] e^{-t/T_n} - T_n' e^{-t/T_\sigma} \right\} \qquad 2.10)$$

Equation 2.10) gives the variation of $\frac{d\phi}{dt}$ with time, for a pure capacitive network on approaching balance, in terms of the circuit constants. In order to express this result graphically, it is proposed to consider the relationship in two parts, and superpose the results. Thus:-

$$\phi' = \phi_A' + \phi_B'$$

where $$\phi_A' = \frac{V_n (C_1' - C_1)}{T_n'^2 (T_n - T_\sigma)^2} \left\{ T_n' - t(T_n - T_\sigma) \right\} e^{-t/T_n}$$

$$\phi_B' = \frac{-V_n (C_1' - C_1)}{T_n'^2 [T_n - T_\sigma]^2} e^{-t/T_\sigma}$$

$\underline{\phi_A'}$. When $t = 0$, $\phi_A' = \frac{V_n (C_1' - C_1)}{(T_n - T_\sigma)^2}$

$\phi_A' = 0$ when $t = \frac{T_n'^2}{(T_n - T_\sigma)} = T_n + \frac{T_n T_\sigma}{(T_n - T_\sigma)}$ or ∞.

Turning points are given by

$\frac{d\phi_A'}{dt} = 0$ or $t = 2T_n + \frac{T_n T_\sigma}{(T_n - T_\sigma)}$ or ∞.

$\underline{\phi_B'}$ When $t = 0$, $\phi_B' = -\frac{V_n (C_1' - C_1)}{(T_n - T_\sigma)^2}$

when $\phi_B' = 0$ when $t = \infty$

$\phi' = \phi_a' + \phi_e'$

When $t = 0$, $\phi' = 0$.

$T_\sigma < T_n$

In practice, T_σ is small with respect to T_n. The waveforms for ϕ_a', ϕ_e', and ϕ', under these conditions are shown in Fig.35)

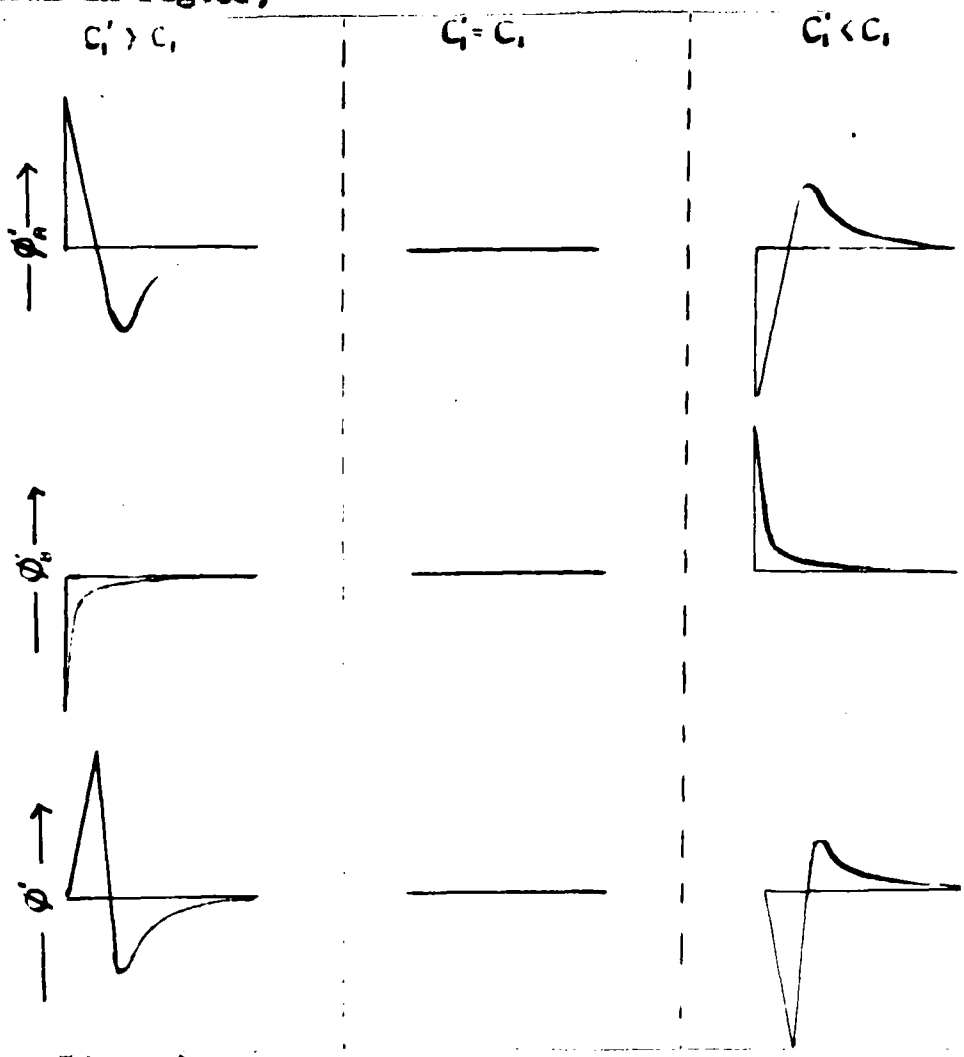

Fig.35) Graphical representation of mathematical results for pure capacitive bridge arms, (σ finite, $T_\sigma < T_n$).

From equation 2.10), ϕ' is proportional to $(C_1' - C_1)$. When $C_1' = C_1$, $\phi' = 0$, the waveform becomes a straight line, the bridge output is zero.

$T_\sigma \triangleq T_n$

When $T_\sigma = T_n$, $\left[\frac{4\sigma C_1 C_1'}{C_1 + C_1'} = n\sqrt{C_1 + C_1'}\right]$,

$\phi' \bullet\!\!-\!\!\bullet \phi$, ϕ' becomes indeterminate [cf. Equ^{n} 2.10]

and the relationship breaks down.

$T_\sigma > T_n$

The waveforms for ϕ_a', ϕ_b', and ϕ, when $T_\sigma > T_n$, are shown in Fig.36).

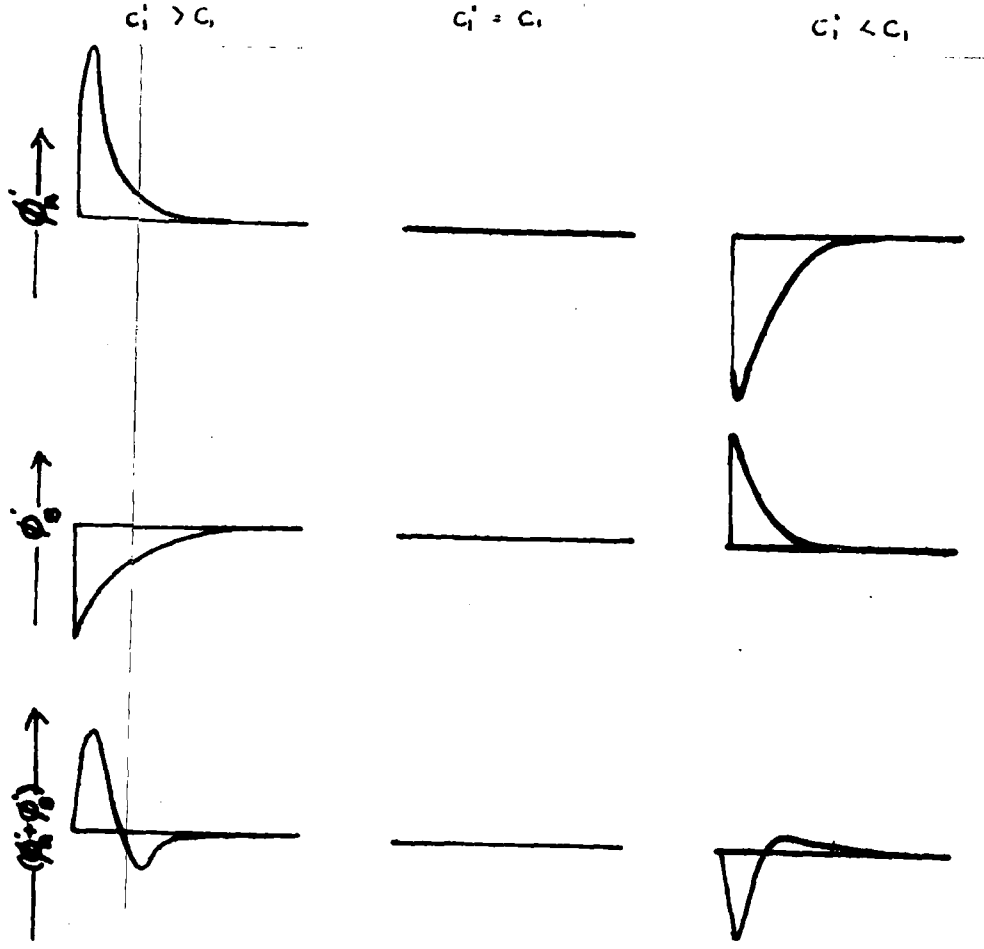

Fig.36) Graphical representation of mathematical results for pure capacitive bridge arms, (σ finite, $T_\sigma > T_n$).

From a comparison of Figs.35) and 36), it can be seen that for maximum sensitivity T_σ should be less than T_n. When this is so the response of the bridge is governed largely by the ring circuit BCDEFB,(cf.Fig.33). When $T_\sigma > T_n$, however the bridge response is governed mainly by the generator circuit. The first working condition of the apparatus is therefore that the generator impedance,

$$\sigma < \frac{n\,[C_1 + C_1']}{4\,C_1 C_1'}^{3/2} \qquad \text{2.11)}$$

3). <u>The effect of a finite rate of rise of the pulse edge.</u>

In the ideal case, the rate of rise of the pulse edge is infinite and the generator impedance $\sigma = 0$. In order to investigate the effect of a finite rate of rise of the pulse edge, it is proposed to compare the above results,(σ finite), with those for the ideal case,($\sigma = 0$).

When $\sigma = 0$, $T_\sigma = 0$,

equation 2.10) becomes:-

$$\phi' = \frac{V_0\,(C_1' - C_1)}{T_n^2}\left[T_n - t\right]e^{-t/T_n} \qquad \text{3.1)}$$

When $t = 0$,

$$\phi' = \frac{V_0\,[C_1' - C_1]}{T_n^2}$$

$\phi' = 0$ when $t = T_n$ or ∞.

Turning points are given by:-

$$\frac{d}{dt}(\phi') = \frac{V_0\,[C_1' - C_1]}{T_n^2}\,e^{-t/T_n}\left[\frac{t}{T_n} - 2\right]$$

$t = 2T_n$ or ∞.

The waveforms for ϕ' as C_1 is varied through C_1' are shown in Fig.37). ϕ' is directly proportional to $(C_1' - C_1)$. When $C_1' = C_1$, the waveform becomes a straight line, the bridge output is zero.

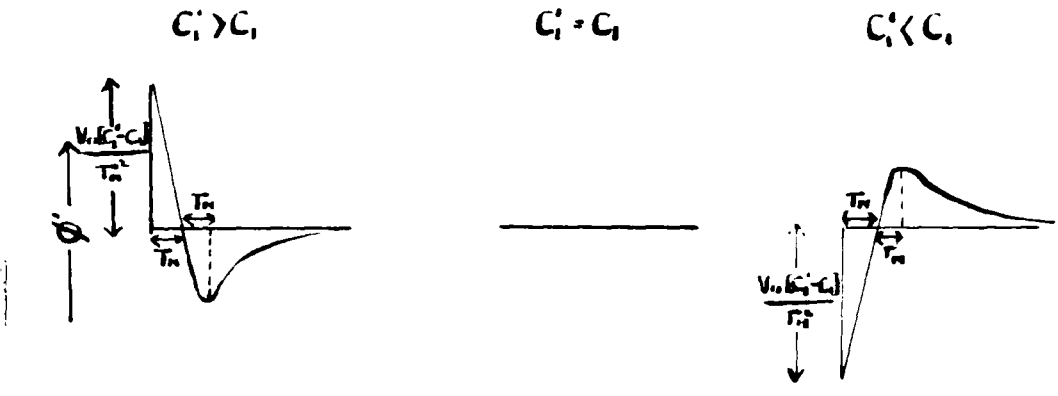

Fig.37) Graphical representation of mathematical results for pure capacitive bridge arms, ($\sigma \neq 0$, $T_\sigma = 0$).

From a comparison of Fig.37) and Figs.35) and 36), it can be seen that the effect of a finite rate of rise of the pulse edge is to impose a finite rate of growth of the initial spike, and to increase the time constant of the initial spike.

4). Capacitance, C_s', and series resistance, R_s', in parallel with the capacitance C_1' in the comparison arm of the bridge, ($N = C_s'$ and R_s' in series, $t_n = t_s$, $q_n = q_s'$), (cf.Fig.38).

The differential equations of the circuit become:-

$$K\frac{d\phi}{dt} + \phi - n\left[\frac{dq_1'}{dt} + \frac{dq_s'}{dt} - \frac{dq_2'}{dt}\right] = 0 \qquad \text{4.1)}$$

$$V(t) = -n\frac{d\phi}{dt} + \frac{q_2'}{C_1'} + \sigma\left[\frac{dq_1'}{dt} + \frac{dq_s'}{dt} + \frac{dq_2'}{dt}\right] \qquad \text{4.2)}$$

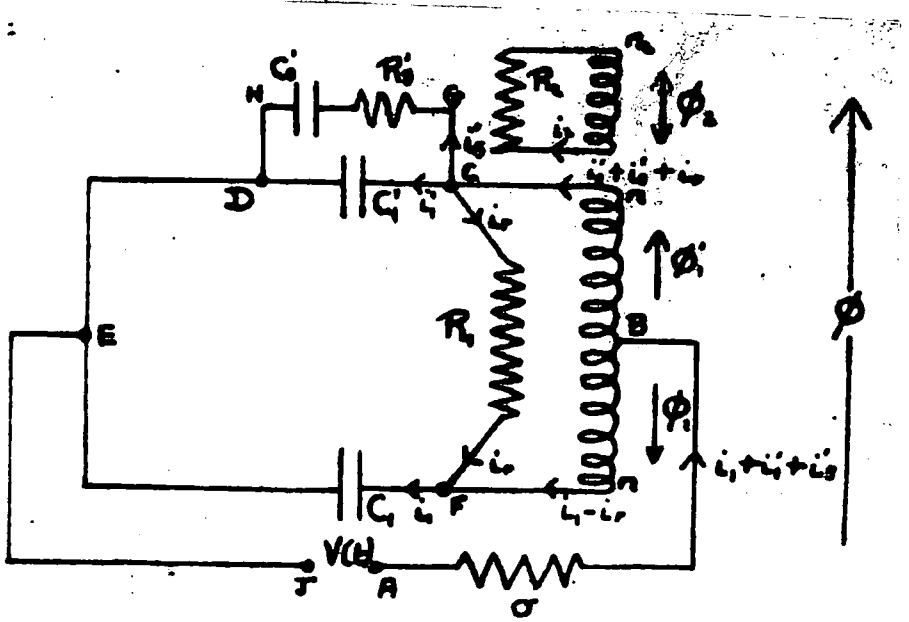

Fig. 38). Differential transformer bridge with capacitance and series resistance in parallel with capacitance in comparison arm .

$$V(t) = +n\frac{d\phi}{dt} + \frac{q_1'}{C_1'} + \sigma\left[\frac{dq_1}{dt} + \frac{dq_1'}{dt} + \frac{dq_3'}{dt}\right] \qquad \text{4.3)}$$

$$\frac{q_1'}{C_1'} - \frac{q_3'}{C_3'} - R_3'\frac{dq_3'}{dt} = 0 \qquad \text{BB} \qquad \text{4.4)}$$

Consider the generator impedance as negligible, ($\sigma = 0$).

Boundary conditions:-

$$V(t) = 0 \quad \text{for} \quad t < 0$$

$$V(t) = V \quad \text{for} \quad t > 0$$

For $t \leq 0$, $q_1 = 0$, $q_1' = 0$, $\phi = 0$, $q_3' = 0$,

For $t > 0$, $q_1 = q_1$, $q_1' = q_1'$, $\phi = \phi$, $q_3' = q_3'$.

Using the Laplace Transform, the subsidiary equations become:-

$$\bar{\phi}\,[\rho K+1] - n\rho\,\bar{q}_1 + n\rho\,\bar{q}_1 - n\rho\,\bar{q}_2 = 0 \qquad \text{4.5)}$$

$$-n\rho\,\bar{\phi} + \frac{1}{C_1}\,\bar{q}_1 = \frac{V}{P} \qquad \text{4.6)}$$

$$+n\rho\,\bar{\phi} + \frac{1}{C_1}\,\bar{q}_1 = \frac{V}{P} \qquad \text{4.7)}$$

$$\frac{\bar{q}_2}{C_1} - \bar{q}_2 R_2 \left[\rho + \frac{1}{C_2 R_2}\right] = 0 \qquad \text{4.8)}$$

From 4.8), $\bar{q}_1 = \bar{q}_2 C_1 R_2 \left[\rho + \frac{1}{C_2 R_2}\right]$ 4.9)

Substituting 4.9) in 4.5), 4.6), and 4.7),

$$\bar{\phi}\,[\rho K+1] - n\rho\,\bar{q}_2\left[1 + C_1 R_2\left(\rho + \frac{1}{C_2 R_2}\right)\right] + n\rho\,\bar{q}_1 = 0 \qquad \text{4.10)}$$

$$-n\rho\,\bar{\phi} + \frac{1}{C_1}\,\bar{q}_1 = \frac{V}{P} \qquad \text{4.11)}$$

$$+n\rho\,\bar{\phi} + \bar{q}_2 R_2\left[\rho + \frac{1}{C_2 R_2}\right] = \frac{V}{P} \qquad \text{4.12)}$$

Solving for $\bar{\phi}$:-

$$\bar{\phi} = \frac{V}{P\Delta}\begin{vmatrix} -n\rho\left[1 + C_1 R_2\left(\rho + \frac{1}{C_2 R_2}\right)\right] & +n\rho & 0 \\ 0 & \frac{1}{C_1} & 1 \\ R_2\left[\rho + \frac{1}{C_2 R_2}\right] & 0 & 1 \end{vmatrix}$$

where $\Delta = \begin{vmatrix} (\rho K+1) & -n\rho\left[1+C_1'R_s'\left(\rho+\frac{1}{C_s'R_s'}\right)\right] & +n\rho \\ -n\rho & 0 & \frac{1}{C_s} \\ +n\rho & R_s'\left[\rho+\frac{1}{C_s'R_s'}\right] & 0 \end{vmatrix}$

$$\therefore \phi' = \frac{V}{\rho\Delta}\left\{-\frac{n\rho}{C_1}\left[1+C_1'R_s'\left(\rho+\frac{1}{C_s'R_s'}\right)\right] + n\rho R_s'\left[\rho+\frac{1}{C_s'R_s'}\right]\right\}$$

$$= \frac{V_0[C_1-C_1']R_s'}{\Delta\ C_1}\left[\rho+\frac{1}{C_s'R_s'} - \frac{1}{(C_1'-C_1)R_s'}\right] \qquad \text{4.13)}$$

$$\Delta = [\rho K+1]\left[-\frac{R_s'}{C_1}\left(\rho+\frac{1}{C_s'R_s'}\right)\right] - \frac{n\rho^2}{C_1}\left[1+C_1'R_s'\left(\rho+\frac{1}{C_s'R_s'}\right)\right] - n\rho^2R_s'\left[\rho+\frac{1}{C_s'R_s'}\right]$$

$$= \frac{-n'[C_1+C_1']R_s'}{C_1}\left[\rho+\frac{1}{C_s'R_s'}\right]\left[\rho^2+\rho\frac{K}{n'[C_1+C_1']}+\frac{1}{n'[C_1+C_1']}\right] \qquad \text{4.14)}$$

provided C_s' is small with respect to (C_1+C_1').

$$\Delta = \frac{-n'[C_1+C_1']R_s'}{C_1}\left[\rho+\frac{1}{C_s'R_s'}\right][\rho-\alpha][\rho-\beta]$$

where α and β are roots of the equation:-

$$\rho^2 + \rho\frac{K}{n'[C_1+C_1']} + \frac{1}{n'[C_1+C_1']}$$

When $K' < 4n'[C_1+C_1']$, α and β are imaginary. This indicates that the system will oscillate.

Condition for damping is given by:-

$$K = \frac{4n'}{R_1} + \frac{n_2'}{R_2} \geq 2n\sqrt{C_1+C_1'}.$$

Consider the simplest case when damping just occurs:-

Then $K = 2n\sqrt{C_1+C_1'}$,

and $$\alpha = \beta = \frac{-K}{2n'[C_1+C_1']} = \frac{-1}{n\sqrt{C_1+C_1'}}.$$

$$\Delta = -n'R_s'\frac{(C_1'+C_1)}{C_1}\left[p+\frac{1}{C_s'R_s'}\right]\left[p+\frac{1}{n\sqrt{C_1+C_1'}}\right]^2$$

From 4.13),

$$\bar{\phi} = \frac{V[C_1'-C_1]\left[p+\frac{1}{C_s'R_s'}-\frac{1}{R_s'(C_1-C_1')}\right]}{n[C_1+C_1']\left[p+\frac{1}{C_s'R_s'}\right]\left[p+\frac{1}{n\sqrt{C_1+C_1'}}\right]^2}$$

$$\bar{\phi}' = \frac{\overline{d\phi}}{dt} = p\bar{\phi} = \frac{V[C_1'-C_1]\,p\left[p+\frac{1}{C_s'R_s'}-\frac{1}{R_s'[C_1-C_1']}\right]}{n[C_1+C_1']\left[p+\frac{1}{C_s'R_s'}\right]\left[p+\frac{1}{n\sqrt{C_1+C_1'}}\right]^2}$$

Let $C_s'R_s' = T_s$,
$R_s'[C_1-C_1'] = T_D$
and $n\sqrt{C_1+C_1'} = T_n$

Then, from 4.14)

$$\bar{\phi}' = \frac{V_n[C_1'-C_1]\,p\left[p+\frac{1}{T_s}-\frac{1}{T_D}\right]}{T_n'\left[p+\frac{1}{T_s}\right]\left[p+\frac{1}{T_n}\right]^2} \qquad 4.15$$

By Heaviside's Expansion Theorem:-

$$\phi' = \frac{V_n[C_1'-C_1]}{T_n'}\left\{\left|\frac{d}{dp}\left[\frac{\left[p+\frac{1}{T_s}-\frac{1}{T_D}\right]p}{\left(p+\frac{1}{T_s}\right)}\right]\right|_{p=-\frac{1}{T_n}} e^{-t/T_n} + \left|\frac{\left[p+\frac{1}{T_s}-\frac{1}{T_D}\right]p}{\left(p+\frac{1}{T_s}\right)}\right|_{p=-\frac{1}{T_n}} te^{-t/T_n}\right.$$

$$\left. + \left|\frac{p\left[p+\frac{1}{T_s}-\frac{1}{T_D}\right]}{\left(p+\frac{1}{T_n}\right)^2}\right|_{p=-\frac{1}{T_s}} e^{-t/T_s}\right\}$$

$$\phi' = \frac{V_n[C_1' - C_0]}{T_n'}\left\{\left[1 - \frac{T_n'T_s}{T_0[T_n - T_s]^2} + t\left[\frac{T_s}{T_0[T_n - T_s]} - \frac{1}{T_n}\right]\right]e^{-t/T_n} + \frac{T_n'T_s\, e^{-t/T_s}}{T_0[T_n - T_s]^2}\right\} \qquad 4.16)$$

Equation 4.16) gives the variation of $\frac{d\phi}{dt}$ with time for a network consisting of a series resistance and capacitance in parallel with a capacitance, on approaching balance, in terms of the circuit constants. Two cases are of particular interest:- i) $C_1 = (C_1' + C_s')$ or $T_0 = T_s$

ii) $C_1 = C_1'$ or $T_0 = 0$

1) $\underline{C_1 = (C_1' + C_s')_{or}\ T_0 = T_s}$

Putting $T_0 = T_s$ in equation 4.16):-

$$\phi' = \frac{V_n C_s'}{T_n'}\left\{\left[1 - \frac{T_n'}{(T_n - T_s)^2} + \frac{t.T_s}{T_n(T_n - T_s)}\right]e^{-t/T_n} + \frac{T_n'}{(T_n - T_s)^2}e^{-t/T_s}\right\} \qquad 4.17)$$

Consider this relationship in two parts, and superpose the results:- $\phi' = \phi_n' + \phi_0'$

where $\phi_n' = \frac{V_n C_s'}{T_n'}\left[1 - \frac{T_n'}{(T_n - T_s)^2} + \frac{t.T_s}{T_n(T_n - T_s)}\right]e^{-t/T_n}$

$$\phi_0' = \frac{V_n C_s'}{(T_n - T_s)^2}\, e^{-t/T_s}$$

$\underline{\phi_n'}$ when $t = 0$, $\phi_n' = \frac{V_n C_s'}{T_n'}\left[1 - \frac{T_n'}{(T_n - T_s)^2}\right]$

$\phi_n' = 0$ when $t = \frac{T_n[T_n - T_s]}{T_s}\left[1 + \frac{T_n'}{(T_n - T_s)^2}\right]$

$$= T_n + \frac{T_n'}{(T_n - T_s)} \quad \text{or} \quad \infty.$$

Turning points are given by $\frac{d\phi'_B}{dt} = 0$, or $t = 2T_n + \frac{T_n'}{T_n - T_s}$ or ∞.

ϕ'_B When $t = 0$, $\phi'_B = \frac{V_n C_s'}{(T_n - T_s)^2}$

$\phi'_B = 0$ when $t = \infty$

$\phi' = \phi'_A + \phi'_B$ When $t = 0$, $\phi' = \frac{V_n C_s'}{T_n'}$ ——————— 4.18)

The waveforms for ϕ'_A, ϕ'_B and ϕ' are shown in Fig.39), for $T_s < T_n$ When $T_s = T_n$, $\phi' = \infty$, and the relationship breaks down.

From equation 4.18), the height of the initial spike when $C_1 = (C_1' + C_s')$ is proportional to C_s'.

ii) $C_o = C_1'$ or $T_o = 0$

Putting $T_o = 0$ in 4.16:-

$$\phi' = \frac{V_n C_s'}{T_n'} \left\{ \frac{1}{(T_n - T_s)} \left[t - \frac{T_n'}{T_n - T_s} \right] e^{-t/T_n} + \frac{T_n'}{(T_n - T_s)^2} e^{-t/T_s} \right\} \quad \text{——————— 4.19}$$

Considering this relationship in two parts and superposing the results:- $\phi' = \phi'_A + \phi'_B$

where $\phi'_A = \frac{V_n C_s'}{T_n' (T_n - T_s)} \left[t - \frac{T_n'}{T_n - T_s} \right] e^{-t/T_n}$

$$\phi'_B = \frac{V_n C_s'}{(T_n - T_s)^2} e^{-t/T_s}$$

ϕ'_A When $t = 0$, $\phi'_A = \frac{-V_n C_s'}{(T_n - T_s)^2}$

$\phi'_A = 0$ when $t = T_n \left[1 + \frac{T_s}{T_n - T_s} \right]$ or ∞.

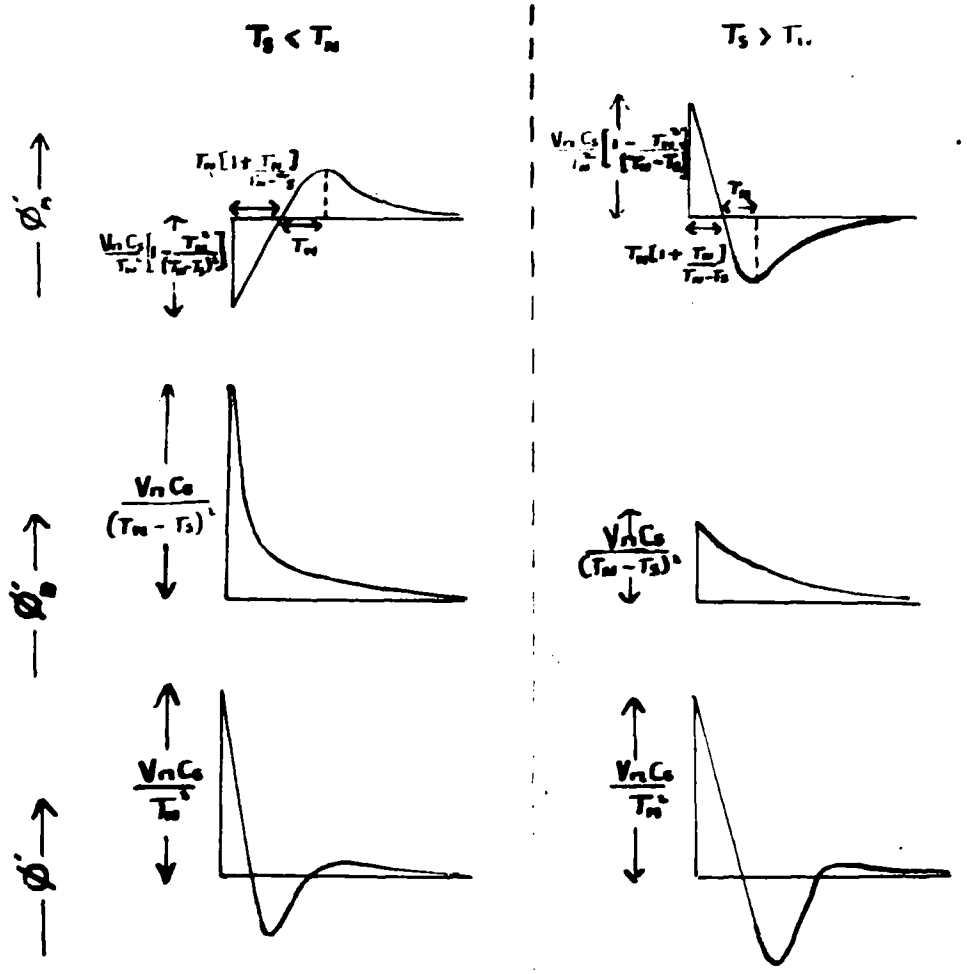

Fig.39). Graphical representation of mathematical results for series resistance capacitence network across one arm, (T_p negligible, $T_p = T_s$).

Turning points are given by $\frac{d\phi'_s}{dt} = 0$,

or $t = 2T_n + \frac{T_n T_s}{T_n - T_s}$ or ∞.

ϕ'_s when $t = 0$, $\phi'_s = \frac{V_n C_s}{(T_n - T_s)^2}$.

$\phi'_s = 0$ when $t = \infty$

$\phi' = \phi_n' + \phi_s'$ When $t = 0$, $\phi' = 0$. ——— 4.20)

The waveforms for ϕ_n', ϕ_s' and ϕ' under these conditions are shown in Fig.40) for $T_s < T_n$. When $T_s = T_n$, ϕ' becomes indeterminate and the relationship breaks down [cf. Equ^{n} 4.19]

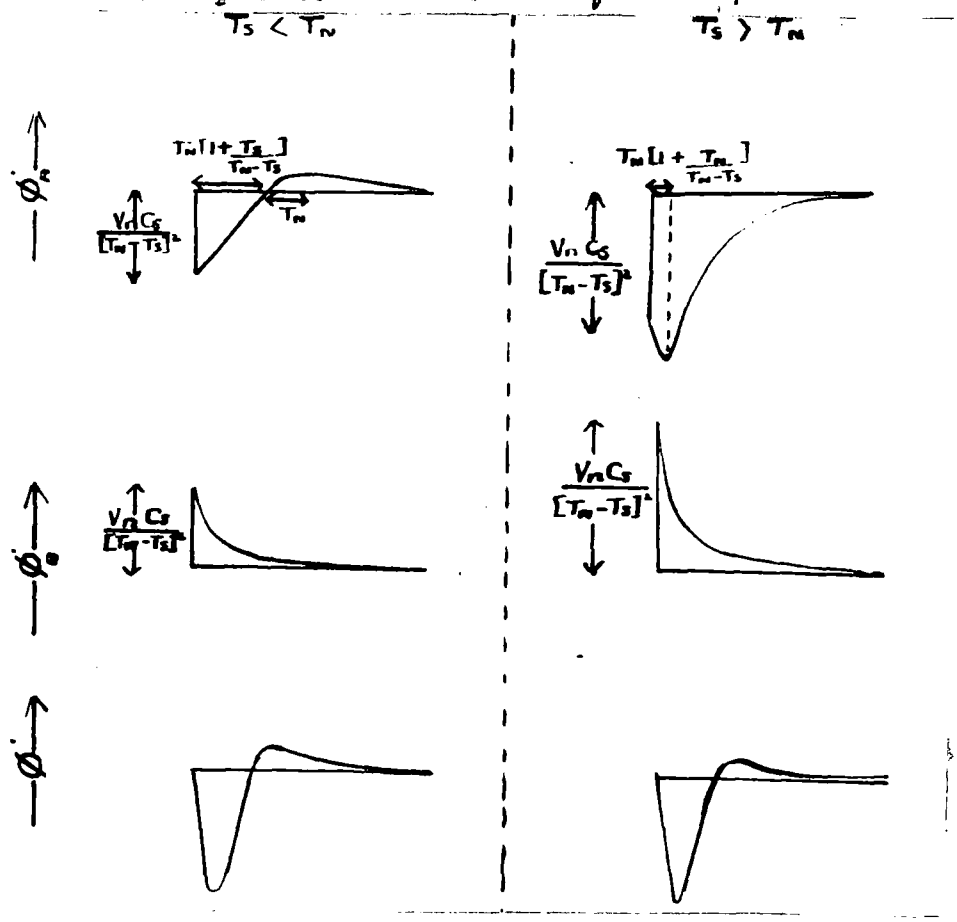

Fig.40). Graphical representation of mathematical results for series resistance capacitance network across one arm, (ϕ negligible, $T_0 = 0$).

From equation 4.20) it can be seen that when $C_1 = C_1'$ there is no initial spike in the output waveform. Comparing this with equ^{n} 4.18 ~~From this,~~ it may be concluded that the change in C_1 from $(C_1' + C_s')$ to C_1' is accompanied by the disappearance of the initial spike.

5). Resistance R_p' in parallel with the capacitance C_1', ($R_N = R_p'$, $i_n = i_p'$, $q_n = q_p'$), (cf. Fig. 41).

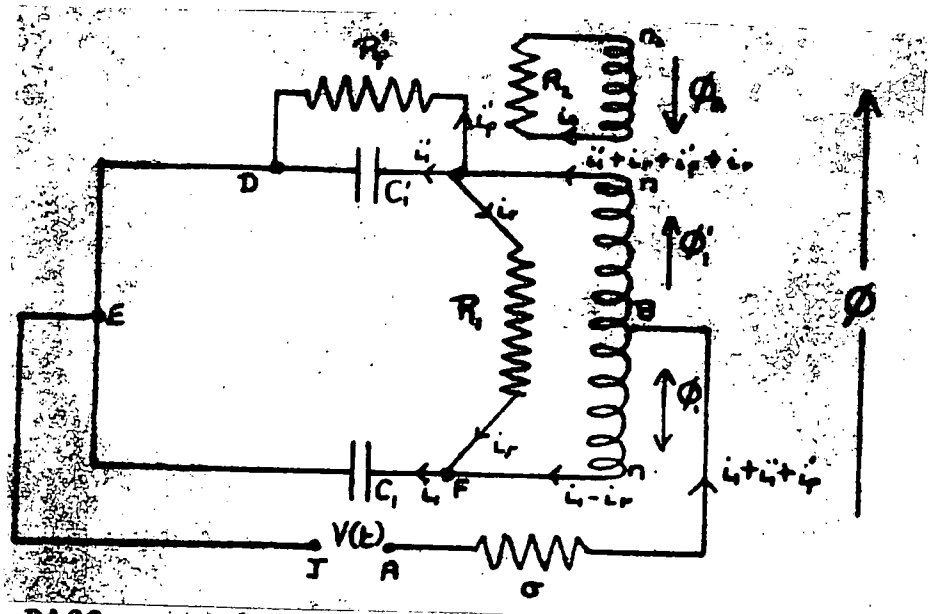

Fig. 41). Differential transformer bridge with capacitance and parallel resistance in the comparison arm.

The differential equations to the circuit become:-

$$K\frac{d\Phi}{dt} + \Phi - n\left[\frac{dq_1'}{dt} + \frac{dq_p'}{dt} - \frac{dq_1}{dt}\right] = 0 \qquad \text{5.1)}$$

$$-n\frac{d\Phi}{dt} + \frac{q_1}{C_1} + \sigma\left[\frac{dq_1'}{dt} + \frac{dq_p'}{dt} + \frac{dq_1}{dt}\right] = V(t) \qquad \text{5.2)}$$

$$+n\frac{d\Phi}{dt} + \frac{q_1'}{C_1'} + \sigma\left[\frac{dq_1'}{dt} + \frac{dq_p'}{dt} + \frac{dq_1}{dt}\right] = V(t) \qquad \text{5.3)}$$

$$\frac{q_p'}{C_1'} - R_p'\frac{dq_p'}{dt} = 0 \qquad \text{5.4)}$$

Consider the generator impedance as negligible, ($\sigma = 0$).

Boundary conditions:-

$$V(t) = 0 \quad \text{For } t < 0, \quad V(t) = V \text{ for } t > 0.$$

For $t \leq 0$, $q_1 = 0$, $q_1' = 0$, $q_f = 0$, $\phi = 0$.

For $t > 0$, $q_1 = q_1$, $q_1' = q_1'$, $q_f = q_f$, $\phi = \phi$

Using the Laplace Transform, the subsidiary equations become:-

$$\bar{\phi}[K_f p + 1] - n_f p[\bar{q}_1 + \bar{q}_f - \bar{q}_1'] = 0 \qquad \text{5.5)}$$

$$-n_f p\bar{\phi} + \frac{\bar{q}_1}{C_1} = \frac{V}{p} \qquad \text{5.6)}$$

$$+n_f p\bar{\phi} + \frac{\bar{q}_1'}{C_1'} = \frac{V}{p} \qquad \text{5.7)}$$

$$\frac{\bar{q}_1'}{C_1'} - p R_f' \bar{q}_f' = 0 \qquad \text{5.8)}$$

From 5.8) $$\bar{q}_f' = \frac{1}{p C_1' R_f'} \bar{q}_1' \qquad \text{5.9)}$$

Substituting equation 5.9) in 5.5), the subsidiary equations become:-

$$\bar{\phi}[K_f p + 1] - \bar{q}_1' n_f\left[p + \frac{1}{C_1' R_f'}\right] + n_f p \bar{q}_1 = 0 \qquad \text{5.10)}$$

$$-n_f p\bar{\phi} + \frac{\bar{q}_1}{C_1} = \frac{V}{p} \qquad \text{5.6)}$$

$$+n_f p\bar{\phi} + \frac{\bar{q}_1'}{C_1'} = \frac{V}{p} \qquad \text{5.7)}$$

Solving for $\bar{\phi}$:-

$$\overline{\phi} = \frac{V}{\rho \Delta} \begin{vmatrix} -n\left[\rho + \frac{1}{C_1' R_\rho'}\right] & +n\rho & 0 \\ 0 & \frac{1}{C_1'} & 1 \\ \frac{1}{C_1'} & 0 & 1 \end{vmatrix}$$

where $$\Delta = - \begin{vmatrix} (K_\rho + 1) & -n\left[\rho + \frac{1}{C_1' R_\rho'}\right] & +n\rho \\ +n\rho & 1/C_1' & 0 \\ -n\rho & 0 & \frac{1}{C_1'} \end{vmatrix}$$

$$\overline{\phi}' = \frac{-V}{\rho \Delta}\left\{\frac{n}{C_1'}\left[\rho + \frac{1}{C_1' R_\rho'}\right] - \frac{n\rho}{C_1'}\right\} = -\frac{V n [C_1' - C_1]\left[\rho + \frac{1}{R_\rho'(C_1' - C_1)}\right]}{\rho C_1 C_1' \Delta} \qquad 5.11)$$

$$\Delta = \left\{-\frac{(K_\rho + 1)}{C_1 C_1'} - \frac{n'\rho}{C_1'}\left[\rho + \frac{1}{C_1' R_\rho'}\right] - \frac{n'\rho^2}{C_1'}\right\} = -\frac{n'[C_1 + C_1']}{C_1 C_1'}\left[\rho^2 + \rho \cdot \frac{K + \frac{n'}{R_\rho'}}{n'(C_1 + C_1')} + \frac{1}{n'(C_1 + C_1')}\right]$$

$$= -\frac{n'[C_1 + C_1']}{C_1 C_1'}[\rho - \alpha][\rho - \beta] \qquad 5.12)$$

where α and β are the roots of the equation

$$\rho^2 + \rho \cdot \frac{K + n'/R_\rho'}{n'(C_1 + C_1')} + \frac{1}{n'(C_1 + C_1')}$$

When $\left(K + \frac{n'}{R_\rho'}\right)^2 < 4n'[C_1 + C_1']$, α and β are imaginary. This indicates that the system will oscillate.

Condition for damping is given by:-

$$K + \frac{n^2}{R_p} = \frac{4n^2}{R_1} + \frac{n^2}{R_2} + \frac{n^2}{R_p'} \geq 2n\sqrt{C_1+C_1'} \qquad \text{5.13)}$$

Consider the simplest case, when damping just occurs.

Then $K + \frac{n^2}{R_p'} = 2n\sqrt{C_1+C_1'}$, $\alpha = \beta = -\frac{K+\frac{1}{R_p'}}{2n^2[C_1+C_1']}$

$$= \frac{1}{n\sqrt{C_1+C_1'}}.$$

$$\therefore D = -\frac{n^2[C_1+C_1']}{C_1C_1'}\left[p + \frac{1}{n\sqrt{C_1+C_1'}}\right]^2$$

From 5.11),

$$\overline{\phi} = \frac{V[C_1'-C_1]\left[p + \frac{1}{R_p'(C_1'-C_1)}\right]}{n[C_1+C_1']\,p\left[p + \frac{1}{n\sqrt{C_1+C_1'}}\right]^2}$$

$$\overline{\phi'} = \overline{\frac{d\phi}{dt}} = p\overline{\phi} = \frac{V[C_1'-C_1]\left[p + \frac{1}{R_p'(C_1'-C_1)}\right]}{n[C_1+C_1']\left[p + \frac{1}{n\sqrt{C_1+C_1'}}\right]^2} \qquad \text{5.14)}$$

Let $R_p'[C_1'-C_1] = T_G$

and $n\sqrt{C_1+C_1'} = T_n$

From 5.14), $\overline{\phi'} = \frac{V n[C_1'-C_1]\left[p + \frac{1}{T_G}\right]}{T_n^2\left[p + \frac{1}{T_n}\right]^2}$ 5.15)

By Heaviside's Expansion Theorem:-

$$\overline{\phi} = \frac{V n[C_1'-C_1]}{T_n^2}\left\{\left|\frac{d}{dp}\left[p - \frac{1}{T_G}\right]\right|_{p=-\frac{1}{T_n}} e^{-t/T_n} + \left|p - \frac{1}{T_G}\right|_{p=-\frac{1}{T_n}} t e^{-t/T_n}\right\}$$

$$= \frac{V n[C_1'-C_1][T_n+T_G]}{T_n^2 T_G}\left\{t - \frac{T_n T_G}{T_n+T_G}\right\} e^{-t/T_n} \qquad \text{5.16)}$$

Equation 5.16) gives the variation of $\frac{d\phi}{dt}$ with time for a network consisting of a parallel resistance and capacitance, in terms of the circuit constants.

When $t = 0$, $\phi' = \frac{V_n [C_1' - C_1]}{T_n^2}$ ——————— 5.17)

$\phi' = 0$ when $t = \frac{T_n T_c}{T_n + T_c}$ ——————— 5.18)

or ∞

Turning points are given by $\frac{d\phi'}{dt} = 0$,

or $t = T_n + \frac{T_n T_c}{T_n + T_c}$ or ∞.

The waveforms for ϕ' under these conditions are shown in Fig.42), for T_c positive, $(C_1 < C_1')$, $T_c = 0$, $(C_1 = C_1')$. and T_c negative, $(C_1 > C_1')$.

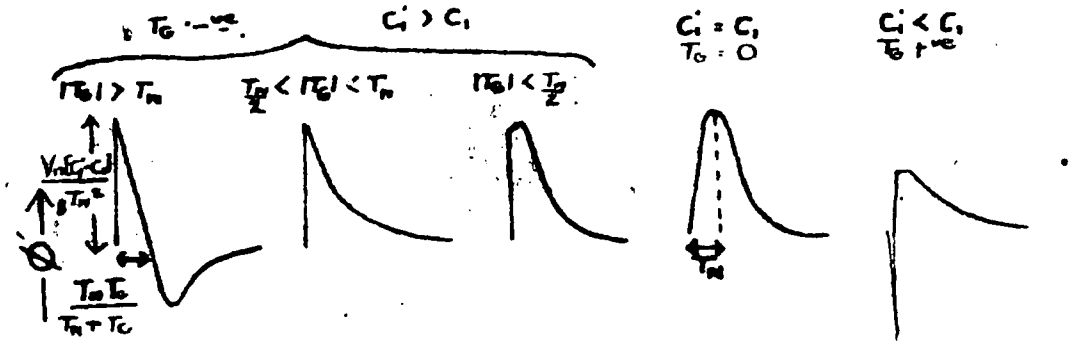

Fig. 42). Graphical representation of mathematical results for parallel resistance across one arm, (C negligible).

From equation 5.17) it can be seen that the height of the initial spike in this case is proportional to $(C_1' - C_1)$. When $C_1 = C_1'$ no initial spike is present. Also, from

equation 5.18), the time constant of the initial spike, ($t\phi'-\sigma$), is much smaller for T_σ positive than for T_σ negative.

6). <u>Series resistance and capacitance, ($C_s' R_s'$), and parallel resistance, (R_p'), in parallel with the capacitance C_1' in the comparison arm of the bridge,</u> (N = $C_s' R_s'$ in series, in parallel with R_p'), (of. Fig. 43).

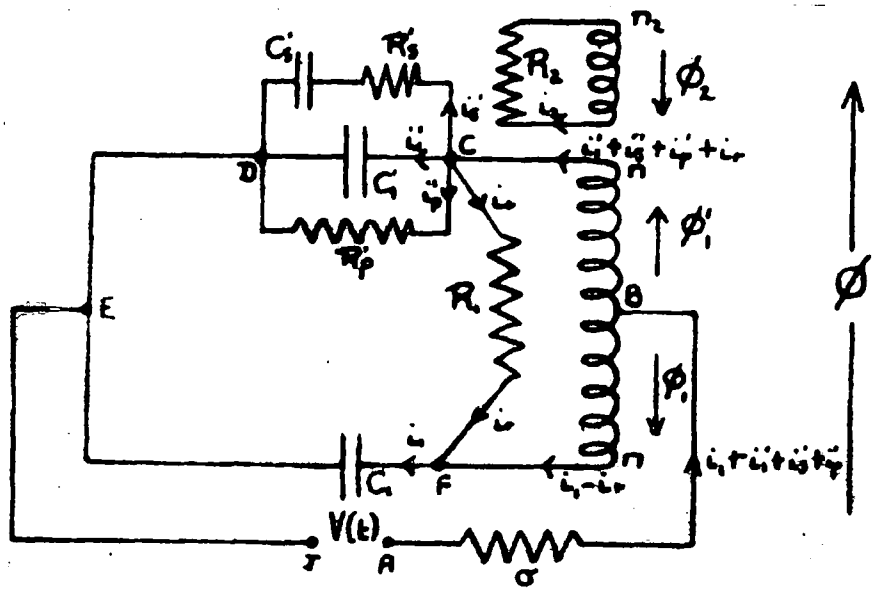

Fig. 43). Differential transformer bridge with capacitance and series resistance, and capacitance and parallel resistance in the comparison arm.

The differential equations to the circuit become:-

$$K\frac{d\phi}{dt} + \phi - n\left[\frac{dq_1'}{dt} + \frac{dq_s'}{dt} + \frac{dq_p'}{dt} - \frac{dq_1}{dt}\right] = 0 \qquad \text{6.1)}$$

$$-n\frac{d\phi}{dt} + \frac{q_1}{C_1} + \sigma\left[\frac{dq_1'}{dt} + \frac{dq_s'}{dt} + \frac{dq_p'}{dt} + \frac{dq_1}{dt}\right] = V(t) \qquad \text{6.2)}$$

$$n\frac{d\phi}{dt} + \frac{q_1'}{C_1'} + \sigma\left[\frac{dq_1'}{dt} + \frac{dq_2'}{dt} + \frac{dq_f'}{dt} + \frac{dq_1'}{dt}\right] = V(t) \qquad \text{6.3)}$$

$$\frac{q_1'}{C_1'} = R_f'\frac{dq_f'}{dt} = \frac{q_2'}{C_2'} + R_2'\frac{dq_2'}{dt} \qquad \text{6.4)}$$

Consider the generator impedance to be negligible, ($\sigma = 0$).

Boundary conditions:-

$V(t) = 0$ for $t < 0$, $\quad V(t) = V$ for $t \geq 0$,

For $t \leq 0$, $q_1 = 0$, $q_1' = 0$, $q_2' = 0$, $q_f' = 0$, $\phi = 0$,

For $t > 0$, $q_1 = q_1$, $q_1' = q_1'$, $q_2' = q_2'$, $q_f' = q_f'$, $\phi = \phi$.

Using the Laplace Transform, the subsidiary equations become:-

$$\bar{\phi}[Kp+1] - np[\bar{q}_1' + \bar{q}_2' + \bar{q}_f' - \bar{q}_1] = 0 \qquad \text{6.5)}$$

$$-np\bar{\phi} + \frac{\bar{q}_1}{C_1} = \frac{V}{p} \qquad \text{6.6)}$$

$$+np\bar{\phi} + \frac{\bar{q}_1'}{C_1'} = \frac{V}{p} \qquad \text{6.7)}$$

$$\frac{\bar{q}_1'}{C_1'} = pR_f'\bar{q}_f' = \bar{q}_2'R_2'\left[p + \frac{1}{C_2'R_2'}\right] \qquad \text{6.8)}$$

From 6.8) $$\bar{q}_1' = \bar{q}_2'C_1'R_2'\left[p + \frac{1}{C_2'R_2'}\right] \qquad \text{6.9)}$$

$$\bar{q}_f' = \bar{q}_2'\frac{R_2'}{pR_f'}\left[p + \frac{1}{C_2'R_2'}\right] \qquad \text{6.10)}$$

Substituting 6.9) and 6.10) in 6.5), 6.6), and 6.7),

$$\bar{\phi}\left[K_p+1\right] + n_p\bar{q}_1 - n q_2'\left[p + C_1'R_2'\left(p+\frac{1}{C_2'R_2'}\right)\left(p+\frac{1}{C_1'R_p'}\right)\right] = 0 \qquad \text{6.11)}$$

$$-n_p\bar{\phi} + \frac{\bar{q}_1}{C_1} = \frac{V}{p} \qquad \text{6.12)}$$

$$+n_p\bar{\phi} + \bar{q}_2'\left[p+\frac{1}{C_2'R_2'}\right]R_2' = \frac{V}{p} \qquad \text{6.13)}$$

Solving for $\bar{\phi}$:-

$$\bar{\phi} = \frac{V}{p\Delta}\begin{vmatrix} -n\left[p + C_1'R_2'\left(p+\frac{1}{C_2'R_2'}\right)\left(p+\frac{1}{C_1'R_p'}\right)\right] & +n_p & 0 \\ 0 & \frac{1}{C_1} & 1 \\ R_2'\left[p+\frac{1}{C_2'R_2'}\right] & 0 & 1 \end{vmatrix}$$

where $\Delta =$

$$\begin{vmatrix} K_p+1 & -n\left[p+C_1'R_2'\left(p+\frac{1}{C_2'R_2'}\right)\left(p+\frac{1}{C_1'R_p'}\right)\right] & +n_p \\ -n_p & 0 & \frac{1}{C_1} \\ +n_p & R_2'\left[p+\frac{1}{C_2'R_2'}\right] & 0 \end{vmatrix}$$

$$\therefore \phi' = \frac{V}{p\Delta}\left\{-\frac{n}{C_1}\left[p + C_1'R_2'\left(p+\frac{1}{C_2'R_2'}\right)\left(p+\frac{1}{C_1'R_p'}\right)\right] + n_p R_2'\left[p+\frac{1}{C_2'R_2'}\right]\right\}$$

$$\phi' = \frac{-V_n}{p\Delta C_1}\left\{\left[p+\frac{1}{C_2'R_2'} + \frac{1}{R_2'(C_1'-C_1)}\right]\left[p+\frac{1}{R_p'(C_1'-C_1)}\right]R_2'(C_1'-C_1) - \frac{1}{R_p'(C_1'-C_1)}\right\} \qquad \text{6.14)}$$

$$\Delta = -\frac{R_2'n'(C_1+C_1')}{C_1}\left[p+\frac{1}{C_2'R_2'}\right]\left[p^2 + p\cdot\frac{K+\frac{n}{R_p'}}{n'(C_1+C_1')} + \frac{1}{n'(C_1+C_1')}\right] \qquad \text{6.15)}$$

provided C_2' is small with respect to (C_1+C_1').

$$\Delta = -\frac{R_5' n^2 [C_1+C_1']}{C_1}\left[p+\frac{1}{C_5' R_5'}\right][p-\alpha][p-\beta]$$

where α and β are roots of the equation,

$$p^2 + p\cdot\frac{K+\frac{n^2}{R_p'}}{n^2[C_1+C_1']} + \frac{1}{n^2[C_1+C_1']}.$$

When $\left[K+\frac{n^2}{R_p'}\right]^2 < 4n^2[C_1+C_1']$, α and β are imaginary. This indicates that the system will oscillate.

Condition for damping is given by:-

$$K+\frac{n^2}{R_p'} = 4\frac{n_1^2}{R_1'} + \frac{n_2^2}{R_2'} + \frac{n^2}{R_p'} \geq 2n\sqrt{C_1+C_1'} \qquad \text{6.16)}$$

Consider the simplest case when damping just occurs.

Then $K+\frac{n^2}{R_p'} = 2n\sqrt{C_1+C_1'}$ and $\alpha = \beta = -\frac{K+\frac{n^2}{R_p'}}{2n^2[C_1+C_1']}$

$$\therefore \Delta = -R_5' n^2 \frac{[C_1+C_1']}{C_1}\left[p+\frac{1}{C_5' R_5'}\right]\left[p+\frac{1}{n\sqrt{C_1+C_1'}}\right]^2$$

From 6.14),

$$\Phi = \frac{V\left\{\left[p+\frac{1}{C_5'R_5'}+\frac{1}{R_5'[C_1'-C_1]}\right]\left[p+\frac{1}{R_p'[C_1'-C_1]}\right]R_5'[C_1'-C_1] - \frac{1}{R_p'[C_1'-C_1]}\right\}}{p R_5' n [C_1+C_1']\left[p+\frac{1}{C_1'R_5'}\right]\left[p+\frac{1}{n\sqrt{C_1+C_1'}}\right]^2}$$

$$\overline{\phi}' = \frac{d\overline{\theta}}{dt} = p\overline{\phi}$$

$$= \frac{V\left\{\left[p+\frac{1}{C_5'R_5'}+\frac{1}{R_5'[C_1'-C_1]}\right]\left[p+\frac{1}{R_p'[C_1'-C_1]}\right]R_5'[C_1'-C_1] - \frac{1}{R_p'(C_1'-C_1)}\right\}}{R_5' n [C_1+C_1']\left[p+\frac{1}{C_1'R_5'}\right]\left[p+\frac{1}{n\sqrt{C_1+C_1'}}\right]^2} \qquad \text{6.17)}$$

Let $C_5'R_5' = T_5$, $\quad R_5'[C_1'-C_1] = -T_0$

$n\sqrt{C_1+C_1'} = T_n$, $\quad R_p'[C_1'-C_1] = -T_G$

Then from 6.17),

$$\phi' = \frac{-V_n[C_1-C_1']\left\{(p+\frac{1}{T_s}-\frac{1}{T_0})(p-\frac{1}{T_0})T_0 - \frac{1}{T_0}\right\}}{T_0 T_n^2 [p+\frac{1}{T_s}][p+\frac{1}{T_n}]^2} \qquad 6.18)$$

By Heaviside's Expansion Theorem:-

$$\phi' = \frac{-V_n(C_1-C_1')}{T_0 T_n^2}\left\{\left|\frac{d}{dp}\frac{\left[(p+\frac{1}{T_s}-\frac{1}{T_0})(p-\frac{1}{T_0})T_0 - \frac{1}{T_0}\right]}{(p+1/T_s)}\right|_{p=-\frac{1}{T_n}} e^{-t/T_n}\right.$$

$$+\left|\frac{\left[(p+\frac{1}{T_s}-\frac{1}{T_0})(p-\frac{1}{T_0})T_0-\frac{1}{T_0}\right]}{(p+\frac{1}{T_s})}\right|_{p=-\frac{1}{T_n}} t\,e^{-t/T_n} + \left|\frac{\left[(p+\frac{1}{T_s}-\frac{1}{T_0})(p-\frac{1}{T_0})T_0-\frac{1}{T_0}\right]}{(p+\frac{1}{T_n})^2}\right|_{p=-\frac{1}{T_s}} e^{-t/T_s}\left.\right\}$$

$$= \frac{V_n[C_1'-C_1]}{T_n^2}\left\{\left[1-\frac{T_n T_s}{T_0(T_n-T_s)}+t\left(\frac{T_s}{T_0(T_n-T_s)}-\frac{1}{T_n}-\frac{1}{T_0}\right)\right]e^{-t/T_n} + \frac{T_n T_s}{T_0(T_n-T_s)}\,e^{-t/T_s}\right\} \qquad 6.19)$$

Equation 6.19 gives the variation of $\frac{d\phi}{dt}$ with time for a network consisting of a series resistance and capacitance in parallel with a parallel resistance and capacitance, on approaching balance in terms of the circuit constants.

Comparing this result, (Eq.6.19), with the result for the series resistance capacitence network, (Eq.4.16), it can be seen that the presence of parallel resistance, (represented by the factor $T_0 = R_p'(C_1'-C_1)$) modifies the coefficient of t in the equations, slightly. That is to say, it affects only the time rate and not the general shape of the waveform. Once ~~agd~~

again, when $t = 0$, $\phi = 0$, for $C_1 = C_1'$, and ϕ' is proportional to C_s' for $C_1 = (C_1' + C_s')$ (cf. Fig.44).

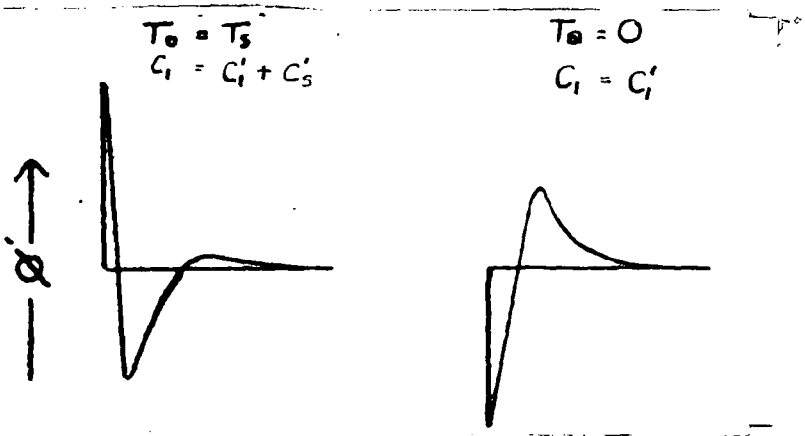

Fig.44). Graphical representation of mathematical results for series resistance and capacitance and parallel resistance and capacitance across one arm, (σ negligible).

7). Conclusions drawn from the mathematical theory of the circuit.

i) Response of simple networks. In the theory deduced above it can be predicted that the bridge output waveforms for various networks in the comparison arm of the bridge are as follows. For pure capacitive arms the predicted waveform at balance is a straight line. Off-balance, the waveform is oscillatory in nature, the frequency of the decaying oscillation depending on the properties of the ring circuit. The dominating time constant is therefore relatively large. The output waveform for the capacitance and series resistance network at balance, (defined by equal total capacitances in the two bridge arms), is characterised by the sharp spike at the co commencement of the trace. The height of this initial spike ~~is proportional to the capacitance~~

is proportional to the capacitance associated with series resistance. The time constant associated with the spike is in general smaller than that associated with unbalanced capacitive arms. The waveforms for the series resistance capacitance network are in direct contrast with the sharp rise followed by the slow decay typical of the parallel resistance capacitance network at balance. The combination of series resistance and capacitance ,and parallel resistance and capacitance, appears to exhibit the characteristics of the separate networks superimposed; that is to say, the initial spike arising from the capacitance and series resistance branch followed by the slow decay typical of the parallel resistance capacitance branch, and the possibility of a second maximum.

The waveforms predicted for the simple networks indicated above are similar to those deduced from the charge-time variations for those networks in Ch.II. It will be seen later that they are also in good agreement with experimental observation.

ii) <u>The working conditions of the circuit.</u>

<u>a) Damping.</u> From equation 5.13) the condition for damping in the case of the combined series resistance capacitance and parallel resistance capacitance network is given by:-

$$\frac{4n^2}{R_1^2} + \frac{n_2^2}{R_2^2} + \frac{n^2}{R_p^2} \geq \cdot 2n\sqrt{C_1 r C_1} = 2T_n$$

In practice, $R_1 = 8K$,

$R_2 = 10K$

$R_p' > 1M$

$n' =$ (Flux/unit current in each primary)

$=$ Primary inductance $= 0.11$ Henries.

$n_1 : n_2 = 150 : 450$

$C_1 \simeq C_1' > 300 \mu\mu F$

Substituting these values,

$$(2T_n)_{max.} = 16.2 \mu secs.$$

$$\frac{4n'^2}{R_1} + \frac{n_1'^2}{R_2} + \frac{n'^2}{R_p'} = \frac{0.44}{8 \times 10^3} + \frac{0.99}{10 \times 10^3} + \frac{0.11}{10^6} = 154 \mu secs.$$

Condition for damping holds in practipe.
($\frac{n'^2}{R_p'}$ is small with respect to $\left(\frac{4n'^2}{R_1} + \frac{n_1'^2}{R_2}\right)$,in practice, and can therefore be neglected. The condition for damping is there fore not appreciably affected by the presence of the parallel resistance network)

Theoretically the damping condition indicates that ~~dempin~~ damping is possible when either R_1 or $R_2 = \infty$. In practice, however, this was not so.

b) Current through the differential transformer primary arising from the series resistance capacitence network.

From equation 4.14), it can be seen that the mathematical deduction of the waveform for the series resistance

capacitance network is based on the proviso that the current i_s', through the differential transformer primary arising from the series resistance capacitance network, should be small, i.e. that C_s' is small with respect to $(C_1' + C_1)$. If C_s' is not small with respect to $(C_1' + C_1)$ the results obtained in practice were not necessarily invalid however.

In practice, $\left[\frac{C_s'}{C_1 + C_1'}\right]_{max.} = \frac{50}{200} = 25\%$

c). Experimental ranges of time constants which are involved in the mathematical theory.

Time constant.	Min^{n}.value.	Max^{n}.value.
$T_n = n\sqrt{C_1 + C_1'}$.	4·7 μ secs.	8·1 μ secs.
$T_\sigma = \frac{4 - C_1 C_1'}{(C_1 + C_1')}$	0·6 μ secs.	1·8 μ secs.
$T_s = C_s' R_s'$	0·5 μ secs.	25 μ secs.

T_σ is always less than T_n. The condition specified in equ^{n}. 2.11) holds.

T_s covers a wider range of values than T_n. From a study of the waveforms deduced for the capacitance and serbes resistance

network,(cf.Fig.39), it would appear that if $\tau_s \gg \tau_h$, $\phi_g' \propto e^{-t/\tau_s}$ would predominate. The final waveform would then lie completely above the horizontal axis.

V. A QUALITATIVE EXPERIMENTAL STUDY OF THE RESPONSE OF VARIOUS ELECTRICAL NETWORKS TO AN APPLIED PULSE.

Using the circuit shown in Fig.45), a study was made of the response of the electrical networks discussed above to an applied pulse.

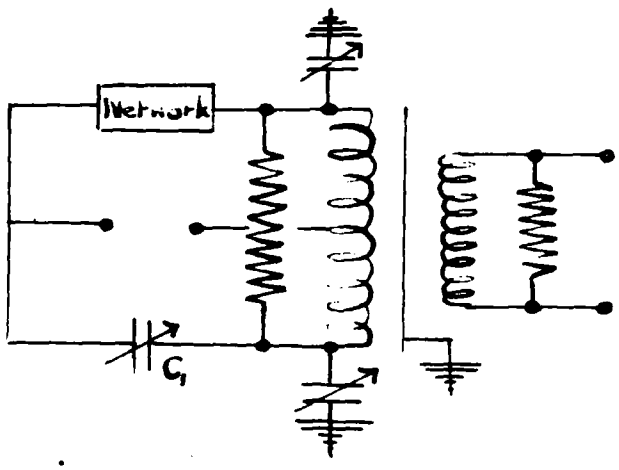

Fig. 45). Bridge circuit used for qualitative tests on various networks.

1).Capacitance,C1.(cf.Fig.46). With pure capacitive arms the output waveform at balance was approximately a straight line as predicted by the theory. The small initial spikes indicate that a certain amount of loss was inherent in the circuit, but this was comparatively negligible. Off-balance

$C_1 \lessgtr C_1'$, the waveform was as predicted apart from the superposition of the effects due to this inherent loss.

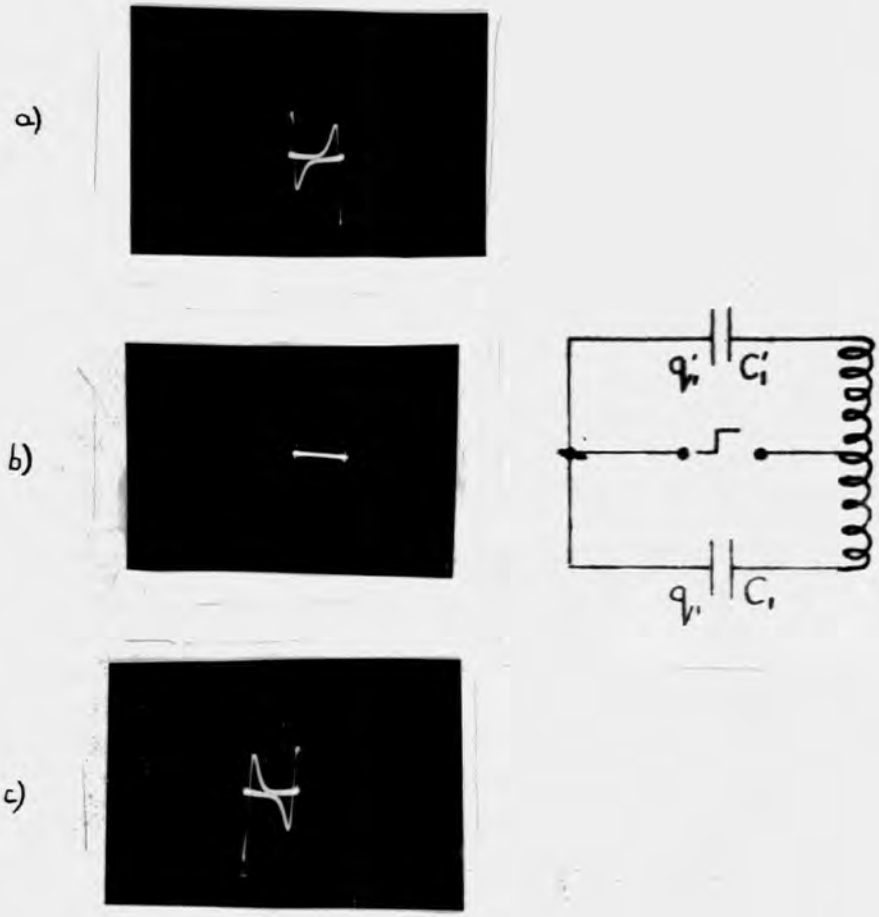

Fig.46). Output waveforms for pure capacitive arms:-
a) $C_1 < C_1'$,
b) $C_1 = C_1'$,
c) $C_1 > C_1'$.

Using the calibration described in Chapter III, it was observed that the time constant of the initial spike was of the order of 10 μ-secs. for unbalanced capacitive arms. According to the mathematical theory this time constant should approximately equal T_n, which is estimated at 10 μ-secs.

indicating good agreement between experiment and theory. The ballistic balance indication for pure capacitive arms was very critical.

ii). Capacitance and series resistance, C_1' and R_1', (cf. Fig. 47).

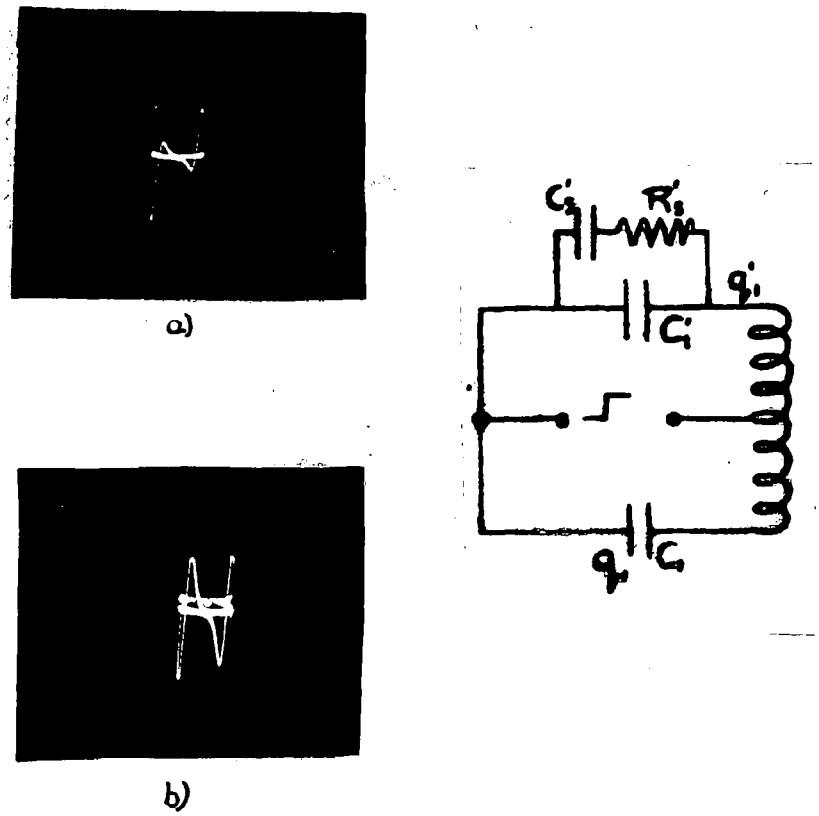

Fig. 47). Output waveforms for network of capacitance and series resistance:- a), $C_1 = C_1' + C_1'$,
b), $C_1 = C_1'$.

When this network is placed in parallel with the capacitance C_1' in the comparison arm of the bridge, and balanced against the capacitance C_1 in the measuring arm of the bridge,

(i.e., $C_1 = C_1' + C_2'$), the distinguishing feature of the output waveform was the presence of the sharp initial spike at balance. The time constant of this initial spike was of the order of $\frac{2}{3}$ or 3 μ-secs., appreciably smaller than was observed for unbalanced capacitive arms. This result was in agreement with mathematical prediction, and a series of tests were carried out to prove that the initial spike was a characteristic of the type of network, and did not arise from extraneous causes. These tests will be described later.

It was observed that as C_1 was decreased from the value $C_1'+C_2'$, the initial spike gradually decreased to zero.

c). Resistance, R_p, in parallel with capacitance, C_1', (cf. Fig. 48)
It was observed that as C_1 was varied through C_1' the waveform for capacitance and parallel resistance passed through the transitions predicted by the mathematical theory. When $C_1 = C_1'$ no initial spike was observed. The ballistic balance indication was far from critical for this type of network.

d). Combination of series resistance and capacitance and parallel resistance and capacitance, ($C_2'R_2'$ in parallel with C_1' and R_1'), (cf. Fig. 49).

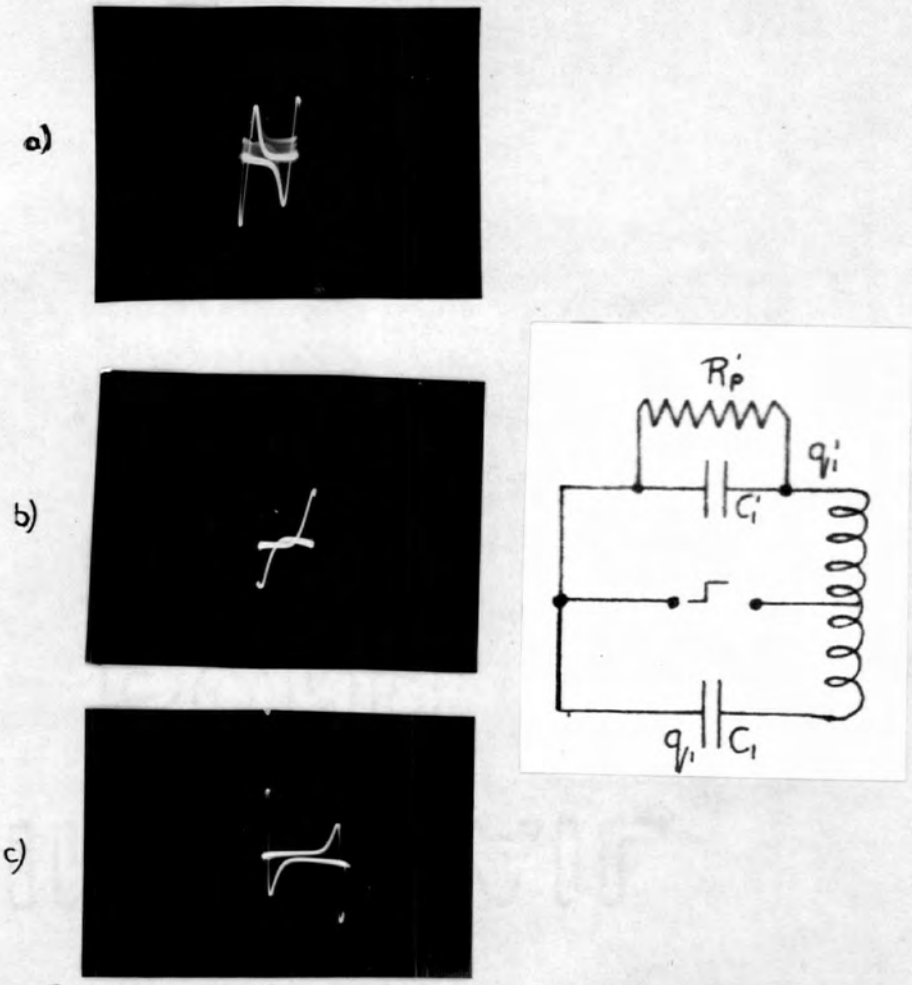

Fig.48). Output waveforms for networksof capacitance and parallel resistance:- a) $C_1 < C_1'$, b) $C_1 = C_1'$, c) $C_1 > C_1'$.

When $C_1 = C_1'$ the characteristic festure of both series resistance and capacitance, and parallel resistance and capacitance were exhibited by this waveform, i.e., the sharp initial spike followed by a slow decay. It was concluded from this that, in accordance with the mathematical theory the series resistance capacitance branch gave rise to the

sharp initial spike, and the parallel resistance branch to a slow decay towards the end of the trace.

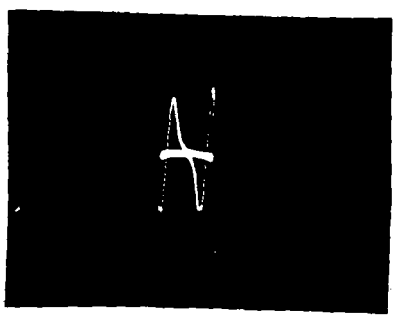

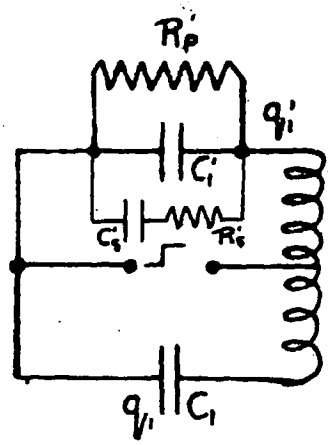

Fig.49). Output waveforms for network of series resistance and capacitance across parallel resistance and capacitance:- a) $C_1 = C_1' + C_1'$,
~~b) $C_1 = C_1'$.~~

Tests on the origin of the initial spike in the output waveform for the capacitance and series resistance network. In order to investigate further the hypothesis that the initial spike arising in the output waveform for the capacitance and series

resistance network was a characteristic of that network as opposed to the parallel resistance capacitance network, and also that it did not arise wholly or partly from extraneous causes, the following tests were carried out:-

i) A circuit was set up by means of which it was possible to vary the relative amounts of series resistance in the two bridge arms, the total resistance being kept constant,(cf.Fig.50) As R_s was increased from zero through $R_g = R_g$ to a maximum, it was observed that the initial spike passed from a maximum in one direction through zero to a maximum in the opposite direction.

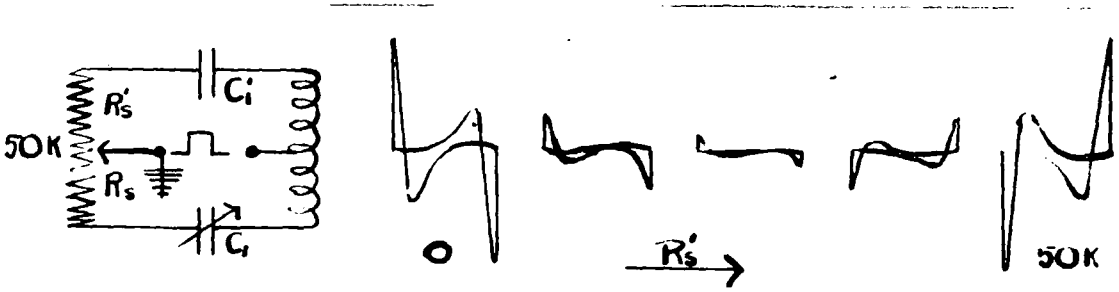

Fig. 50). Bridge output waveforms on varying the relative amounts of series resistance in the bridge arms.

In contrast to this the corresponding circuit for parallel resistance at no time exhibited an initial spike,(cf.Fig.51). This test indicated that the initial spike was a characteristic of the capacitance and series resistanee network as distinct from the parallel resistance network only.

ii) To ensure that the initial spike was not arising wholly or in part from any special condition, not visible on the cathode-ray oscillograph, at the corner of the applied pulse, the pulse was blunted slightly by placing small r resistances in the positive supply lead to the bridge. It was observed that this did not affect the initial spike apart from the rest of the trace. It was therefore assumed that the initial spike was a characteristic of the capacitance and series resistance type of network, and that its existence was not dependent on any special condition existing at the corner of the applied pulse.

The qualitative study of the response of the simple electric networks indicated above, to an applied pulse carried out using the differential transformer bridge, revealed the characteristic features of those responses. These agreed well with mathematical predictions, and the results indicated the ability of the instrument to differentiate between the different types of network.

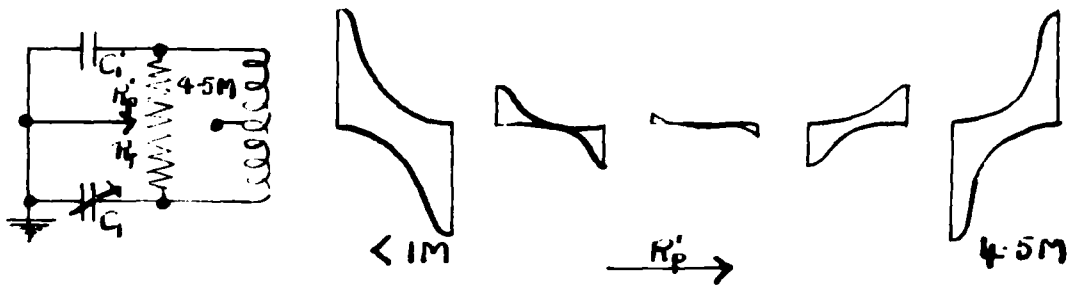

Fig.51). Bridge output waveforms on varying the relative amounts of parallel resistance in the bridge arms.

VI. A QUALITATIVE STUDY OF THE RESPONSE OF VARIOUS DIELECTRICS TO AN APPLIED PULSE.

Having investigated the response of some simple electrical networks to an applied pulse, and observed their characteristic features, the next stage was a study of the response of certain dielectrics. By identifying the main features of the output waveform for a given dielectric with the characteristics of one or more of the networks discussed above, it was hoped to build up an electrical network equivalent to the dielectric. It was fully realised that such a network would be neither a complete nor absolute representation of the dielectric, but would merely serve as a device in terms of which certain properties of the dielectric could be measured.

The dielectric chosen for initial investigations was glass. The structure of glass has been studied extensively by X-ray and other methods. In general it appears to consist of an extended network of atoms showing only short distance order ordering. This network is made up of small highly charged positive ions, such as silicon, boron, etc., each surrounded by several oxygen ions to form a lattice. The interstices which necessarily occur, are often occupied wholly or partly by metallic ions such as sodium, potassium, etc. The modern picture of the mechanism of conduction and relaxation

in glasses, based on the theory developed by Frohlich[10] and others, and put forward recently by Gevers and Du Pre[16], is as follows:- the metallic ions are in continual thermal vibration around an equilibrium position. In order to jump from one interstice to another, the ion must gain sufficient energy to overcome the potential barrier surrounding it. In the absence of an external field, any such jumps which do take place are completely random in direction. Hence the resultant effect is zero. Upon the application of an external electric field, however, the ions tend to move more in one direction than the other, thus giving rise to a conduction current. The probability of an ion making a jump depends on the strength of the applied field, and also on the depth and steepness of the surrounding potential barrier. The equilibrium position of an ion depends also on the applied field and varies with the applied field. Small deformations of the network surrounding the ion occur, and 'after effects' occur giving rise to a series of excitation energies, and hence a series of relaxation times. These losses are known to occur at comparatively low frequencies, probably within the frequency range of the instrument described above. This factor, combined with the relative ease of obtaining suitable specimens in a convenient form, determined the choice of glass as the dielectric on which initial observations were made.

The bridge circuit was adapted for the study of the response of actual dielectrics to an applied pulse by replacing the network in the comparison arm of the bridge by a condenser made up of the dielectric under investigation. For the initial investigations the glass dielectric was in the form of a test tube. The electrodes were of mercury with which the tube was filled and surrounded,(cf.Fig.52).

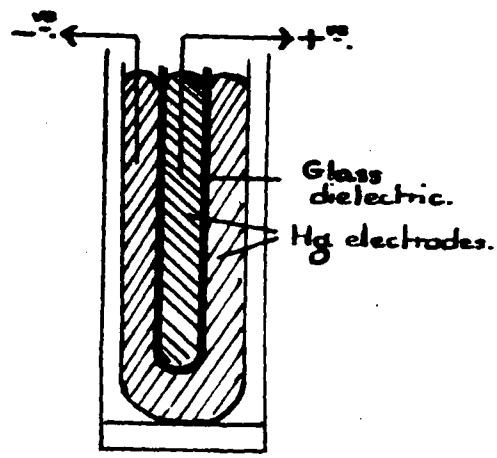

Fig.52) Form of lossy condenser used for qualitative tests.

Specimens of Hysil and of Soda glass were first investigated Comparing the responses of these with the responses obtained of various networks, it was observed that both Hysil and Soda glass exhibited the initial spike characteristic of the series resistance capacitance network. Also it appeared that whereas with Soda glass the characteristics of heavy conduction

were exhibited, Hysil glass showed comparatively little evidence of conduction,(cf.Fig.53). These results were in general accordance with other experimental evidence[12].

a) b)

Fig.53). Bridge output waveforms for:- a) Soda glass, b) Hysil glass.

In all, the following glasses were investigated:-

Type of glass.	Composition.	Form of specimen.	Supplied by:-
i) Soda glass, (XS).	SiO_2 71%, Na_2O 17% CaO 6.7%, MgO 3.2% $Al_2O_3 + Fe_2O_3$ 0.5%	Tube, (300$\mu\mu$F)	Lemington Glass works
ii) Hysil glass	SiO_2 80.4% Na_2O 4.2% CaO 0.3% B_2O_3 12.4% Al_2O_3 2.7%	Tube, (300$\mu\mu$F)	Science Labs.
iii) Pyrex Brand glass.	SiO_2 80.8%, Na_2O 4.6% As_2O_3 0.2%, B_2O_3 3.2% Al_2O_3 1.9%,	Tube, (300$\mu\mu$F)	Wear Glass works.
iv) Borosilicate glass(W1)	SiO_2 78.5%, B_2O_3 15.5% Na_2O 3.5%, K_2O 2.5% $Al_2O_3 + Fe_2O_3$ 2.0% CaO 0.5%.	Tube, (300$\mu\mu$F)	Lemington Glass works

Table IV,(cont.).

Type of glass.	Composition.	Form of specimen.	Supplied by:-
v) Lead glass (L1).	SiO_2 56.5%, PbO 30.0% KO 7.0%, NaO 5.0% CaO 0.3%, MgO 0.1% BO_3 0.2%, $Al_2O_3 + Fe_2O_3$ 0.6%	Tube, (300$\mu\mu$F)	Lemington Glass works
vi) Photographic plate.		Plate, (30$\mu\mu$F).	Science Labs.

Table IV. Details of glasses whose response waveforms were investigated.

A study of the response waveforms for these glasses led to the following conclusions,(cf.Fig.54). Pyrex Brand glass and Borosilicate (W1) glass exhibited similar features to Hysil glass in varying degrees. Lead glass,(L1), was practically loss-free. Soda glass,(X8), exhibited heavy conductance losses in addition to the non-instantaneous losses represented by the initial spike. Comparison of the results for photographic plate with the other glass samples is difficult due to the great difference in the relative capacitances involved. Whereas the glass specimens i) to v) were tubular in form, and the corresponding condensers were approximately 300$\mu\mu$F, the photographic plate sample was used in a parallel plate condenser whose capacitance was 30 $\mu\mu$F. However it would appear that the losses are great for photographic plate. The electrodes of the parallel plate

condenser consisted of two circular metal plates whose surfaces were accurately ground.

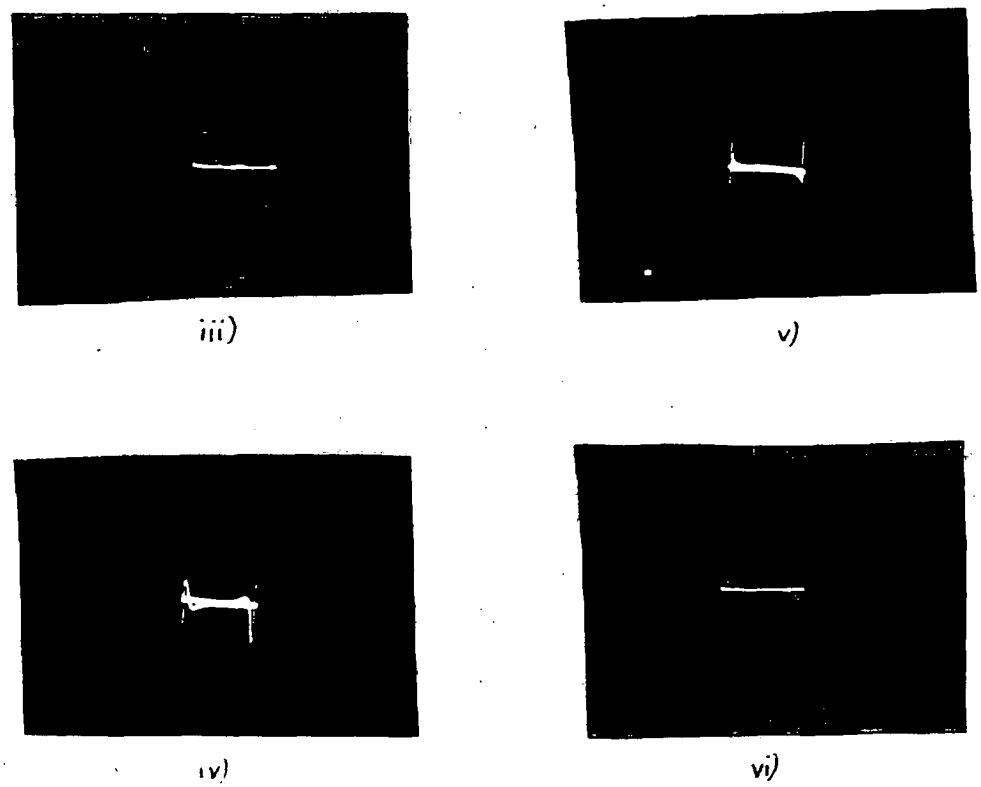

Fig.54). Response waveforms for:-
i) Soda glass } (cf. Fig 53) iv) Borosilicate glass (W1)
ii) Hysil glass } v) Lead glass (L1)
iii) Pyrex Brand glass vi) Photographic plate.

The parallel plate condenser described above provided a simple and convenient means of making rapid observations on the dielectric loss of various substances obtainable in sheet form. By a comparison of the output waveforms it was possible to estimate the relative amounts of loss. As an example of this, the substances indicated in Table V were investigated.

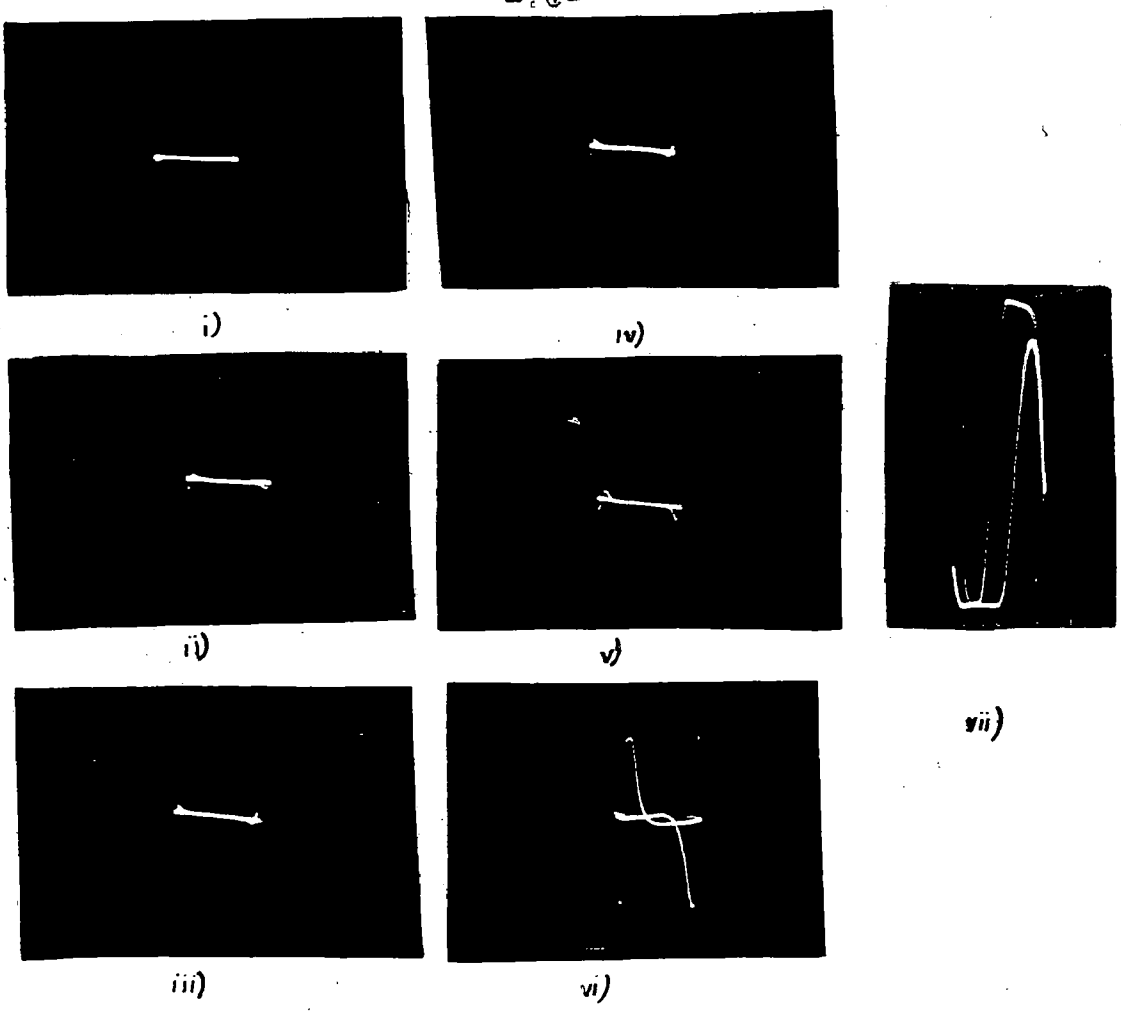

Capacitance = 30μμF.

	Material.	Comments on loss.
i)	Polythene.	Negligible.
ii)	Mica.	Very small.
iii)	Perspex.	Very small.
iv)	Ebonite.	Very small.
v)	Paxolin.	Small.
vi)	Asbestos and cement compound.	Large, conduction and non-instantaneous losses.
vii)	Ice.	Extremely large conduction and non-instantaneous losses.

Table V. Output waveforms for various materials.

VII. A QUANTITATIVE STUDY OF THE RESPONSE OF VARIOUS ELECTRICAL NETWORKS TO AN APPLIED PULSE.

It was shown in the preceeding chapter that a striking similarity existed between the responses to an applied pulse of certain dielectrics and electrical networks respectively. The possibility thus arose of measuring the properties of such a dielectric in terms of an equivalent network of linear circuit elements, using the apparatus which has been developed. In order to be able to do this with confidence, it was necessary to prove the ability of the instrument to analyse precisely the networks discussed in the previous chapter. The bridge circuit used for this purpose is shown in Fig.55). All stray capacitances to earth and other possible sources of error were reduced to a minimum as described in Chapter III.

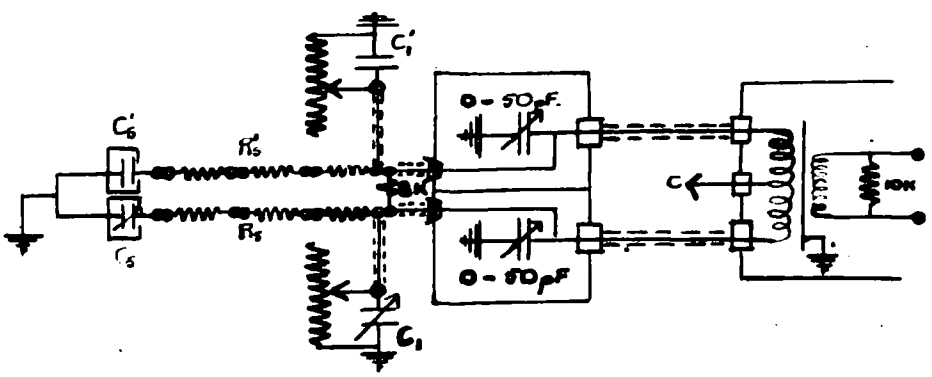

Fig.55). Bridge circuit used for quantitative analysis of various electrical networks.

Analysis of networks. [cf. Fold-out diagram, p.186]

i) Capacitance. For pure capacitive bridge arms, ($R_1 R_1' C_1 C_1' R_1 R_1'$ disconnected) the method of analysis was as follows:-

a) The differential transformer secondary was adjusted with respect to the primary as described in Chapter III, to reduce the effects of inherent strays in the circuit to a minimum.

b) Applying a sinusoidal input to the bridge C_1 was adjusted for minimum output current using the ballistic indicating circuit described in Chapter III. Under these conditions the impedance moduli of the two bridge arms were equal and $C_1 = C_1'$.

The range of values for C_1 and C_1' was from 30 to 300 $\mu\mu$F. The error in C_1 for a given reading of C_1' was less than 1 $\mu\mu$F over the entire capacitance range.

ii) Capacitance and series resistance. The outstanding feature of the response curve for the series-resistance capacitance network when balanced against a pure capacitance($C_1 = C_1' + C_1'$), was the initial spike of comparatively large amplitude and small time constant. Theoretical predictions indicated that when C_1 was reduced to a value C_1' the initial spike would decrease to zero. Hence it would appear that the value of C_1 obtained on eliminating the initial spike should equal C_1' whilst the difference between that value and the value of C_1 giving ballistic balance (i.e. $C_1 = C_1' + C_1'$,provided R_1' is small) should be a measure of C_1'. The instrument should

therefore be capable of separating out the percentage of the total capacitance associated with series resistance. In order to test this, a series of measurements was undertaken on series-resistance capacitance networks of known components over a wide range of values. The method of analysis was as follows:

a) The differential transformer secondary was adjusted with respect to the primary to reduce the effects of inherent strays in the circuit to a minimum.

b) With C_s, R_s and R_s' disconnected, R_s short-circuited, C_1 was adjusted for ballistic balance of the bridge arms using sinusoidal bridge input. Then $C_1 = C_1' + C_1''$.

c) Applying square-wave bridge input, C_1 was reduced until the initial spike decreased to zero. Then $C_1 = C_1'$.

d) Connecting in C_s, R_s short-circuited, and applying sinusoidal bridge input, C_s was adjusted for ballistic indication of balance. Then $C_1 = C_1''$, and $C_s = C_s'$.

e) Applying the square-wave input to the bridge, R_s was adjusted for straight line output wave-form, giving $R_s = R_s'$.

The accuracy with which the series resistance capacitance network could be measured was represented graphically by plotting the error in C_s, $(C_s' - C_s)$, against the time constant $C_s'R_s'$. A range of time constants from $C_s'R_s' = 2\mu$-secs, to $C_s'R_s' = 25\mu$-secs, was covered. The error in C_s' over that range of time constants never exceeded $\pm 2\mu\mu F$, and the distribution of error ~~appeared to be quite random~~ was not systematic. It was later ascertained

that with care time constants as low as 1 μ-sec. could be dealt with satisfactorily. A Table and graph of results is given in Fig.56.

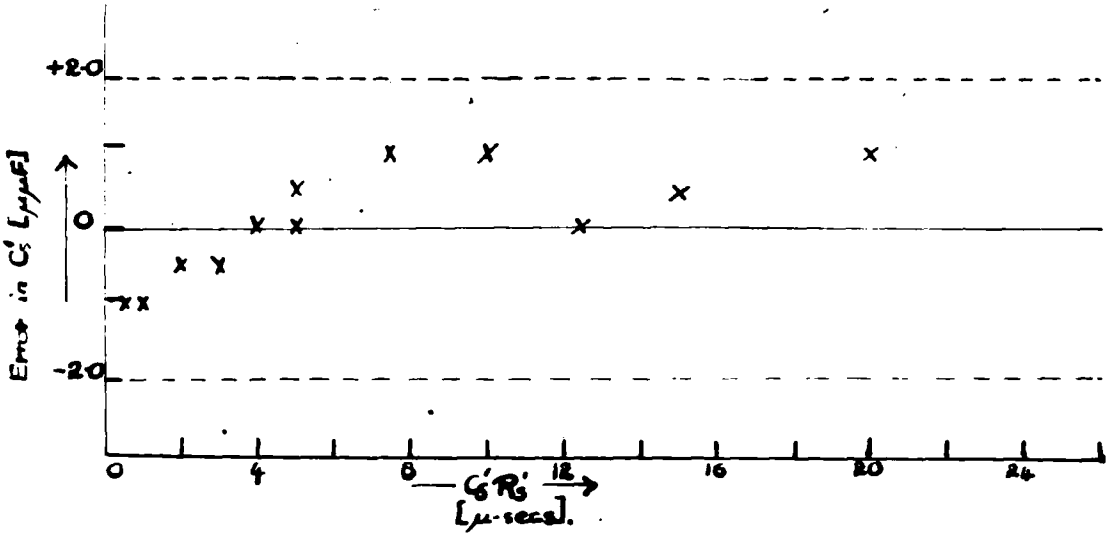

$C_s'R_s'$ (μ-secs.).	Error in C_s' ($\mu\mu$F)
1.0	-1.0
2.0	-1.0
3.0	-0.5
4.0	-0.5
5.0	0
6.0	0
7.0	+0.5
8.0	+1.0
10.0	+1.0
12.5	0
15.5	+0.5
20.0	+1.0

Fig.56). Variation of error in C_s' with time constant $C_s'R_s'$.

In general, the adjustment of R_s could be obtained within $\pm 10K$.

From these tests it was concluded that the instrument was capable of analysing a series resistance capacitance network over the range of values indicated above, within reasonable limits of accuracy.

iii) Capacitance and parallel resistance. (C_s and C_s' disconnected). It has already been observed that a network involving parallel resistance exhibits a relatively slow decay towards the end of the response curve. The smaller the parallel resistance the slower the decay, and the greater the current through the differential transformer secondary at ballistic balance.

In order to adjust the parallel resistance in the measuring arm of the bridge, (R_p), to balance that in the comparison arm of the bridge, (R_p'), a sinusoidal input was applied to the bridge. Using the ballistic balance indicator to observe the current through the differential transformer secondary R_p was adjusted until minimum secondary current was observed This method proved satisfactory for values of R_p' up to about 15M. Above this value R_p' was considered infinite from the point of view of this apparatus.

The adjustment of the parallel resistance was necessarily followed by a readjustment of the capacitive balance, again, using the ballistic balance indicator. As R_p' decreases the apparent value of C_i' tends to infinity, and the readjustment of the capacitive balance after balancing out R_p' becomes increasingly important.

iv) Combination of series resistance and capacitance and parallel resistance and capacitance. It was found possible to analyse this type of network satisfactorily by combining the methods used for the series resistance capacitance network and the parallel resistance capacitance network, as described above, [cf. pp 101 and 103]. The procedure was as follows:-

a) Effects due to inherent strays were eliminated as before.

b) The parallel resistance component was balanced out using the ballistic balance indicator.

c) The fraction of the total capacitance associated with series resistance was separated out by means of observations on the initial spike of the waveform.

d) The adjustment of the series resistance was made from observation on the waveform as a whole.

A series of tests carried out on the analysis of this network indicated that the instrument was capable of accurate analysis over the following rangesof values:-

C_i' = 100 to 300 $\mu\mu$F, C_s' = 5 to 50 $\mu\mu$F, R_s' = 100K to 500K,

R_p' = 1M to 15 M (see Table VI)

Table VI

Correct values of components of network.				Measured values of components of networks.			
C_1'	C_2'	R_1'	R_2'	C_1'	C_2'	R_1'	R_2'
200 μμF.	50 μμF.	200K.	11M.	201.5μμF.	51.5μμF.	185K.	11M.
"	40 μμF.	"	"	201.5μμF.	41.0μμF.	180K.	11M.
"	30 μμF.	"	"	201.0μμF.	31.0μμF.	180K.	11M.
"	20 μμF.	"	"	202.0μμF.	21.0μμF.	220K.	11M.
300 μμF.	50 μμF.	150K.	11M.	302.0μμF.	51.0μμF	240K.	11M.
"	40 μμF.	"	"	302.5μμF	40.5μμF	240K.	11M.
"	30 μμF.	"	"	302.5μμF	31.0μμF	240K.	11M.
"	20 μμF.	"	"	302.0μμF	20.0μμF	250K.	11M.
500 μμF	50 μμ F.	100K.	11M	500.5μμF	49.0 μμF	110K.	11M.
" μμF.	40 μμ F	"	"	500.5μμF	39.5μμF	110K	11M
" μμ F.	30 μμ F	"	"	500.5μμF	29.5μμ F	100K	11M
" μμ F.	20 μμF	"	"	500.0μμF	18.5μμ F	100K	11M
200 μμ F.	50 μμF.	500K.	14M	201.0μμF	50.0μμF	490K	15M.
" μμ F.	40 μμ F	"	"	201.5μμ F	38.5μμF	500K	14M.
" μμ F.	30 μμF	"	"	201.5μμF	29.5μμF	500K	15M.
" μμ F.	20 μμF	"	"	200.5μμ F	19.5μμF	520K	15M.
300 μμF.	50 μμ F.	330K.	1M	301.5μμF	51.5μμF	260K	12M
" μμ F.	40 μμ F.	"	"	300.0μμ F	39.0μμF	270K	12M
" μμ F.	30 μμ F.	"	"	301.0μμF	31.0μμF	270K	12M
" μμ F.	20 μμF	"	"	302.0μμ F	20.0μμF	280K	12M

According to the mathematical theory, the main factor determining the working range of the instrument was the time constant $T_n = n\sqrt{C_1 + C_2}$, (cf. Ch. IV). If T_n is much smaller than the time constant, $T_s = C_s' R_s'$ of the series resistance capacitance branch of the network under investigation, the mathematical theory indicates that the instrument is unable to separate out the capacitance associated with series resistance. In practice, maximum value of T_s was 25 μ-secs., as compared with T_n = 8μsecs. In order to extend the working range of the instrument to larger values of T_s, it would be necessary to use a differential transformer of larger primary inductance thus increasing T_n. At the other end of the scale, the smallest time constant with which the instrument could deal satisfactorily was 1 μ sec. According to the mathematical theory it would appear that the limit was set in this case by the rate of rise of the pulse edge, i.e., by the impedance of the generator, increasing the rate of rise of the pulse edge, the possibility arises of extending the working range of the instrument to cover time constants less than 1 μ sec.

VIII. MEASUREMENTS ON THE DIELECTRIC PROPERTIES OF PYREX GLASS, SODA GLASS, AND ICE.

1) Pyrex glass.

It has already been observed that the response curves for glass are similar to that for the combined series-resistance capacitance, and parallel-resistance capacitance network. Having ascertained that the instrument was able to analyse such a network accurately within certain limits, the stage was reached when it was feasible to measure the properties of glass in terms of this equivalent network. By so doing it was hoped that further information would be obtained regarding the effect on the dielectric properties , of the constitution and previous history of the specimen investigated. In the past the measurements made on the dielectric properties of glass have in general been characterised by the lack of such information. What little evidence there is, leads to the conclusion that these two factors are of the greatest importance in the study of the dielectric properties of glass, and results which do not specify these conditions are comparatively worthless. It was therefore decided to investigate first the effect of the previous history on the dielectric properties of a glass whose constitution is kept fixed.

Glass is characterised by the fact that upon cooling

from the liquid state it solidifies gradually without passing through a definite phase transition as do other solids. The resultant material possesses features of both liquids and solids. The cooling down process is of the greatest importance in the history of the glass since on this process depends the structure of the glass. The more gradual the cooling down process the more chance the atoms have of regrouping themselves and in some cases , when the liquid is cooled down very slowly crystallisation occurs. Usually the glass is allowed to anneal i.e. cool down relatively slowly. No accurate temperature control is maintained during the annealing process. When a glass is not annealed strains are set up in the glass and, unless the glass is a hard glass, such as Hysil or Pyrex glass the glass will usually crack. Obviously then the annealing processes can have considerable bearing on the dielectric properties of the glass. A second factor of major importance is the condition of the surface of the glass. Surface films caused by moisture and impurities can give rise to heavy surface conductivity which can completely mask the dielectric properties of the glass itself.

Measurements were made on samples of Pyrex glass, supplied for the purpose by the Wearside Glass Works, Sunderland. These samples had been stabilised at given temperatures in the temperature range 480 to 800°C., and then cooled rapidly in still air at room temperature. The results of these measurements

were then compared with the results for an ordinarily annealed sample of Pyrex glass. The samples used were tubular in form, 17 cms. long, with an outer diameter of 1.7 cms., and a wall thickness of about 1 mm.

Form of condenser used for quantitative measurements on glass.

The type of condenser used in the initial stages of this work to study the response curves for various glass dielectrics,(cf.Ch.VI)., was not suitable for the application of precise measurements in that the closing of one end of the tube to form a test tube is not a controllable process from the point of view of temperature. Some attention was therefore devoted to the development and construction of a condenser of more suitable form. The most usual form of condenser used in the measurement of the electrical properties of glass consists of a sheet of the glass floating in mercury with a pool of mercury on top(cf.Fig.57).[13].

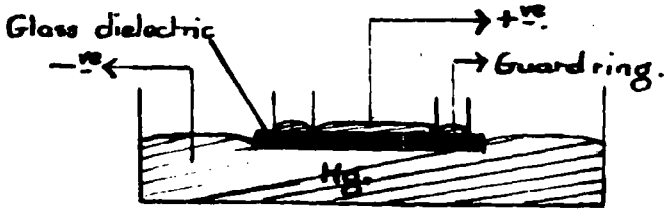

Fig.57) Usual form of condenser for studying the dielectric properties of glass.

This method would, however, necessitate the use of a guard ring of mercury on top of the glass sheet. The proposed method of measurement was not easily adaptable to a guard ring system, however. Also, for the capacitance required, (at least 100$\mu\mu$F) such a condenser would be unduly large and clumsy in form. With tubular glass specimens, however, capacitances up to 300$\mu\mu$F could be obtained with comparative ease, while the use of a guard ring could be effectively replaced by a measurement of the 'end capacitance',i.e., the apparent capacitance for no mercury inside the tube. The form of condenser finally developed is shown in Fig.58)a

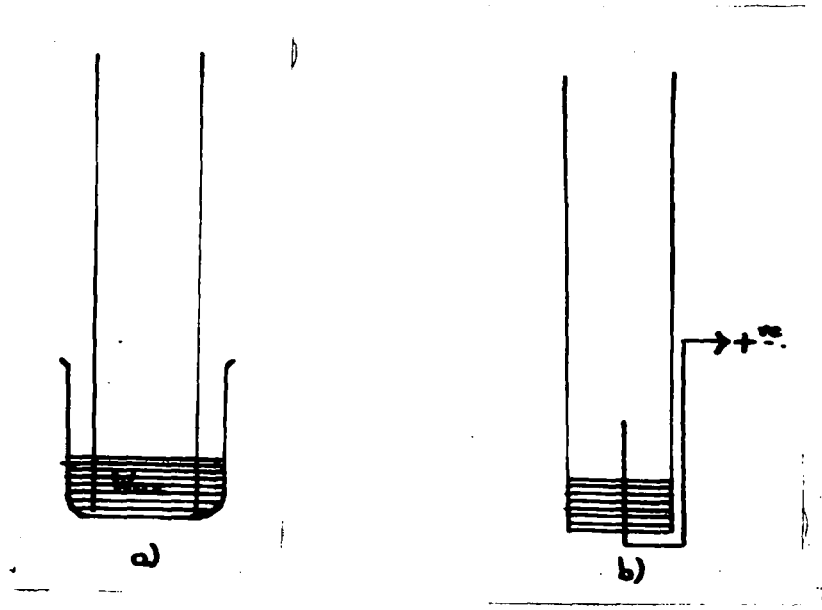

Fig. 58) Construction of condenser for studying the dielectric properties of glass.
(See also, next page).

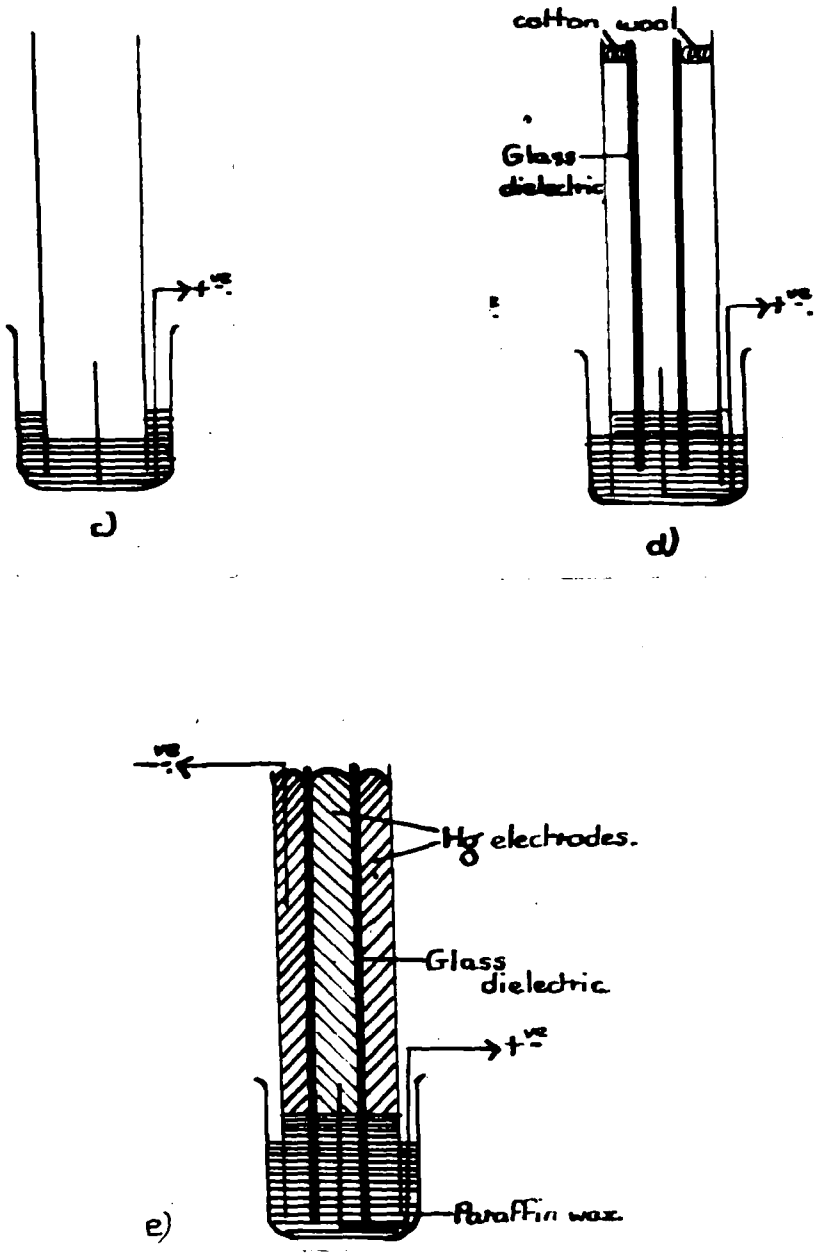

Fig.33,(contd.). Construction of condenser for studying the dielectric properties of glass. (See also, previous page).

pierced by the positive contact wire, and the tube replaced in comparatively cool molten wax,(cf.Fig.58b and58c). The wax was then allowed to cool round the tube, thus fixing it in place. More molten wax was then placed in the outer tube, and the glass sample introduced so that it was surrounded by solidifying wax, and itself surrounded the positive contact wire. Until solidification of the wax took place, the glass sample was held in position by means of pads of cotton wool between it and the outer tube,(cf.Fig.58d). When solidification was complete the cotton wool was removed and mercury placed in the inner and outer tubes.

The use of mercury electrodes is open to some criticism there being the possibility of the formation of inter-face films and air bubbles. Opinion on this matter varies considerably.[14]

Method of measurement of Pyrex glass samples. The bridge arms were adapted for the measurement of dielectrics in terms of an equivalent network as shown in Fig.59). The method of measurement was as follows. Using the condenser constructed as described above, known masses of mercury were placed in the inner tube, and the corresponding total capacitances measured by means of the ballistic indicating circuit. It was found that for Pyrex, the equivalent parallel resistance was greater than 15M. It was therefore assumed to be infinite, and the ballistic balance point obtained directly as described for the

series resistance capacitance network. From these measurements a graph was plotted showing the variation of capacitance with mass of mercury, and the 'end capacitance' obtained by extrapolation to zero mass of mercury. A typical graph is shown in Fig.60).

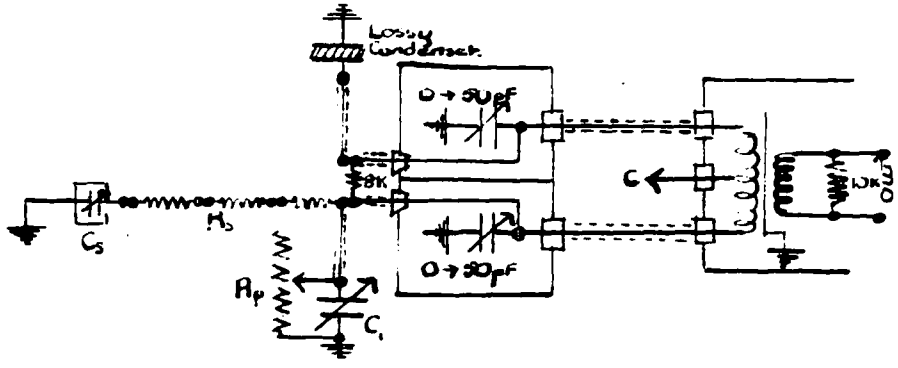

Fig. 59). Bridge circuit adapted for measurement of dielectric properties.

When the total capacitance of the lossy condenser became such that the capacitance associated with series resistance was appreciable, ($> 5\mu\mu F$), a complete analysis of the dielectric was made in terms of the equivalent network. The method of measurement was exactly as for the analysis of a network, (cf. Ch. VII, p. 104). As was expected a perfect balance could not be obtained. The measurement of C_1 and C_s were critical. Adjusting R_s however did not reduce the waveform to a straight line as in the analysis of the electric networks described previously. As R_s was increased from zero, the initial spike decreased to a minimum after which further increase of R_s led to the appearance

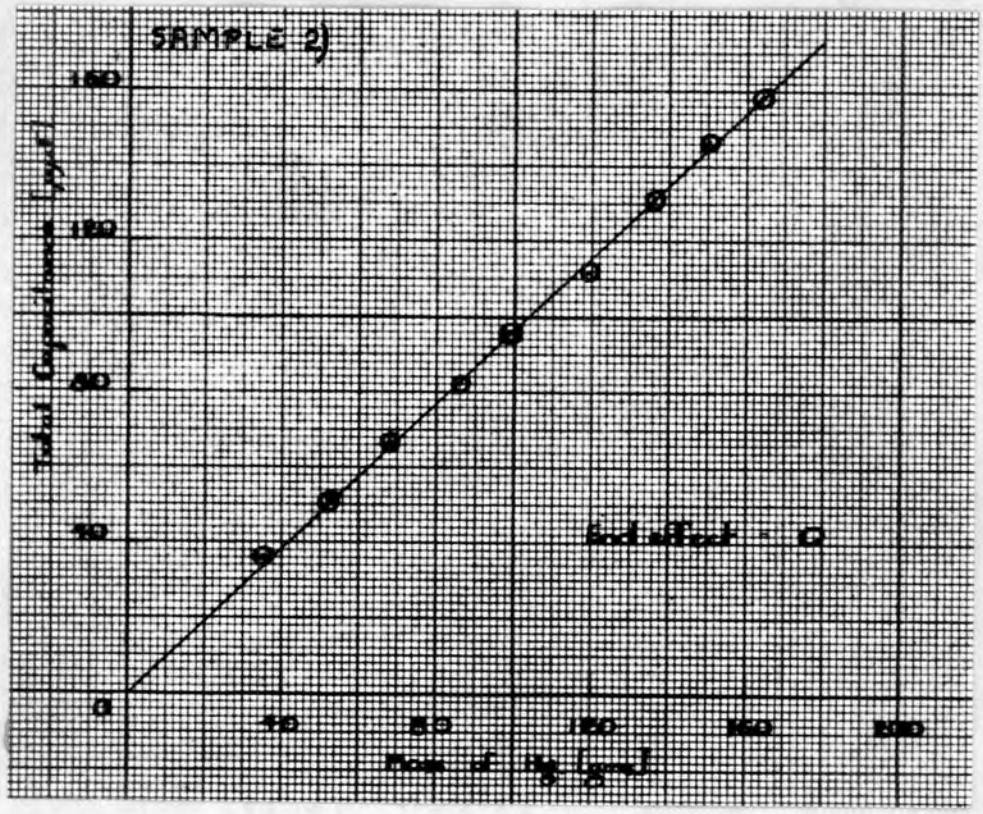

Weight of Hg in inner tube, (gms).	Total capacitance, ($\mu\mu$F).
33.1	36.0
52.2	51.0
67.7	66.5
82.7	82.0
98.9	96.0
118.8	111.5
133.8	131.0
150.2	146.5
163.6	158.5

Fig.69). Typical determination of end capacitance for Pyrex sample.

of a spike in the opposite direction,(cf.Fig.61) The value of R_s for which the original initial spike became a minimum was recorded.

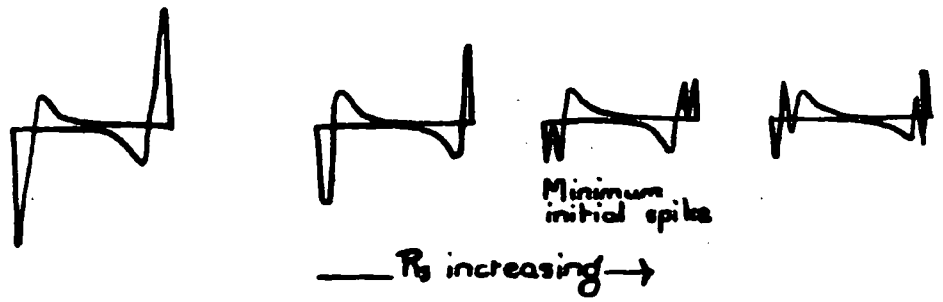

Fig.61) Output waveforms for dielectric on varying R_s of equivalent network.

The imperfect balance obtained under these conditions was an indication of the incompleteness of the equivalence of the network.

As more mercury was added to the inner column, the total capacitance of the lossy condenser increased. Further analyses of the dielectric were made at suitable intervals. Making due allowance for the end capacitance, the percentage of the total capacitance associated with series resistance and the corresponding time constant were calculated for each analysis. An average of the results was then taken. A typical result is shown in Fig.62).

Photo

a) b)

Determination of equivalent network for Pyrex sample.

C_1 ($\mu\mu F$)	C_s ($\mu\mu F$)	R_s (K)	$C_s / C_1 + C_s$ (%)	$C_s R_s$ (μ-secs.).
181.9	4.75	638	2.6	3.0
204.0	5.0	641	2.4	3.2
231.5	6.0	612	2.5	3.7
249.9	6.75	550	2.6	3.9
279.0	8.0	546	2.5	4.4
297.5	9.0	522	2.9	4.7

For this sample, average $C_s / C_1 + C_s$ = 2.6%.
average $C_s R_s$ = 3.8 μ-secs.

c)

Fig.62). Typical result for Pyrex specimen:-
a) Waveform at initial balance,
b) Waveform at final balance,
c) Table of results for typical specimen.

Results of measurements on Pyrex specimens of different temperatures of stabilisation. Full details of the measurements on the Pyrex glass specimens whose temperatures of stabilisation varied from 480 to 600°C, are given in Appendix II. The percentage of total capacitance associated with non-instantaneous losses, ($\frac{C_s}{C_1+C_s}$ %), and the associated time constant, ($C_s R_s$), were calculated for each specimen. Graphs were drawn of the variation of $\frac{C_s}{C_1+C_s}$ and $C_s R_s$ with temperature of stabilisation, (cf.Fig.63). The results indicated that $\frac{C_s}{C_1+C_s}$ increased with temperature of stabilisation to a constant value. The increase was approximately exponential in form. There was a corresponding tendency for the associated time constants to increase with temperature of stabilisation, also.

Measurements were also made on an ordinarily annealed specimen of Pyrex glass. Comparing the results with those obtaind obtained for the stabilised specimens, it was observed that the value of $\frac{C_s}{C_1+C_s}$ % for the annealed glass was equal to the constant value attained by the stabilised glasses of highest temperatures The associated time constant for the annealed specimen was comparitively low, (cf.Fig.63).

Explanation of results in terms of structure of glass specimens Without going very deeply at present into the question of the actual significance of the quantity measured, $\frac{C_s}{C_1+C_s}$ % , it is possible, assuming that $\frac{C_s}{C_1+C_s}$ is a measure of the dielectric

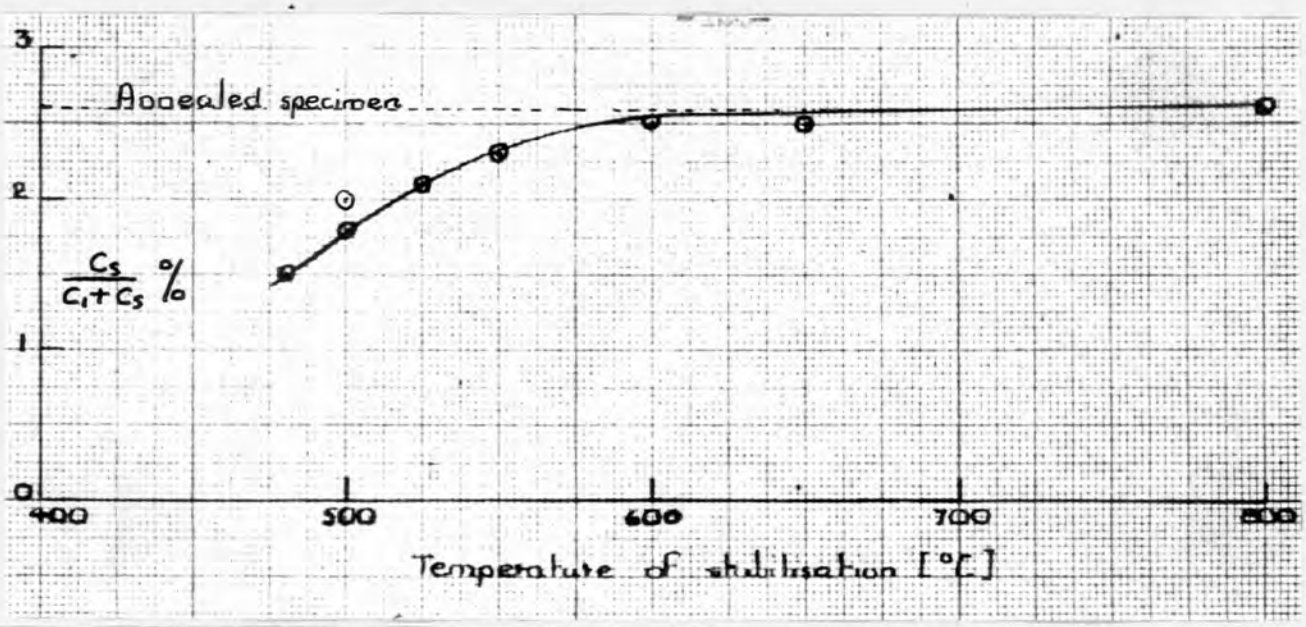

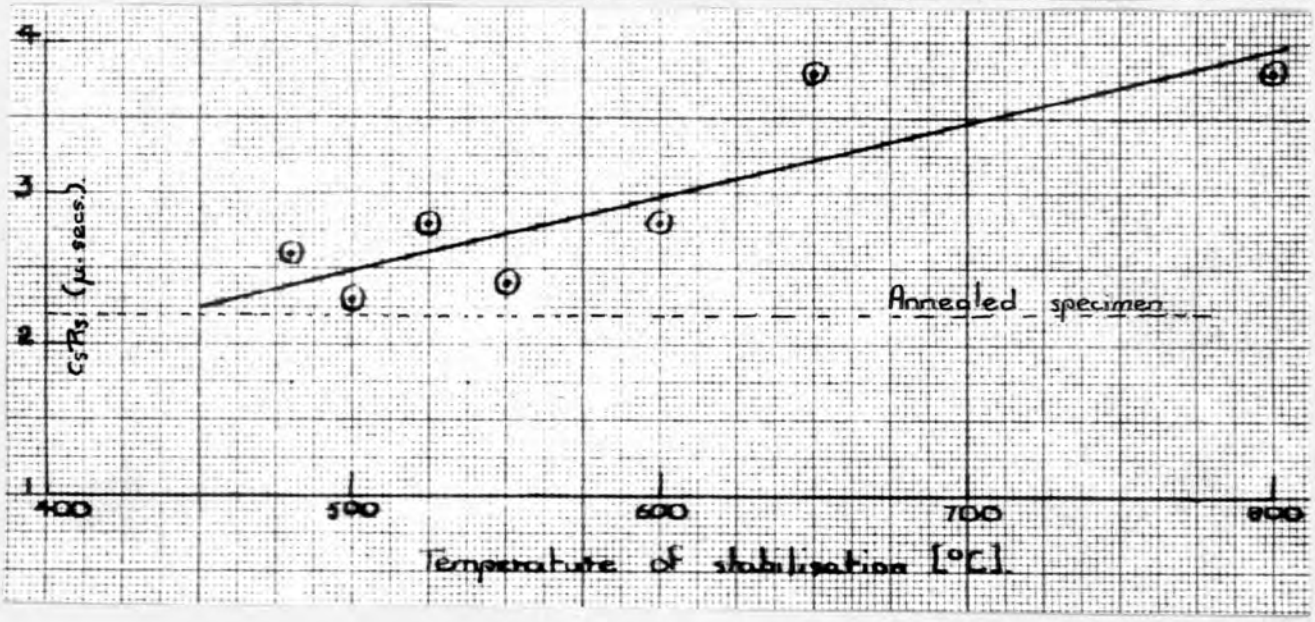

Fig.63). Variation of $C_s / C_i + C_s$, and $C_s R_s$ with temperature of stabilisation for Pyrex samples.

loss in the glass, to consider the above results in terms of the structure of the glass. The structure of glass has already been discussed,(cf.Ch.VI).Experimental observations on the rate of crystal growth in Pyrex glass indicate that the structure of Pyrex glass is in accordance with these views.[5]

Our results indicate that the dielectric loss increased with the temperature of stabilisation of the glass. It is suggested that the stabilisation process followed by rapid cooling results in a freezing in of the properties of the glass characteristic of the temperature of stabilisation of the glass Considering the glass in terms of the structure put forward in Ch.VI, the higher the temperature of the glass, the greater the tendency for continual modification of the potential field in the dielectric. Any such modification of the potential barrier surrounding the metallic ions is followed by a readjustment of the equilibrium positions of those ions.The response of the ions shows some inertia,and is not instantaneous. On the other hand, the higher the temperature the more quickly the ions would respond. This process gives rise to dielectric loss. It would be expected that the greater the temperature of stabilisation the greater the dielectric loss, but the smaller the associated time constant.In practice that loss appears to reach a constant value at the higher temperatures of stabilisation.This may indicate that for the highest temperatures of stabilisation, the time rate of stabilisation becomes so small that it is impossible to cool the glass rapidly enough to freeze

in the required properties. In this case the glass would actually stabilise at some unknown lower temperature, and the dielectric loss measured would be characteristic of that unknown temperature.

The annealed specimen on the other hand would presumably contain in varying degrees the characteristics of the complete temperature range. It would therefore be expected to exhibit maximum loss, which in fact it does. On this hypothesis, however, the time constant associated with the loss would cover a range of values corresponding to the temperature range covered, and it would be expected that the apparatus would analyse the maximum time constant involved. This does not agree with the results.

It can be seen from the above discourse that the results obtained for Pyrex glass can be explained only partially in terms of the structure of the glass. Before attempting to carry the matter further, it is necessary to consider the precise significance of the quantities measured, ($\frac{C_s}{C_1 r C_s}$ % and $C_s R_s$). This will be done in Chapter X of this thesis. [cf. Addenda, p. 183]

ii) Soda glass.

In order to compare the results for Pyrex with another type of glass, some measurements were carried out on an ordinarily annealed specimen of Soda glass. The Soda glass in question was supplied by the Lemington Glass Works. Its composition is given in Ch.VI, (cf. TableV).

The construction of the lossy condenser and the experimental method were exactly as described in the preceeding section, for the specimens of Pyrex. With Soda glass however the equivalent parallel resistance componentwas appreciable. As with the measurements carried out on networks involving parallel resistance, (cf. Ch.VII, p.103), the equivalent parallel resistance was adjusted for minimum bridge output current , using a sinusoidal input to the bridge and the ballistic balance indicator. However, whereas with the network analysis the equivalent parallel resistance was independent of the applied frequency, with Soda glass this was not so. There was considerable variation of the equivalent parallel resistance, and hence of the total capacitance also, with frequency. Using square wave input The measurement of the pure capacitive branch of the equivalent network, (C_1', from the disappearance of the initial spike on the output waveform), was definite. Measurements were made of the equivalent parallel resistance, R_p', and the total capacitance, ($C_1' + C_2'$), at a series of discrete frequencies covering a

frequency range from 300 cycles/sec. to 4.5 Kilocycles/sec. The results were represented graphically by plotting the variation of C_s and R_s with frequency, (cf. Fig.64). In general, as the frequency was increased C_s and R_s decreased. Within the limits of accuracy of the measurements, R_s the series resistance associated with C_s appeared to be constant; hence the time constant $C_s R_s$ apparently decreased with frequency in exactly the same way as did C_s.

Full details of results are to be found in Appendix II.

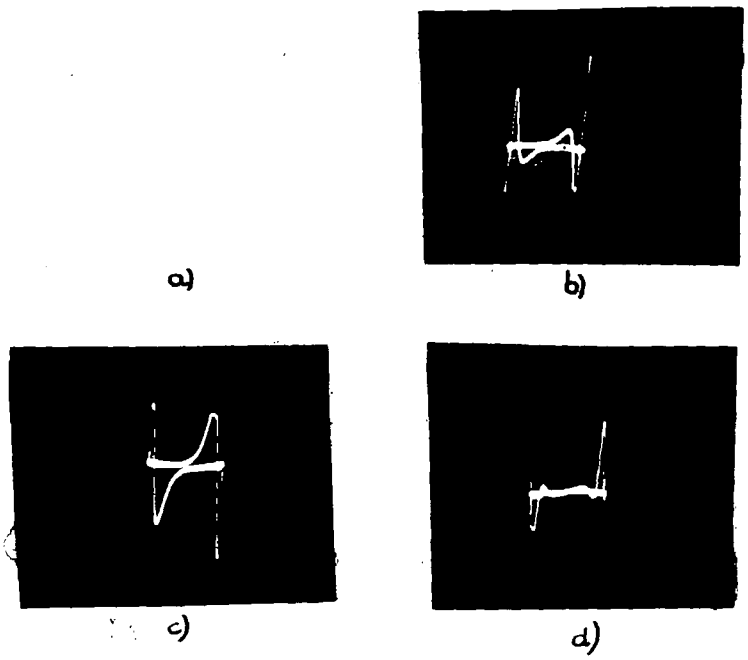

Fig.64). Results for Soda glass:- i) Waveforms,-
a) Initial balance,
b) R_s balanced out,
c) Initial spike eliminated,
d) Final balance.
ii) (see next page), Variation of C_s and R_s with frequency of bridge input.

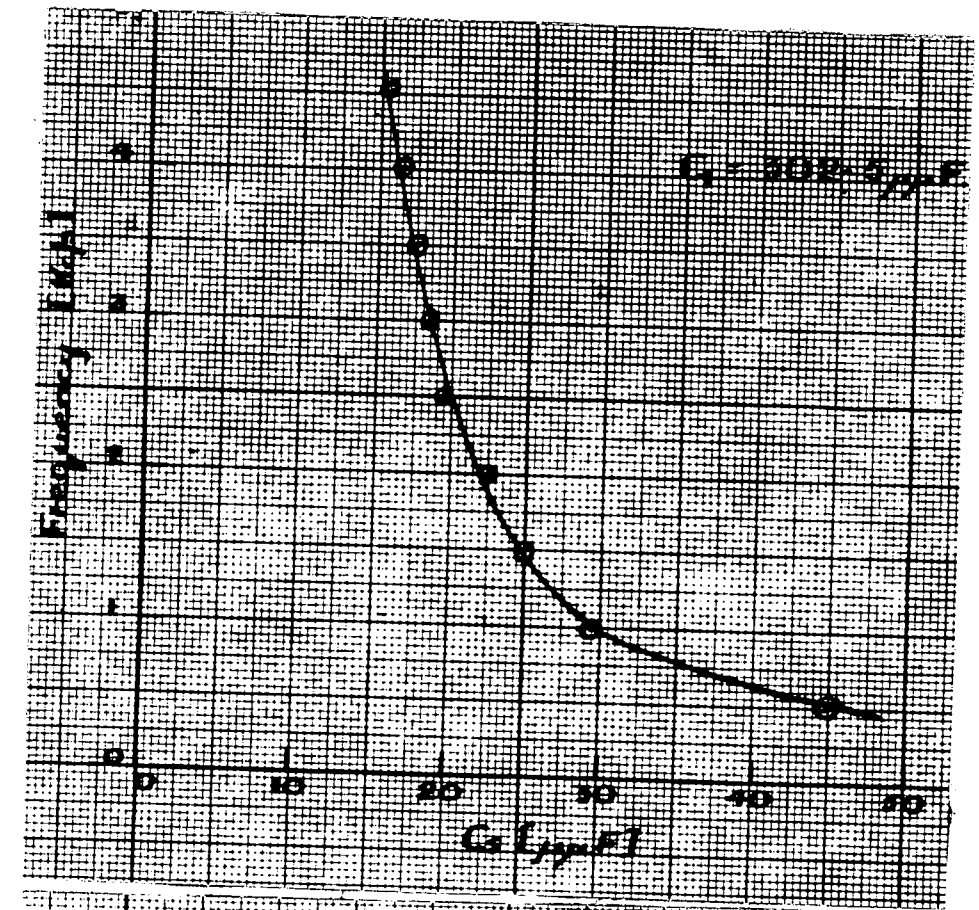

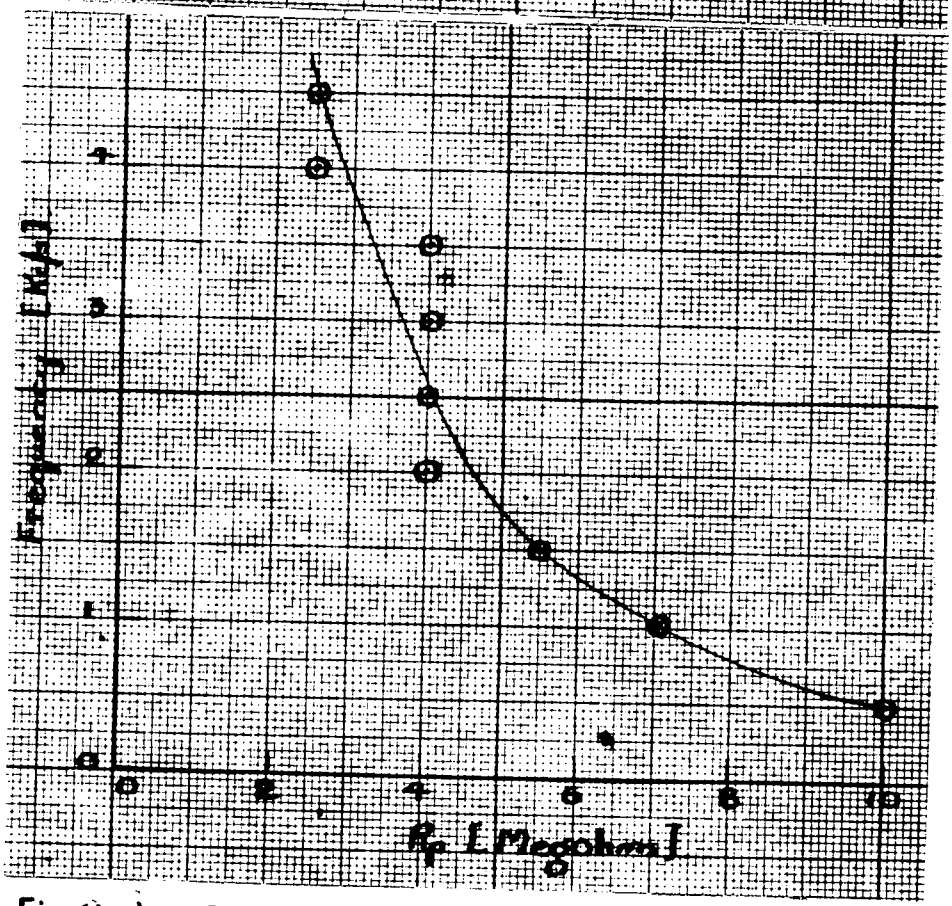

Fig 64 ii) See previous page

iii) Ice.

In the hopes of determining the significance of the measurements carried out on dielectrics using the pulsed differential transformer bridge, it was decided to study some substance whose dielectric properties had already been studied by other methods in the audio-frequency range. The chosen dielectric was ice, the dielectric properties of which were studied in detail recently in the audio-frequency range by J. Lamb.[16] According to Lamb, ice exhibits an absorption maximum which appears to correspond to a single relaxation time, at a frequency of 400 cycles/sec., and a temperature -5°C. It was expected that if a single relaxation time was involved an almost perfect equivalent network would be obtained using the method described in this thesis.

The condenser used for the study of ice is shown in Fig.65).

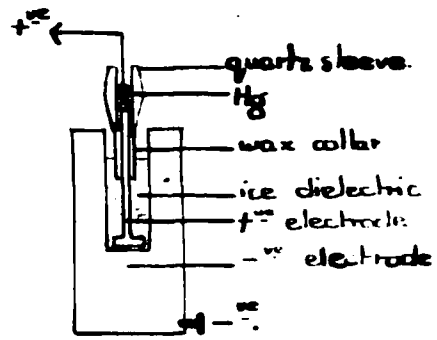

Fig.65) Condenser used in the study of the dielectric properties of ice.

A few drops of distilled water were placed in the outer

cylinder forming the negative electrode. The cylinder was placed on a block of solid carbon-di-oxide and the water allowed to freeze, forming an ice disc. The positive electrode was then placed on the ice disc, and more water added and allowed to freeze. Care was taken that there was no direct contact between the two electrodes and that the ice covered the positive electrode up to and just beyond the wax collar shown in the diagram. This latter precaution eliminated the possibility of direct ~~con~~ conduction between the electrodes across the surface of the ice. The condenser was placed in a container on the carbon-di-oxide block, and packed round with cotton wool to reduce the evaporation of the carbon-di-oxide to a minimum.

The response waveform for ice dielectric upon the application of a square wave to the bridge, is shown in Fig.66).

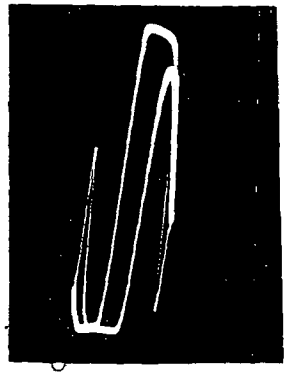

Fig.66) Response waveform for ice.

For these initial measurements on ice no form of temperature control was used. It was observed that as the temperature ~~decreased~~ decreased the length of the initial spike increased.

Measurements were commenced when the waveform appeared to stabilise, (temperature between 0 and -30°C). The measurement of C_i' from the elimination of the initial spike was constant and of the same order of value as the geometric capacitance of the condenser. This indicated that the dielectric loss was associated with the whole of the ice dielectric.

Contrary to expectations the ice dielectric appeared to exhibit considerable parallel conductance. Measurements of R_p' were made by the ballistic balance method, and, as in the case of Soda glass, this measurement appeared to depend on the frequency of the applied sinusoidal input. Observations were made of the variation of the equivalent parallel resistance and of the total capacitance with frequency, over the frequency range, 500 cycles/sec. to 11 Kilocycles/sec. The results were represented graphically as for Soda glass, (cf. Fig.67). The graphs were similar in form to those for Soda glass. The order of parallel resistance exhibited was very low, whilst the fractional capacitance associated with series resistance was extremely large. The final output waveform, when the ice condenser was balanced against the equivalent network for a given frequency of sinusoidal bridge input, was far from perfect.

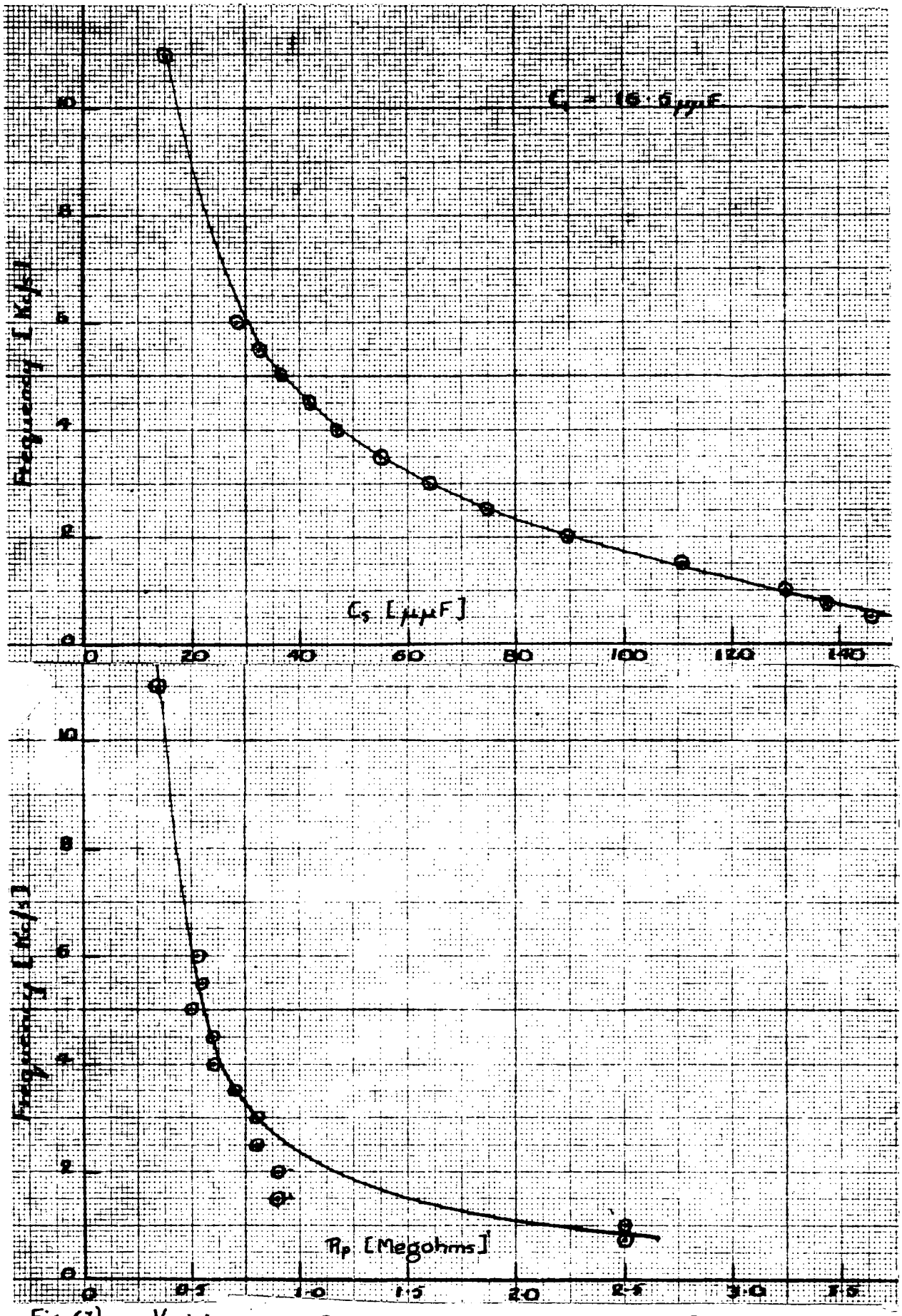

Fig 67). Variation of C_s and R_p with Frequency for Ice

II. DIELECTRIC THEORIES AND MEASUREMENTS.

In order to be able to discuss the results described in the previous chapter of the measurements made on the dielectric properties of Pyrex Brand glass, Soda glass, and ice, it is proposed to consider briefly the electrical properties of dielectrics in general, the methods used to measure those properties, and the subsequent dielectric theories which have been advanced.

1) Experimental methods and results.

Steady field methods.[17] Some mention has already been made of the early experiments carried out on dielectrics using steady fields,(cf. Introduction). Observations were made on the current flowing into the condenser containing the dielectric, upon i) the application of a steady field to the condenser,

ii) short-circuiting the condenser after the application of a steady field for a known interval of time,

iii) insulating the condenser after the application of the conditions indicated above,in ii), for a known time interval.

Under the conditions stated in i) the current flow was considered to consist of three components, namely, the normal charging current of the condenser, the normal conduction current across the dielectric, and the anomalous charging or absorption current resulting from the readjustment of charges in the

dielectric. Under condition Bi), the conduction current was zero, leaving only the normal discharging and enomalous discharging currents, to make up the total discharging current. Under condition iii), a new charge separation developed in the dielectric similar to but less intense than the original charge, (cf. Fig.68).

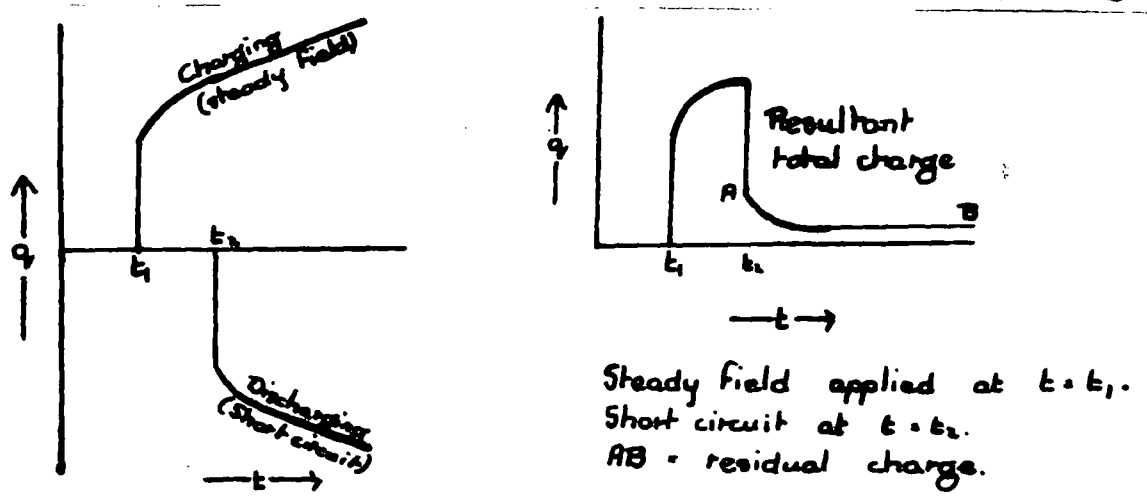

Fig.68). The phenomenon of residual charge.

Sinusoidal field methods. The methods used to study the dielectric properties of a material upon the application of a sinusoidal field can be divided into three main classes, namely, i) thermal methods,

ii) resonance substitution methods,

iii) bridge methods.

i) Thermal methods.

The measurement of dielectric loss in terms of the heat generated as a result of the energy absorption in an alternating

field was originated in 1931 by Harms.[18] The method is suitable for measurements in the high frequency range, say from 1 to 25 Megacycles/sec. More recently this type of measurement has been developed to an accuracy more in line with that of other methods which will be described.[19]

ii) Resonance substitution methods.

Fundamentally this type of method depends on the change in Q-factor and tuning of a resonant circuit upon inserting the dielectric medium under investigation between the condenser plates. The measurement is based on the change in resonant frequency for constant capacitance, or the change in capacitance required to maintain resonance for constant frequency. The method is suitable for frequencies up to 100Megacycles/sec. Above that frequency range it is usual to replace the resonant circuit by elements of transmission lines or waveguides.[20] The accuracy of measurement using waveguides is not so high as that of the usual resonance methods. However the standing wave method of measurement is advantageous in the investigation of small dielectric specimens. There are two possible forms of measurement using waveguides. Either the dielectric medium is used as a terminating load, or the lines themselves are immersed in the dielectric medium. Using the former method frequencies as high as 150,000 Megacycles have been used satisfactorily.

iii) Bridge methods.

The use of bridge methods in the study of dielectrics has already been briefly mentioned,(cf. Introduction). In this type of method the properties of the dielectric are usually measured in terms of an equivalent network of linear circuit elements. In general the values of those elements are dependent on the frequency of the bridge input, and it is necessary to make measurements at a series of discrete frequencies in order to obtain a picture of the dielectric properties over the required frequency range. Bridge methods are widely used for measurements in the lower frequency range up to frequencies of about 1 Megacycles/sec. With careful development and adequate screening, however, bridge measurements can be extended to the decimetre wave region. Typical bridges used for the measurement of dielectric properties are Curtis's bridge,[21] measuring the equivalent series resistance, Grover's bridge,[21] measuring the equivalent parallel resistance, and the Schering bridge, adapted by Dye and Jones[22] to measure to an accuracy of 1% , power factors lying between the limits 0.001 and 0.1.

Frequency dependence of equivalent network.

Attempts have been made to find a network of linear circuit elements equivalent to a dielectric which is independent of the applied frequency in the sense that the values of the circuit elements are independent of the applied frequency. No

simple arrangement has yet been found. Cole,K.S. and Cole,R.H. [23] represented the dielectric properties of various materials by graphs of the variation of the real with the unreal part of the dielectric constant. Theoretically they showed that for a single relaxation time this graph,or complex plane diagram, should be a semi-circle. In this case the dielectric could be represented at all frequencies by an equivalent network containing a capacitance in parallel with a capacitance and series resistance. In practice, Cole,K.S. and Cole, R.H. found that for most materials the complex plane diagram was in the form of a circular arc. To correlate their equivalent network with this result the series resistance had to be replaced by a complex impedance of an experimentally unrealisable type.

Theoretically it would appear that it would be possible to measure the equivalent network at one given frequency, modify that network by the addition of a second branch to apply to a second frequency, then a third, and so on. In this way, an 'extended' network would be obtained which was frequency independent. The experimental difficulties involved, however, are almost insuperable.

Experimental results.

The variations of permittivity and loss angle with frequency have been measured for various materials,- gases, liquids and solids. Although the results vary considerably, they may in

general be classified into two types. Thus for gases and dilute solutions of polar substances, typical results are as shown in Fig.69), the tan δ-frequency variation showing a pronounced peak.

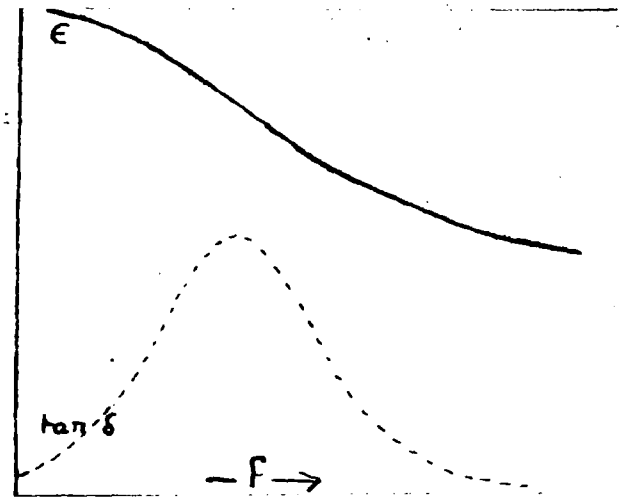

Fig.69) Typical variations of permittivity and loss angle with frequency, for gases and dilute solutions of polar substances.

The majority of solids however exhibit a tan δ-frequency curve which is much flatter, amounting almost to a straight line for some materials,(cf.Fig.70).

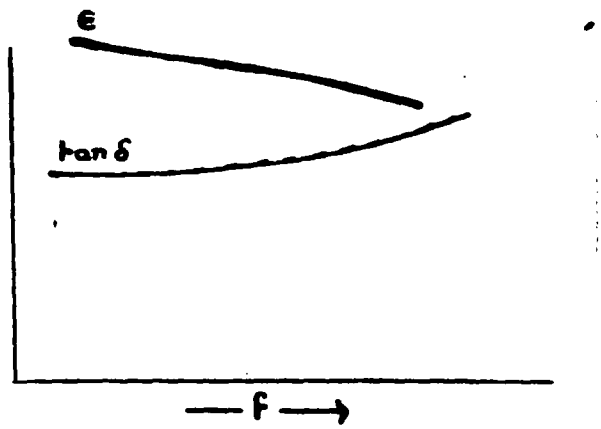

Fig.70) Typical variations of permittivity and loss angle with frequency for solids.

2) Dielectric theories.

Steady fields. The early dielectric theories were put forward in an attempt to explain the electrical properties of dielectrics as observed upon the application of a steady field. Many of these theories were later discarded, but the Superposition Principle, put forward by Hopkinson,[24] is still of general interest. In this work in particular, Hopkinson's Superposition Principle has proved of value in the elucidation of the results. The Principle, in one particular form, states that, upon shortcircuiting a condenser, the initial current is not annulled, but has superposed on it another current of the same time function, but in the opposite direction. On this basis, the electrical behaviour of a dielectric depends to a certain extent on its previous history. Hopkinson's Superposition Principle was later extended to cover the use of sinusoidal fields, and predicted an absorption of energy in the dielectric which depended on the applied frequency.

Maxwell[25] attempted to explain mathematically the phenomenon of residual charge, (described earlier in this Chapter), in terms of the inhomogeneity of the dielectric medium. He considered first the much simplified case of a dielectric consisting of two strata of different permittivities and conductivities. He proved that such a system would exhibit the phenomena of residual charge and absorption. His theory was later extended by Wagner,[26] to cover the case of a medium

containing small spherical inhomogeneities. These theories indicate that inhomogeneity of a material can give rise to the absorption of electrical energy. But the phenomenon of absorption in a material is not necessarily proof of the inhomogeneity of the material. In fact, the phenomenon is exhibited by homogeneous materials also.

Later dielectric theories were based on the molecular structure of the material. In general a material may contain both polar and non-polar molecules. Upon the application of an external field both types of molecule become polarised by induction. The induction processes arise from the displacement of electrons and atoms in the molecules, and are practically instantaneous. Apart from this, Debye[27] suggested that a second polarisation process takes place which is relatively slow, and which arises from the tendency of the permanent dipoles to orientate themselves in alignment with the field. If the applied field is sinusoidal in form, the permittivity and hence the polarisation depend on the frequency of the applied field. Debye assumed that the rotation of the permanent dipoles is opposed by a frictional force. At low frequencies the dipoles are able to follow the variations of the applied field, and there is no energy absorption. As the frequency is increased this condition persists until the duration of the field becomes comparable with the relaxation time of the dipoles. Then the dipoles are unable to respond

immediately to the field. A time lag is introduced and there is a corresponding absorption of energy. As the frequency of the applied field is increased still further, the dipoles are unable to respond at all, and the polarisation arises entirely from the displacement of atoms and electrons in the molecules. Assuming that the interaction between dipoles is negligible, Debye predicted variations of permittivity and loss angle with frequency

, of the form shown in Fig.71).

They are in good agreement with the results observed for gases and dilute solutions of polar substances.

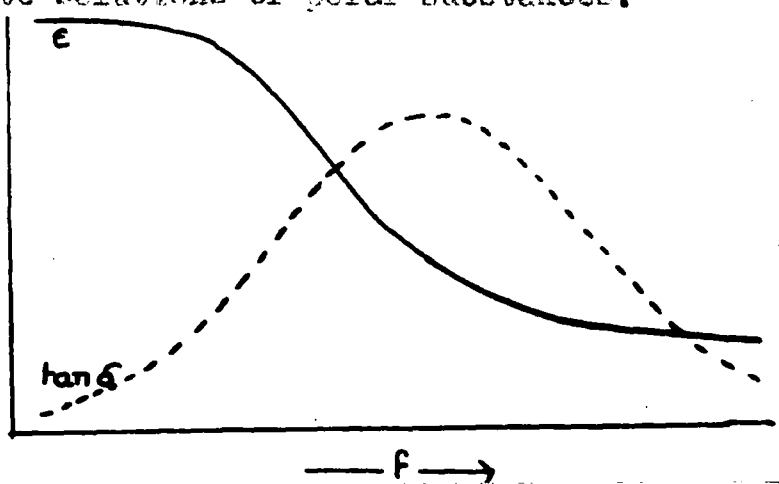

Fig.71) Variation of permittivity and loss angle with frequency predicted by Debye's theory.

In order to account for the flat tanδ-frequency curve characteristic of many solids, Debye extended his theory on the basis that the rotating dipoles would possess a distribution of relaxation times. Such a solution is not wholly satisfactory in that a suitable distribution can always be found to fit any curve.

that a dipole will lie within a certain range of directions is increased. This probability is limited by the Brownian movement of the dipoles; the balance between the thermal disorder and the orienting effect of the applied field can be expressed by means of Boltzmann's Law. The probability therefore of finding a dipole with energy V is proportional to $e^{\frac{-V}{kT}}$, where k=constant, T = temperature.

This conception is strictly true in the case of a truly amorphous material, provided that the concentration of dipoles is small, and that the effects of dipolar interaction can be neglected. But, in a crystalline medium, the dipoles, like the other molecules may be expected to set in preferred directions, determined by the structure of the material. In general, a given dipole is most likely to be found in one particular setting or in the opposite setting,(cf.Fig.72).

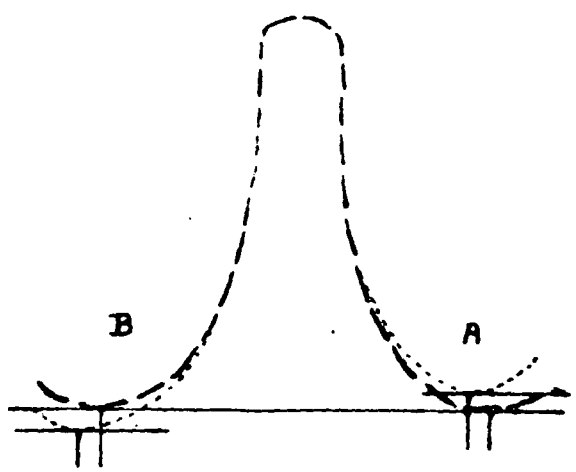

Fig. 72) Potential energy of a dipole with two equilibrium positions. The dotted curve holds in the presence of an external field.

When the polarisation is zero,(no external field), the probability of the dipole being in either of its two equilibrium positions, A or B, is ½. Upon the application of an external field, the probability of the dipole being in position B is increased, and in position A decreased. This leads to a polarisation of the medium in the preferred sense as represented by B.

The combination of the disordering effect of thermal agitation, and the finite rate of attaining equilibrium gives the dipole system the attributes of a quasi-elastic force opposing the setting of the dipole, and a viscous force retarding the response of the dipole.

The development of the theory of the dynamic properties of dielectrics is considerably more complicated than that of the static properties. Since the conception of a complex permittivity is a device applicable only to sinusoidal functions, the response of a dielectric to any other function,-for example, a step function -can only be obtained by

i) a Fourier analysis of the step function,

ii) treatment for each Fourier component separately,

iii) synthesis of results.

Experimentally, the phase relations between the Fourier components are not observable with observations made at discrete frequencies of sinusoidal input.

Although the theories described above do not succeed in explaining the experimental facts completely, they give some indication of the possible causes underlying dielectric lose. Most of the theories, although based on different conceptions of the loss mechanism occuring in dielectrics, lead to strikingly similar mathematical results. In general the experimental variations of permittivity and loss angle with frequency can always be explained in terms of a suitable distribution of time constants, without necessarily throwing any light on the actual nature of the mechanism involved. No direct observation of the separate time constants is possible. If it were, the resulting information would be very revealing as to the structure of the dielectric. As a direct consequence of this, the possibility arises of obtaining a more satisfactory interpretation of the phenomenon of dielectric loss by a study of the behaviour of dielectrics under the application of non-sinusoidal fields.

X. A DISCUSSION OF THE RESULTS OF THIS INVESTIGATION.

This investigation has been concerned primarily with an exploration into the possibilities of the pulsed differential transformer bridge. The development of the bridge was carried out with a view to studying the dielectric properties of materials. Measurements were made on dielectrics of Pyrex Brand glass, Soda glass and ice. The results are of interest more as an indication of the usefulness of the instrument developed, in this field, rather than as a means of obtaining information about the dielectric properties of the materials concerned. With this in mind, it is proposed to consider the significance of the measurements made, and to conclude from the results the usefulness of the pulsed differential transformer bridge in the study of dielectrics.

~~There are~~ Two possible approaches to pulse measurements will be considered. The pulse may be regarded as either a range of Fourier component sinusoids, or, a voltage-step. In this connection, it has been observed that if the response of a dielectric to a voltage step is known, the values of the real and unreal components of the dielectric constant, ϵ_1 and ϵ_2, may be deduced for any given frequency. Furthermore, the use of ϵ_1 and ϵ_2 is an artifice applicable only for sinusoidal fields. Consequently a determination of the time dependence of charge for a condenser to which a voltage step has been applied, may be regarded as

an experimental solution of the problem of determining the properties of the condenser used. Such a solution can be considered complete only if the voltage step is applied so suddenly, and extended so long that the beginning and end of the operation are both discernable in the experimental results, i.e., the points A, P, and the asymptote TR on the charge-time curve should be observable, (cf. Fig. 73). This corresponds to the assumption, where sinusoidal observations are concerned that both the static and the extremely high frequency dielectric constants, ϵ_s and ϵ_∞, are determined.[31] If pure conduction processes are present, the same condition of completeness of the charge-time curve applies, (cf. Fig. 73b). The conduction processes ~~can~~ could be compensated for in the square-wave measurements which were undertaken, reducing the problem to that of studying the charge-time curve illustrated in Fig. 73a).

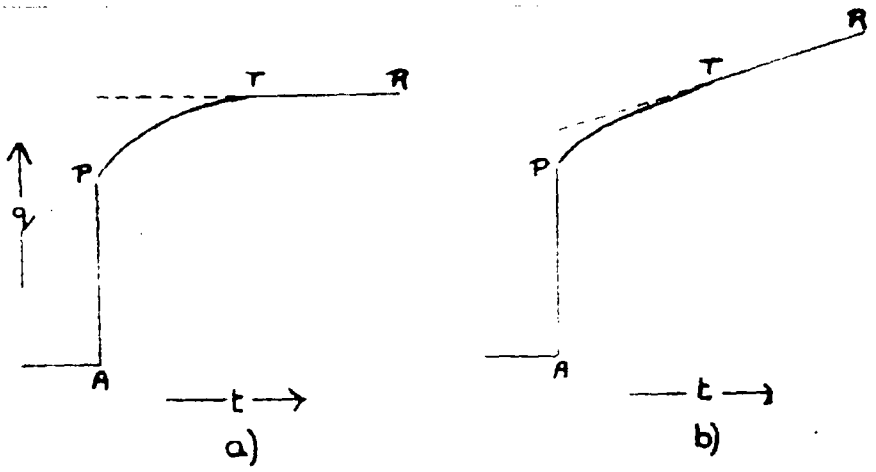

Fig. 73) Charge-time variation for dielectric under application of square-wave:- a) No conduction, b) Conduction present.

An advantage of the old classical methods of observing dielectric properties is that they permit the detailed study of the portion TR of the charge-time curve. The present differential transformer method serves to delineate the region near the beginning of the curve, but it has become apparent during the experimental work that the method does not suffice unless equilibrium is reached,(i.e. the charge-time curve flattens out), in a time comparable with T = 1/repetition frequency. The principle of superposition is useful in elucidating these working conditions.

A square voltage wave may be considered as made up of a set of voltage steps of equal magnitude applied in alternate directions at suitable time intervals,0,T,2T,3T,etc., (cf.Fig.74).

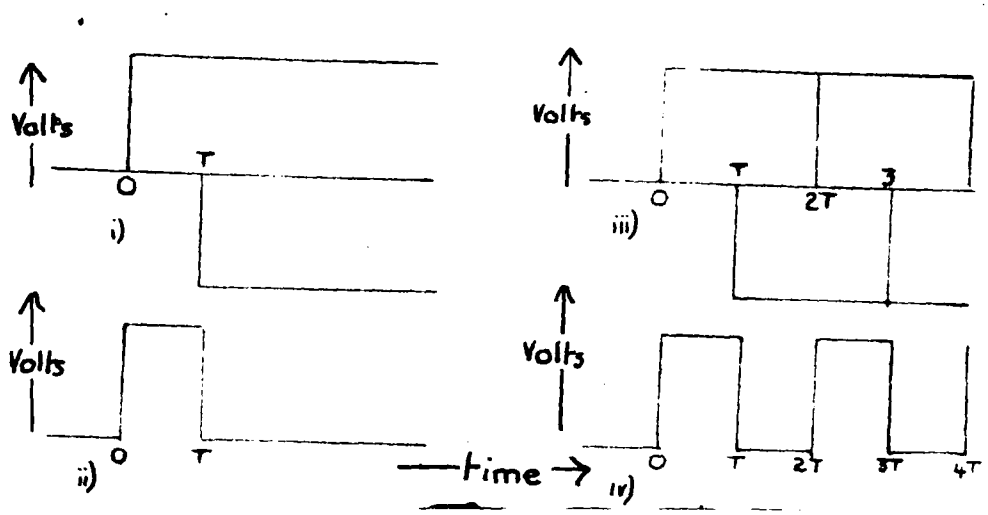

Fig.74) Illustration of building up of square-wave from voltage steps of equal magnitude applied in opposite directions.

If the charge-time curve is known for one complete voltage step, the charge-time curve for a square-wave may be deduced.

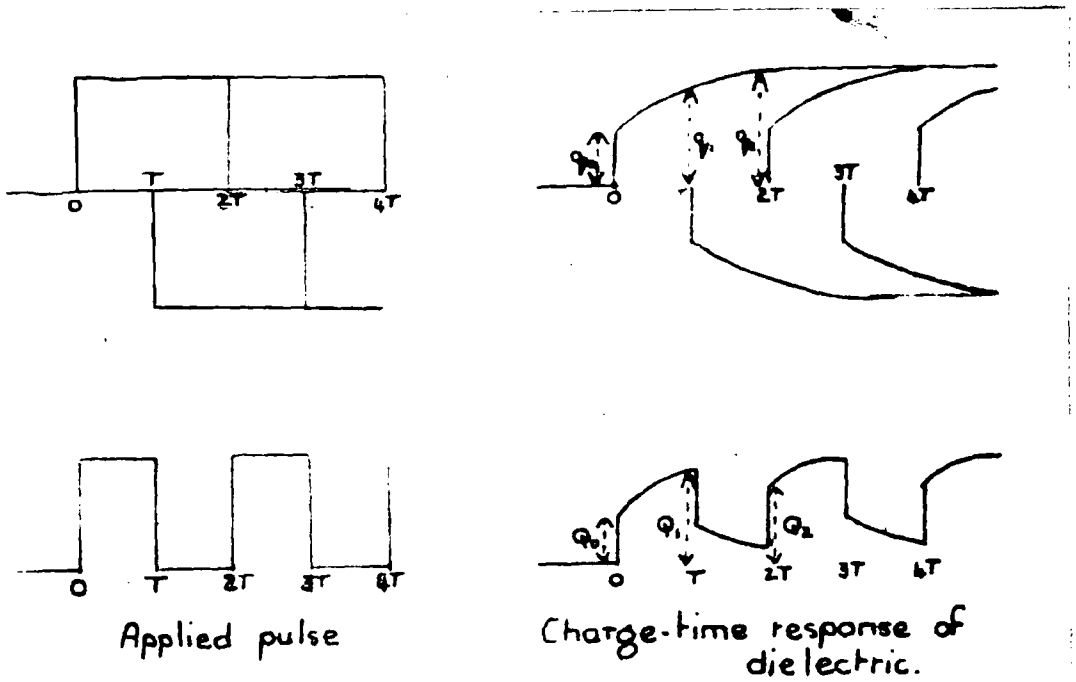

Fig.75) Deduction of charge-time curve of dielectric upon application of square-wave, using the Principle of Superposition.

By the Principle of Superposition(cf.Fig.75):-

$Q_0 = q_0$ $\qquad$ $Q_1 = q_1$

$Q_2 = q_2 - q_1 + q_0$ $\qquad$ $Q_3 = q_3 - q_2 + q_1$

$Q_4 = q_4 - q_3 + q_2 - q_1 + q_0$ $\qquad$ $Q_5 = q_5 - q_4 + q_3 - q_2 + q_1$

$\vdots$ $\qquad$ $\vdots$

$Q_n = q_n - q_{n-1} + q_{n-2} - q_{n-3} \_\_\_\_\_ - q_1 + q_0$ $\qquad$ $Q_{n+1} = q_{n+1} - q_n + q_{n-1} - q_{n-2} \_\_\_\_\_ - q_2 + q_1$

Let equilibrium be obtained at time nT. Then $q_n \doteq q_{n+1} =$ ____

Error in q_n arising from superposition effects,

$$q_n - q_0 = q_n - q_{n-1} + q_{n-2} \text{ ------ } q_0$$

Error in q'_n arising from superposition effects,

$$q_{n-1} - q_1 = q_{n-1} - q_{n-2} + q_{n-3} \text{ ------ } q_1$$

$$= q_{n-2} - q_{n-3} + q_{n-4} \text{ ------ } q_2$$

It would appear that there are two sets of circumstances in which the initial part of the charge-time curve may be correctly delineated by square-wave experiment,-

i) When the curve is complete within time T, where T = 1/2repetition frequency,(cf.Fig.76). In this case,

$q_n = q_{n-1} = q_{n-2} = \text{ ---------- } = q_2 = q_1$; $q_n = q_0$, $q_{n-1} = q_1$.

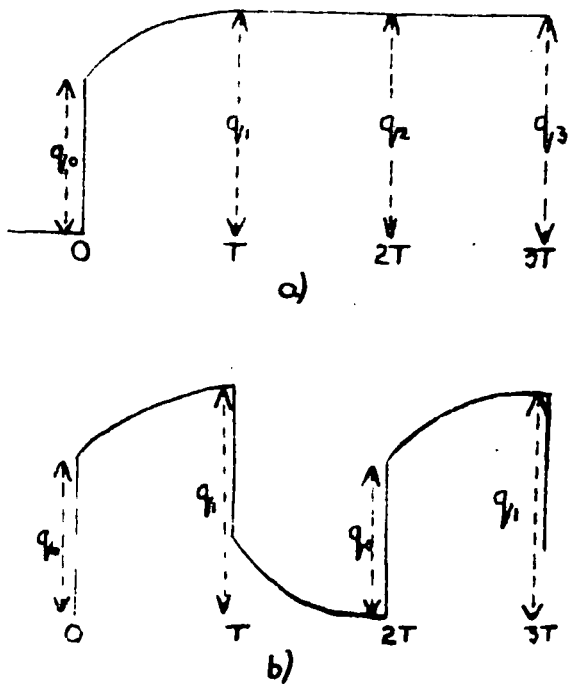

Fig.76) Square-wave response of dielectric whose charge-time curve attains equilibrium within time T = 1/2repetition frequency.

ii) When the curve is not complete within time T = ~~$q_0/rep^n.freq^y$~~ (repetition frequency), but is of such a form that

Error in $Q_n = q_n - q_{n-1} + q_{n-2} \text{ ——— } - q_1$,

$= \sum_{m=2}^{m=n} (q_m - q_{m-1})$, is negligible.

The latter case is not generally helpful, and is effectively equivalent to case i). It may be worth noting that if the curve is extensive and does not show a rapid change of slope, $\Sigma (q_m - q_{m-1})$ has the value of approximately $q_1/2$. It is thus possible that observations at various repetition frequencies would lead to some information on the shape of the latter part of the charge-time curve.

When the charge-time curve is of a defined analytical form, precise deductions may be made. The Debye equations express the behaviour of a medium for which the curve is exponential. These equations are of such convenient form, and simple relaxation processes, which may be taken to represent exponential processes, are so usual that where the curve is not exponential it is commonly regarded as a set of exponential processes of various relaxation times. This artifice is equivalent in many respects to the alternative one of constructing an equivalent network. For if such a network involves only linear circuit elements, the separate meshes exhibit exponential relaxations, (in the absence of free oscillation). Thus it is possible to imagine a wide range of equivalent networks representing a dielectric.

The attitude adopted in the present investigation has been that of attempting to represent probable physical processes occurring in certain dielectrics by means of a network, and then examining the correspondence in form between the oscillograms resulting from the use of such networks, and those resulting from the use of actual dielectric materials. The measurements made on Pyrex glass indicated that the equivalent network used was satisfactory in its representation of the dielectric, in that its component values were independent of the repetition frequency of the square-wave,(or sinusoidal frequency applied for ballistic balance)*. With Soda glass and ice,however, the equivalent network was unsatisfactory in that the values of the components were not independent of repetition rate. It has been seen above that this indicates the occurrence in the material of processes whose time order is greater than T = 1/(repetition frequency).

* In order to obtain information concerning the end of the charge-time trace, sinusoidal fields were used to obtain ballistic balance(cf.Ch.IV). Pulse measurements can be expected to yield information only over the frequency range contained in the pulse. Hence the ballistic measurements made at low frequencies may be considered equivalent to measurements at the repetition rate of the pulse.

With Soda glass, the indication of the occurrence of very slow processes in the medium might possibly be explained in terms of ionic conduction combined with an inter-surface film effect. Conduction due to the movement of Sodium ions in Soda glass is a well-known phenomenon. It appears feasible that with the type of condenser used in this investigation a thin film may be formed between the glass surfaces and the mercury electrodes. Under these conditions the ionic conduction manifested by Soda glass would appear more in the nature of a very slow relaxation process than as a pure conduction process.[32] The corresponding equivalent network would then adopt the form shown in Fig.77) , where C_{s1}' represents the capacitance due to surface film effects, and R_{s1}' the ionic conduction. It would be expected that both C_{s1} and R_{s1} would be large. This point might well be tested by investigating the effects of using different types of electrode, for example, electrodes of Sodium Chloride solution, and silvered electrodes on the glass specimen.

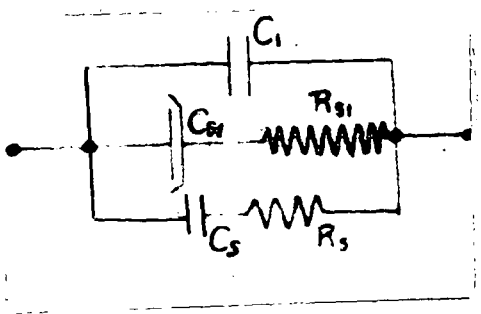

Fig.77) Possible equivalent network for Soda glass, exhibiting inter-surface film effects.

XI. CONCLUSION.

This research has consisted of an investigation into the possibilities of the pulsed differential transformer bridge for:-

i) the measurement of four component capacitance-resistance networks approximating to a condenser filled with natural dielectric,

ii) the examination of certain dielectric media in terms of such a network.

From the work it has been concluded that, using the pulsed differential transformer bridge, four component networks of the type discussed in Ch.II, can be analysed satisfactorily over a wide range of values. The main factors limiting the working range of the instrument in this respect are the design of the differential transformer and the steepness of the pulse edge. The measurements made on actual dielectric media indicate that the method is suitable for the analysis of dielectrics exhibiting loss phenomena of time order greater than (repetition frequency). For dielectrics exhibiting very slow loss processes the method is incomplete. In order to obtain the complete picture of the dielectric it would be necessary to incorporate an auxiliary instrument such as a four-condenser bridge, with which to investigate the end of the charge-time trace. This presents one possible line for future

development, a second being the investigation of the effects of using various types of electrode with Soda glass and similar dielectric media.

33)

APPENDIX I. DESIGN OF BRIDGE OUTPUT AMPLIFIER.

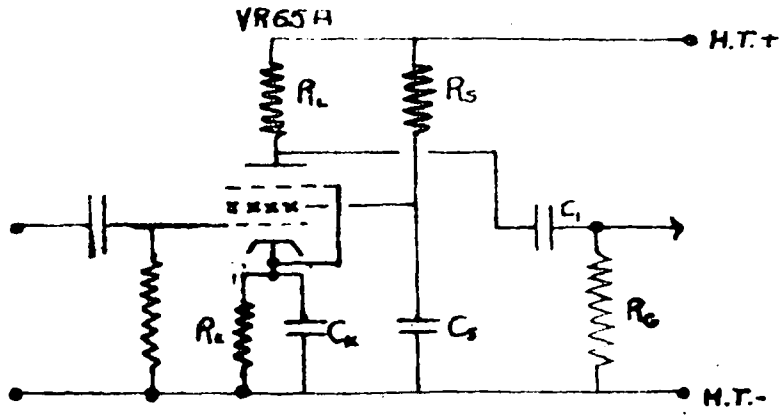

Fig.73). R-C coupled amplifier stage.

Valve:- VR 65A.

Anode voltage, V_L, = 200 volts,

Anode current, I_L, = 10.0 ma.

Screen voltage, V_S, = 200 volts.

Screen current, I_S, = 3.0 ma.

Amplification factor, μ, = 6×10^3.

H.T.Voltage, , = 300 volts.

Frequency range required = 350 cycles/sec. to 2 Megacycles/sec.

Calculation of components, (Static voltages only).

R_K $V_G = I_L \times R_K$. R_K = 140 ohms

R_L $(V - V_L) = I_L \times R_L$. R_L = 10 K

R_S $(V - V_S) = I_S \times R_S$ R_S = 33 K

R_G and C_1. R_G should be as large as possible for peak grid voltages. If $R_G = 10^5$ K, $C_1 = 0.1\mu F$, time constant $C_1 R_G = 10^{-7} \times 10^5 = 10^{-2}$, i.e., this C-R combination will respond satisfactorily to frequencies of 100 cycles/sec. and upwards.

R_K and C_K. If $R_K = 140$ ohms (see above), and $C_K = 25\mu F$., $C_K R_K = 3.5 \times 10^{-3}$, i.e., this C-R combination will respond satisfactorily to frequencies above approximately 300 cycles/sec.

Estimation of amplification at intermediate frequencies of single R-C coupled amplifier stage.

The equivalent circuit of a single R-C coupled amplifier stage is shown in Fig.79), from the point of view of varying voltages.

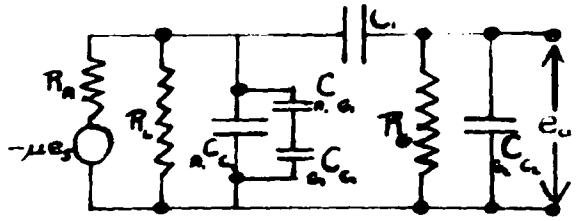

Fig.79). Equivalent circuit of R-C coupled amplifier stage from point of view of varying voltages

At medium frequencies C_1 acts as a shortcircuit to those frequencies, and C_{R_a}, C_{C_1}, C_{R_b}, C_{C_2} and C_{C_1} in series, and C_{C_2} have

negligible effect. Equivalent circuit reduces to that shown in Fig.80).

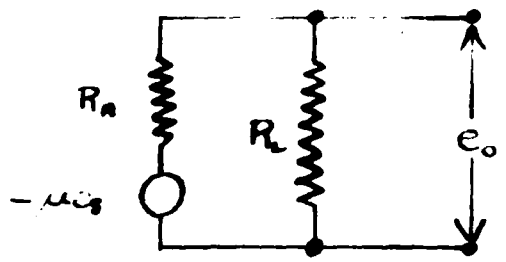

Fig.80). Simplified equivalent circuit applicable at medium frequencies of single stage R-C amplifier.

Then, $e_o = \dfrac{-\mu e_g R_L}{R_A + R_L}$

$$\frac{e_o}{e_g} = \text{stage amplification} = \frac{\mu R_L}{R_A + R_L} = 9$$

For three exactly similar stages,

$$\text{Overall amplification} = \left(\frac{\mu R_L}{R_A + R_L}\right)^3$$

$$= \underline{\underline{729}}$$

APPENDIX II. RESULTS OF MEASUREMENTS ON THE DIELECTRIC PROPERTIES OF PYREX GLASS, SODA GLASS AND ICE.

1). PYREX GLASS.

Sample 1):- ordinarily annealed specimen.

Determination of end capacitance of sample.

Weight of Hg in inner column, (gms.)	Total capacitance ($\mu\mu$F).	Weight of Hg in inner column, (gms.)	Total capacitance, ($\mu\mu$F).
12.1	9.0	137.4	104.5
25.1	20.0	148.1	114.5
40.9	32.5	163.2	126.0
54.8	43.5	176.3	137.5
68.8	52.6	190.0	149.5
86.8	66.9	202.9	157.0
103.9	78.5		
125.3	95.0		

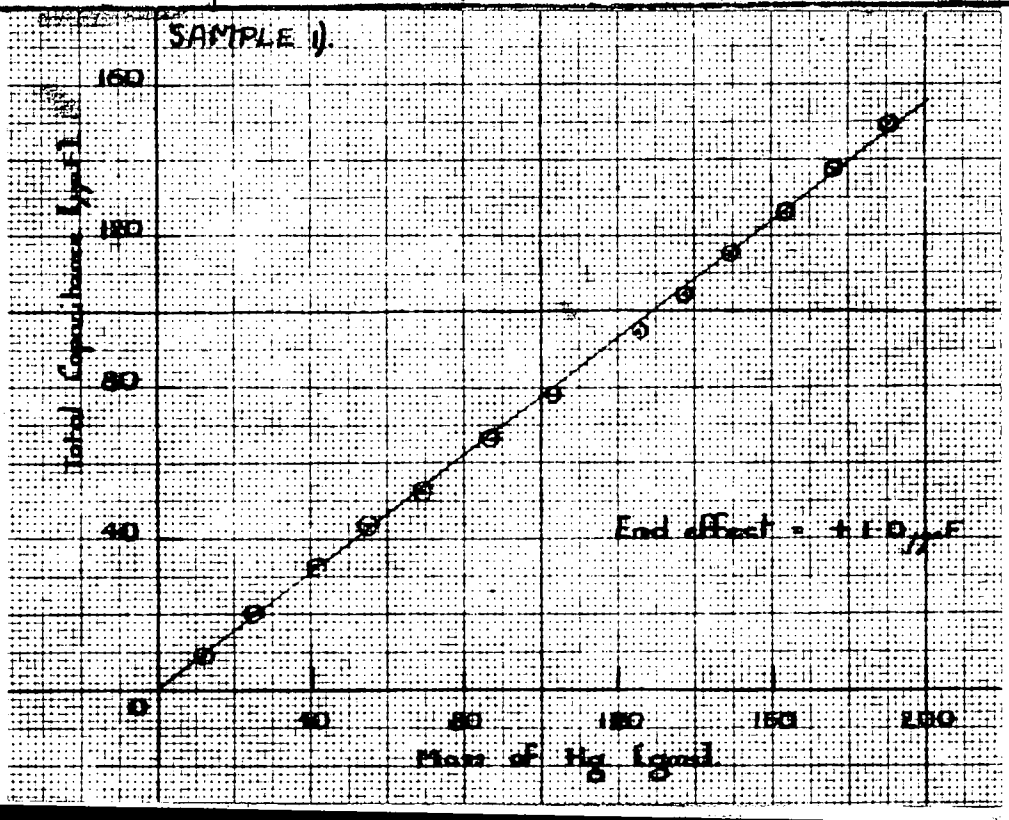

Determination of equivalent network for sample 1).

C_1 ($\mu\mu$ F).	C_s ($\mu\mu$ F).	R_s (K).	C_s/C_1+C_s (%).	C_sR_s (μ-secs.).
152.5	4.0	417.0	2.6	1.7
178.0	4.5	432	2.5	1.9
214.5	6.0	413	2.7	2.5
234.5	6.0	405	2.5	2.4
268.0	7.5	257	2.9	1.9
269.0	7.5	296	2.8	2.3
287.0	8.0	279	2.5	2.1
304.5	8.0	306	2.6	2.5
322.5	8.0	388	2.4	2.8

For sample 1):-

Average C_s / C_1+C_s = 2.6%.

Average $C_s R_s$ = 2.2μ-secs.

Sample 2):- specimen stabilised at 600°C for 2 minutes, then immersed in a bath of Sodium Nitrate at 300°C,(toughened glass).

Determination of end capacitance of sample.

Weight of Hg in inner column (gms.)	Total capacitance, ($\mu\mu$F)	Weight of Hg in inner column,(gms.).	Total capacitance, ($\mu\mu$F).
35.1	36.0	118.8	111.5
52.2	51.0	135.6	131.0
67.7	66.5	150.3	146.5
85.7	82.0	163.6	158.5
98.0	96.0		

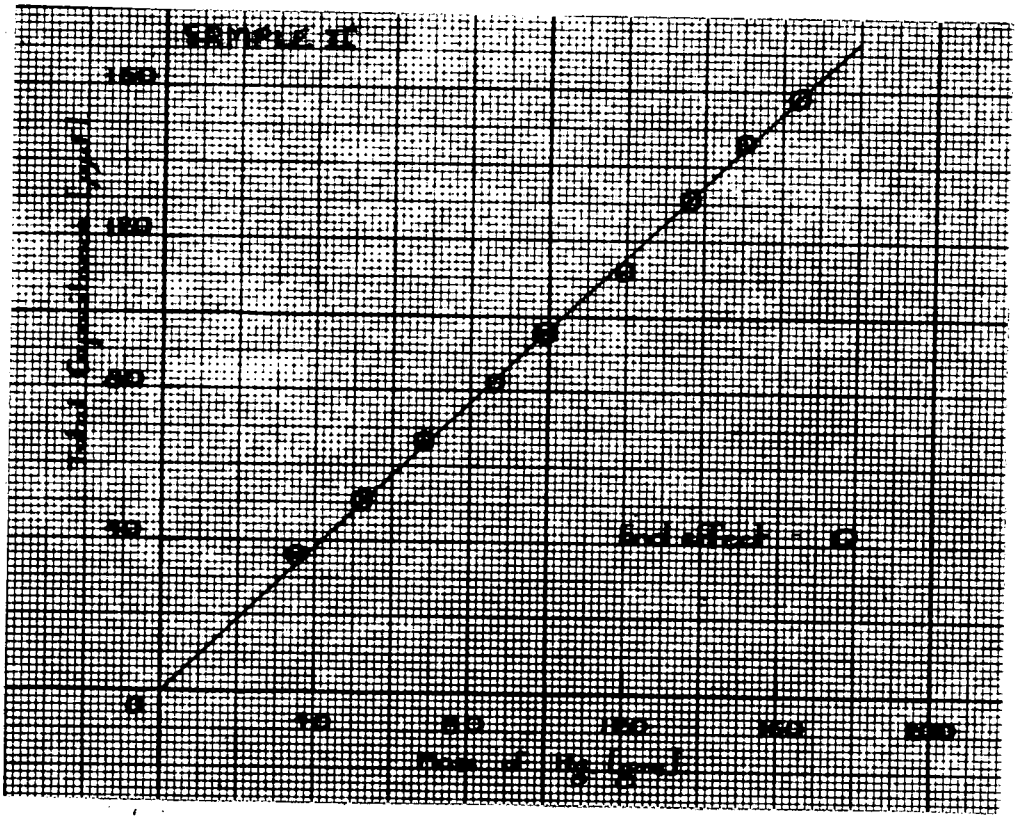

Determination of equivalent network for sample2).

C_1 ($\mu\mu F$)	C_s ($\mu\mu F$)	R_s (K)	$C_s / C_1 + C_s$ (%)	$C_s R_s$ (μ-secs.).
181.0	4.75	635	2.6	3.0
202.0	5.0	641	2.4	3.2
231.5	6.0	612	2.5	3.7
249.9	6.75	589	2.6	3.9
270.3	8.0	546	2.8	4.4
297.5	9.0	532	2.9	4.7

For sample 2):-

Average $C_s / C_1 + C_s$ = 2.6%

Average $C_s R_s$ = 3.8μ-secs.

Sample 3):- specimen stabilised for 1 hour at 650°C, followed by cooling in still air at room temperature.

Determination of end capacitance of sample.

Weight of Hg in inner column,(gms.).	Total capacitance, ($\mu\mu$F).	Weight of Hg in inner column,(gms.).	Total capacitance ($\mu\mu$F).
12.4	4.0	99.2	80.5
20.6	11.5	116.3	98.5
30.8	21.0		
47.7	37.5		
62.1	49.5		
79.9	65.0		

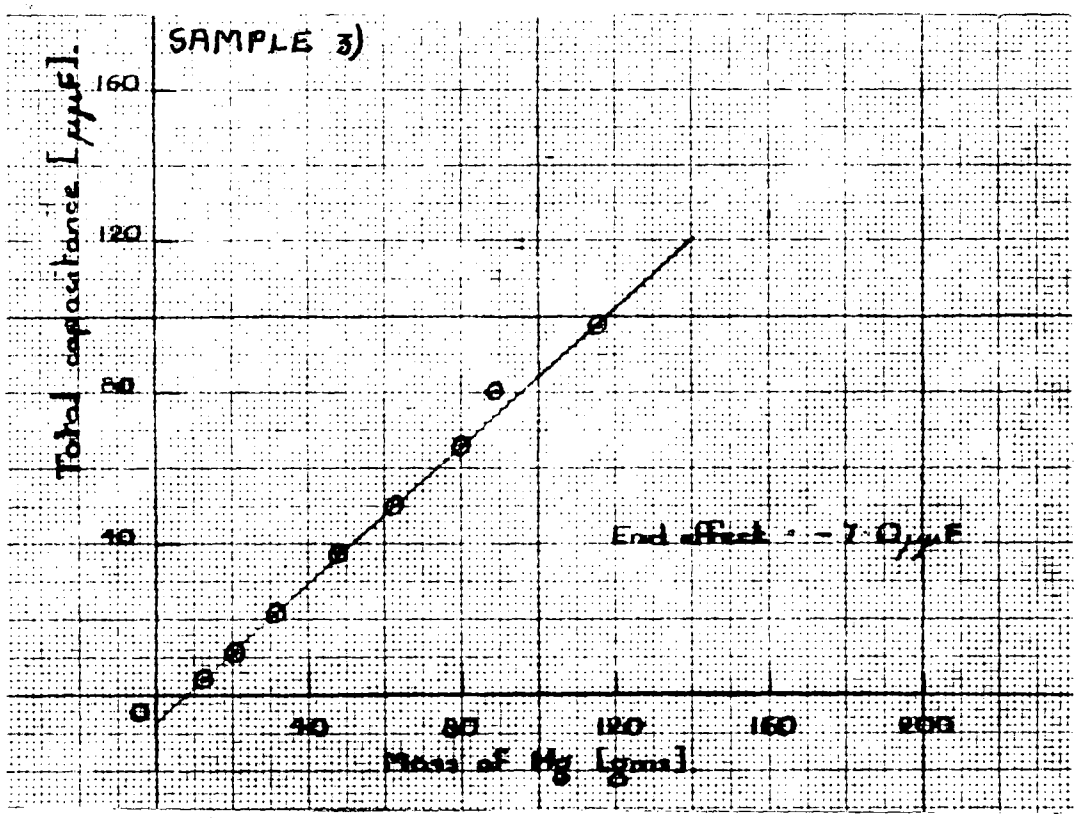

Determination of equivalent network for sample 3).

C_1 ($\mu\mu F$)	C_s ($\mu\mu F$)	R_s (K)	$C_s / C_1 + C_s$ (%)	$C_s R_s$ (μ-secs.).
185.0	4.75	575	2.5	2.7
204.5	5.0	612	2.4	3.1
223.0	5.5	612	2.4	3.3
253.8	7.0	612	2.7	4.3
269.0	7.5	580	2.7	4.0
287.8	7.0	575	2.4	400
309.0	8.5	566	2.7	4.8

For sample 3):-

Average $C_s / C_1 + C_s$ = 2.5%

Average $C_s R_s$ = 3.8 μ-secs.

Sample 8):- specimen stabilised for 30 minutes at 600°C, followed by cooling in still air at room temperature.

Determination of end capacitance of sample.

Weight of Hg in inner column (gms).	Total capacitance ($\mu\mu$F).	Weight of Hg in inner column, (gms.).	Total capacitance, ($\mu\mu$F).
14.0	[illegible]	94.5	88.5
29.8	28.5	107.7	105.5
44.9	43.0	121.3	122.0
61.9	59.0	140.1	138.0
77.0	72.5	156.9	152.5

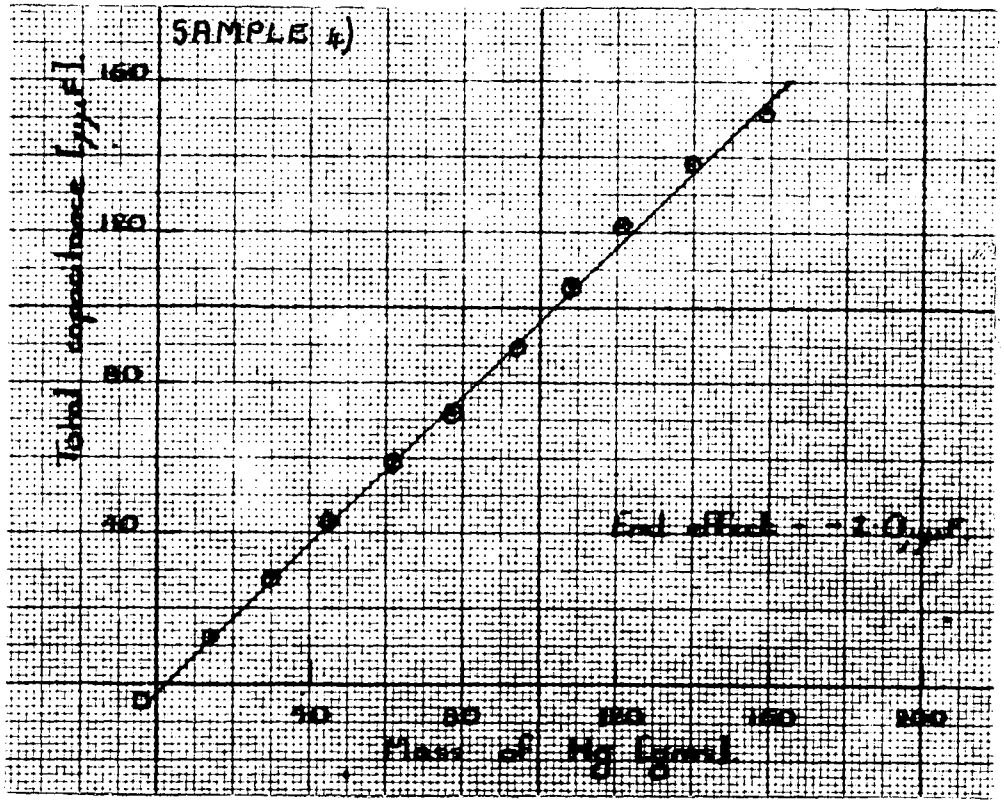

Determination of equivalent network for sample 4).

C_1 ($\mu\mu F$)	C_s ($\mu\mu F$)	R_s (K)	$C_s / C_1 + C_s$ (%)	$C_s R_s$ (μsecs.)
178.0	4.5	571	2.5	2.6
187.5	5.0	559	2.5	2.8
216.0	5.5	584	2.5	3.0
236.5	6.0	441	2.5	2.6
254.0	7.0	413	2.7	2.9
273.0	7.0	413	2.5	2.9
293.0	7.75	343	2.6	2.7
313.0	8.5	345	2.6	2.9

For sample 4):-

Average $C_s / C_1 + C_s$ = 2.5%

Average $C_s R_s$ = 2.8μ-secs.

Sample 5):- stabilised for 20 hours at 550°C followed by cooling in still air at room temperature.

Determination of end capacitance of sample.

Weight of Hg in inner column,(gms.).	Total capacitance, ($\mu\mu$F).	Weight of Hg in inner column,(gms.).	Total capacitance, ($\mu\mu$F).
12.0	9.0	140.2	124.5
20.7	17.5	165.6	145.0
34.7	29.0	193.5	169.5
51.5	42.5		
68.5	58.5		
89.5	83.5		
110.6	95.5		

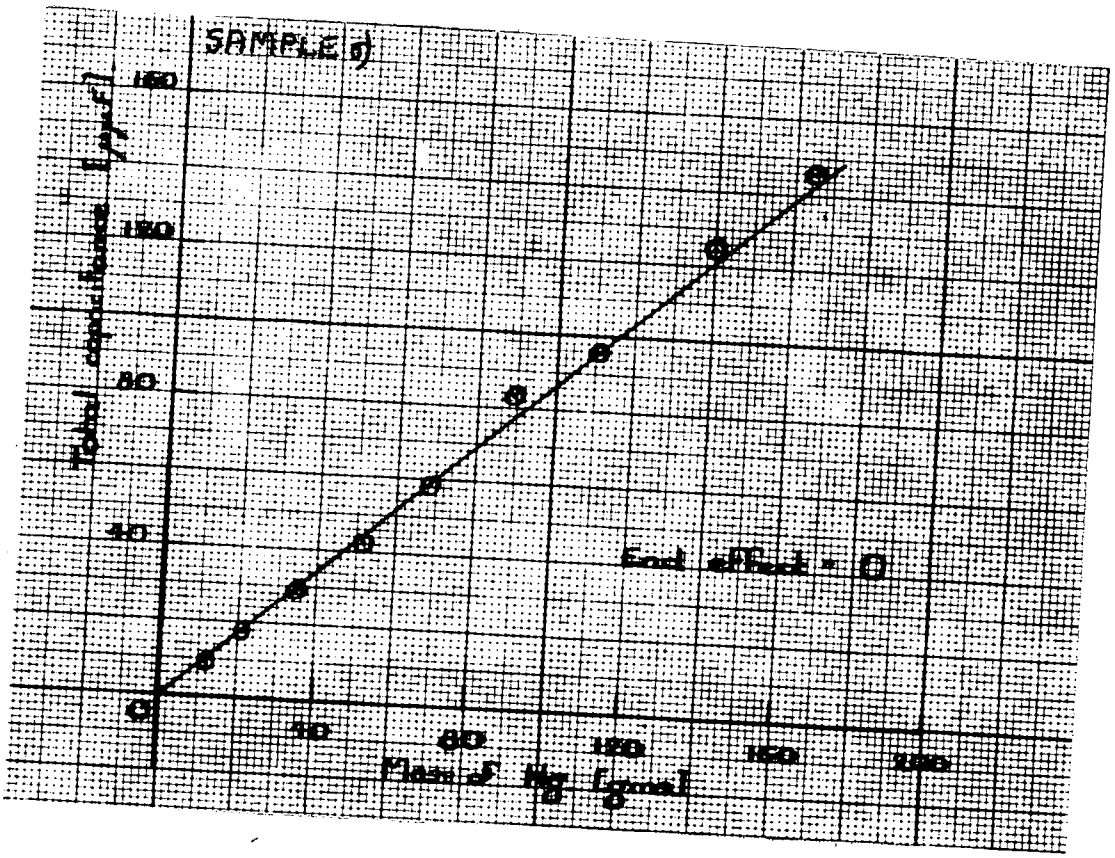

Determination of equivalent network for sample 5).

C_1 ($\mu\mu F$)	C_s ($\mu\mu F$)	R_s (K)	$C_s / C_1 + C_s$ (%)	$C_s R_s$ (μ-secs.)
177.0	4.0	378	2.2	1.5
203.6	4.5	462	2.2	2.1
222.6	5.0	475	2.2	2.4
246.0	6.0	474	2.4	2.8
266.0	6.5	431	2.4	2.8
292.0	7.5	545	2.5	2.5
390.0	8.0	338	2.6	2.7

For sample 5):-

Average $C_s / C_1 + C_s$ = 2.4%

Average $C_s R_s$ = 2.4μ-secs.

Sample 6):- stabilised for 15 hours at 525°C, followed by cooling in still air at room temperature.

Determination of end capacitance of sample.

Weight of Hg in inner column,(gms).	Total capacitance ($\mu\mu F$)	Weight of Hg in inner column,(gms.).	Total capacitance ($\mu\mu F$).
16.5	19.0	102.6	78.0
34.4	44.0	124.2	96.5
49.7	56.8	141.1	121.0
69.2	52.6	158.5	139.0
88.3	67.0	175.6	152.0

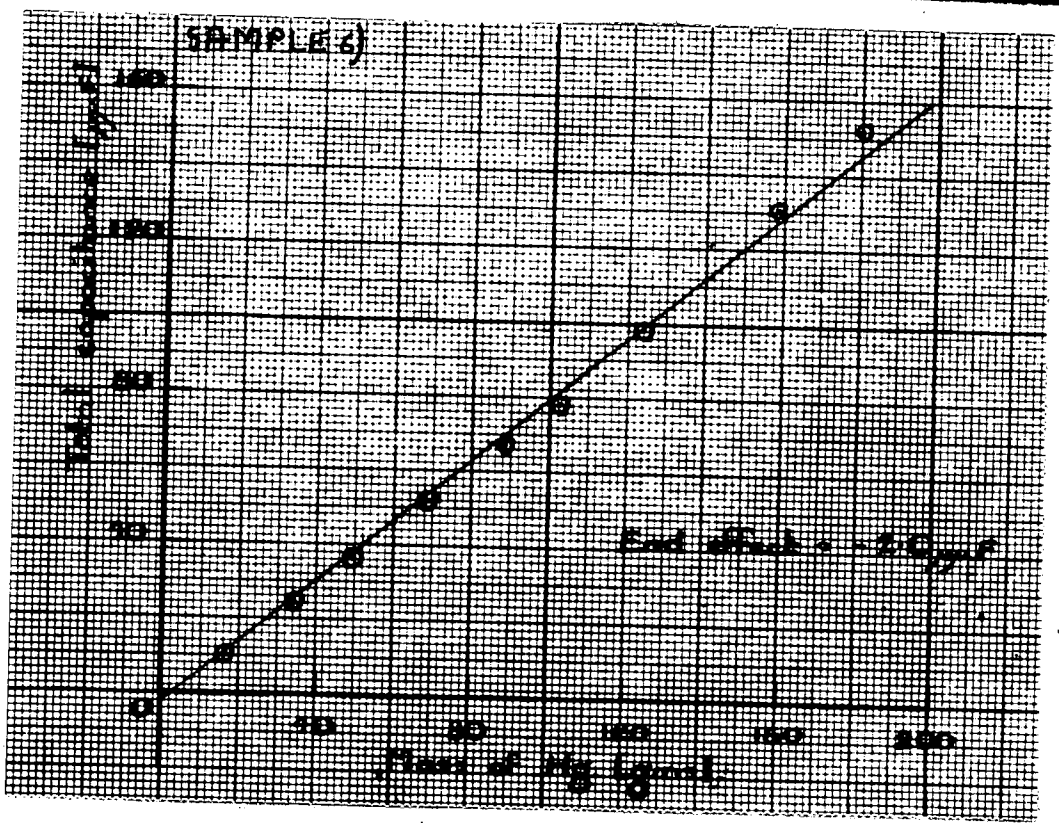

Determination of equivalent network for sample 6).

C_1 ($\mu\mu$F).	C_s ($\mu\mu$F).	R_s (K)	C_s / C_1+C_s ($\mu\mu$F).	C_sR_s (μ-secs.)
226.5	4.75	551	2.1	2.6
250.75	6.5	540	2.2	3.0
276.5	5.75	426	2.0	2.5
297.0	6.5	426	2.1	2.8
313.5	7.25	495	2.3	2.9
327.5	7.5	426	2.2	3.2

For sample 6):- Average C_s / C_1+C_s = 2.15%

Average C_sR_s = 2.8μ-secs.

Sample 7):- stabilised for 72 hours at 500°C, followed by cooling in still air at room temperature.

Determination of end capacitance of sample.

Weight of Hg in inner column, (gms.).	Total capacitance, ($\mu\mu$F).	Weight of Hg in inner column (gmF)	Total capacitance, ($\mu\mu$F).
33.2	27.5	114.3	129.5
45.1	43.0	127.3	149.0
61.1	66.0	140.1	151.0
75.1	86.0	153.7	161.5
88.3	101.5	162.5	173.0
101.7	116.0		

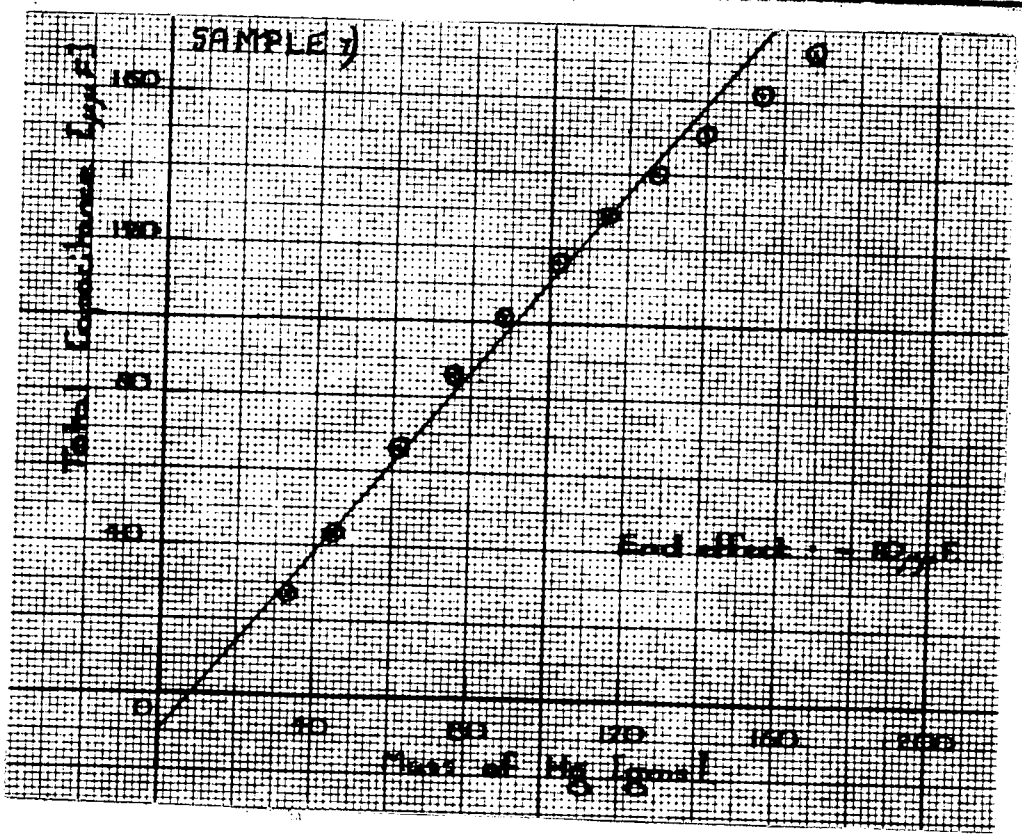

Determination of equivalent network for sample 7).

C_1 ($\mu\mu$F).	C_s ($\mu\mu$F).	R_s (K)	C_s / C_1+C_s (%)	C_sR_s (μ-secs.)
237.0	4.0	448	1.7	1.8
458.0	4.75	417	1.8	2.0
278.0	5.5	425	1.9	2.3
298.0	6.0	413	2.00	2.5
315.0	7.5	343	2.3	2.6
332.0	8.0	304	2.4	2.4

For sample 7):- Average C_s / C_1+C_s = 2.0%

Average C_sR_s = 2.3μ-secs.

Sample 8):- stabilised for 72 hours at 460° C, followed by cooling in still air at room temperature.

Determination of end capacitance of sample.

Weight of Hg in inner column,(gms).	Total capacitance, ($\mu\mu$F).	Weight of Hg in inner column,(gms).	Total capacitance, ($\mu\mu$F).
16.1	14.0	97.9	96.0
39.5	28.5	114.6	116.5
45.9	42.5	134.7	138.0
63.4	60.5	156.3	161.5
82.2	79.5	176.9	181.5

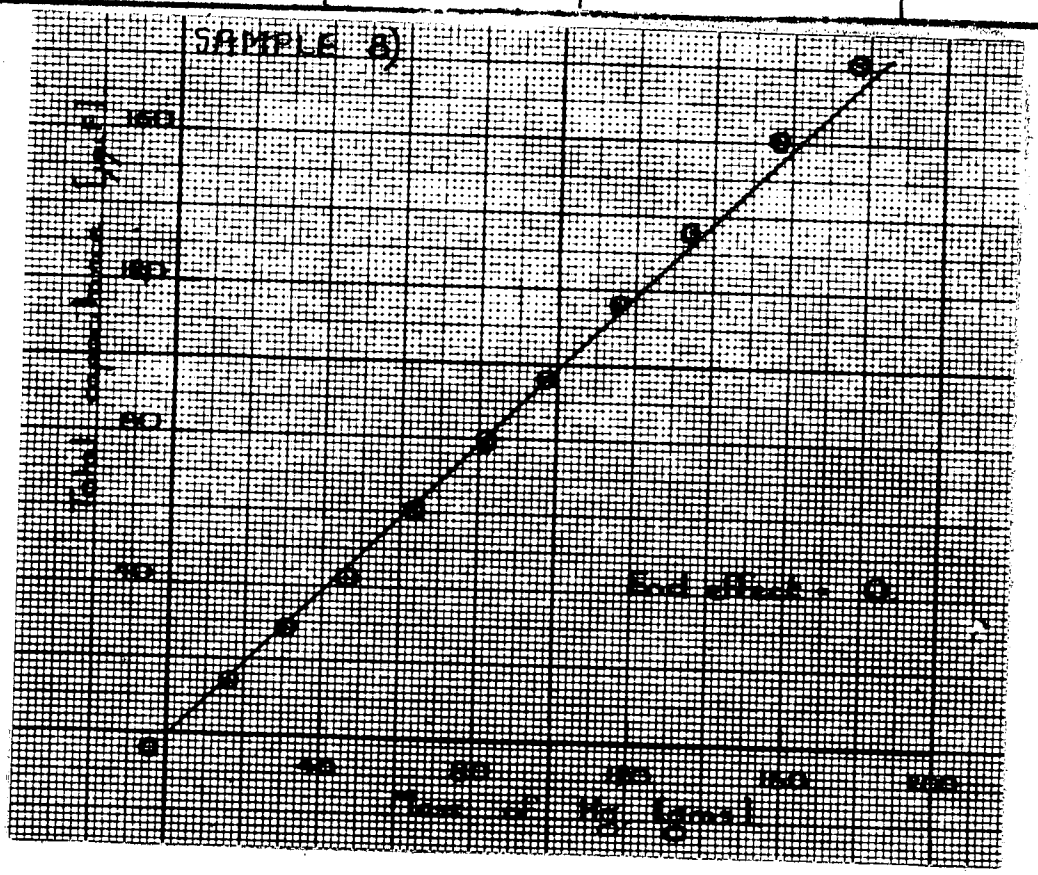

Determination of equivalent network for sample 8).

C_1 ($\mu\mu F$)	C_s ($\mu\mu F$)	R_s (K)	$C_s / C_1 + C_s$ (%)	$C_s R_s$ (μ-secs.).
~~164.0~~	~~4.5~~		~~1.1~~	
189.0	2.5	—	1.30	—
197.5	2.5	—	1.65	—
216.5	3.5	—	1.6	—
237.0	3.50	—	1.5	—
258.5	4.25	—	1.6	—
266.5	4.3	597	1.7	2.6

Note:- For this sample it was impossible to measure $C_s R_s$, except in the last instance, due to the small value of C_s.

For sample 8):- Average value of $C_s / C_1 + C_s$ = 1.5%.
$C_s R_s$ measured in one instance at 2.6μ-secs.

Summary of measurements on the dielectric properties of Pyrex glass.

Sample.	Stabilisation Temperature, (°C).	$C_s / C_1 + C_s$ (%).	$C_s R_s$ (μ-secs)
1).	Ordinarily annealed.	2.6%	2.2 μsecs.
2).	800.	2.6%	3.8 μ secs.
3).	650.	2.5%	3.3 μ secs.
4).	600.	2.5%	2.8 μ secs.
5).	550.	2.4%	2.4 μ secs.
6).	525.	2.15%	2.8 μsecs.
7).	500.	2.0%	2.3 μ secs.
8).	480.	1.5%	2.6 μ secs.

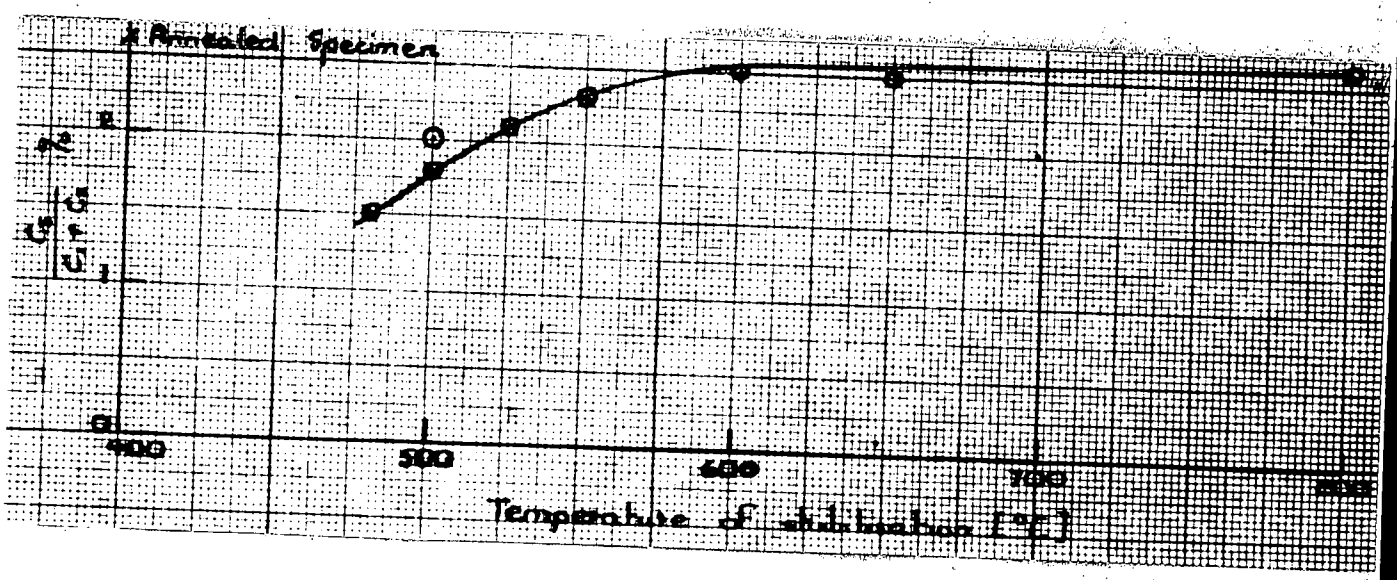

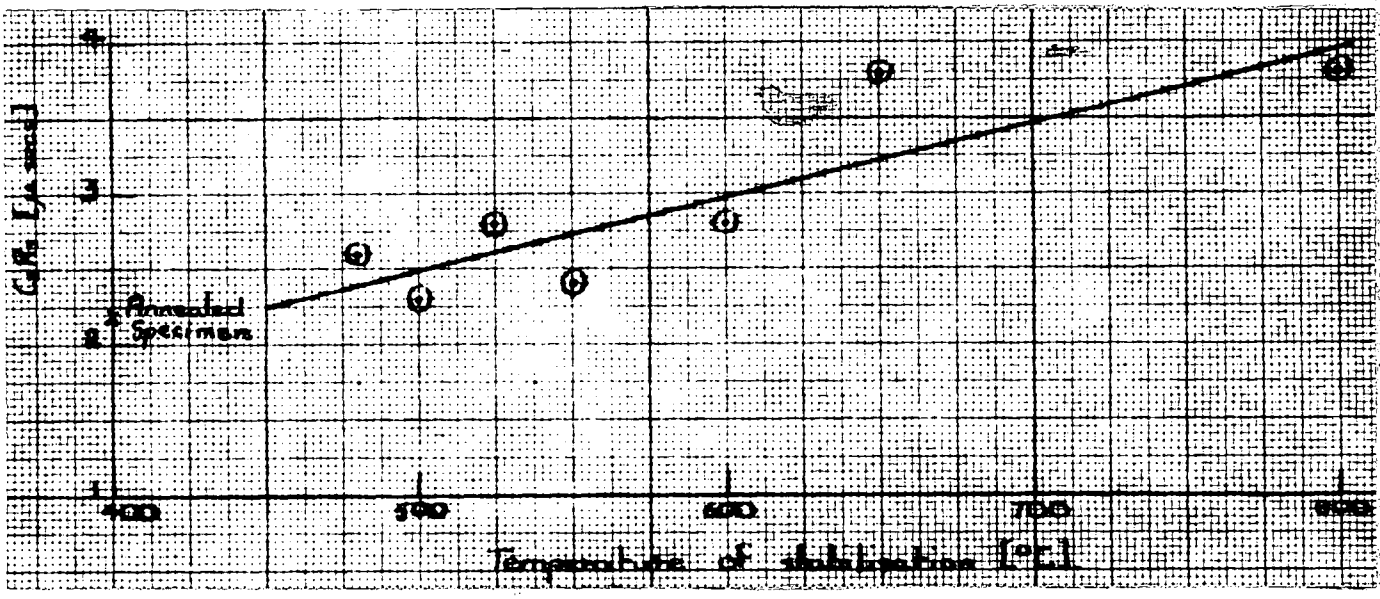
4
3
2
1
400
500
600
700
800
Annealed Specimen
Temperature of stabilization [°C]

2). SODA GLASS.(X6).

Variation of C_s and R_p with frequency of input.

C_1 ($\mu\mu F$)	Frequency (cycles/sec.).	R_p (M)	C_1+C_s ($\mu\mu F$)	C_s ($\mu\mu F$)
302.5	4.5K	2.5	318.0	15.5
	4.0K	2.5	319.0	16.5
	3.5K	4.9	320.0	17.5
	3.0K	4.0	321.0	18.5
	2.5K	4.0	322.0	19.5
	2.0K	4.0	325.0	22.5
	1.5K	5.5	327.5	25.9
	1.0K	7.0	332.0	29.5
	0.5K	10.0	347.5	45.0

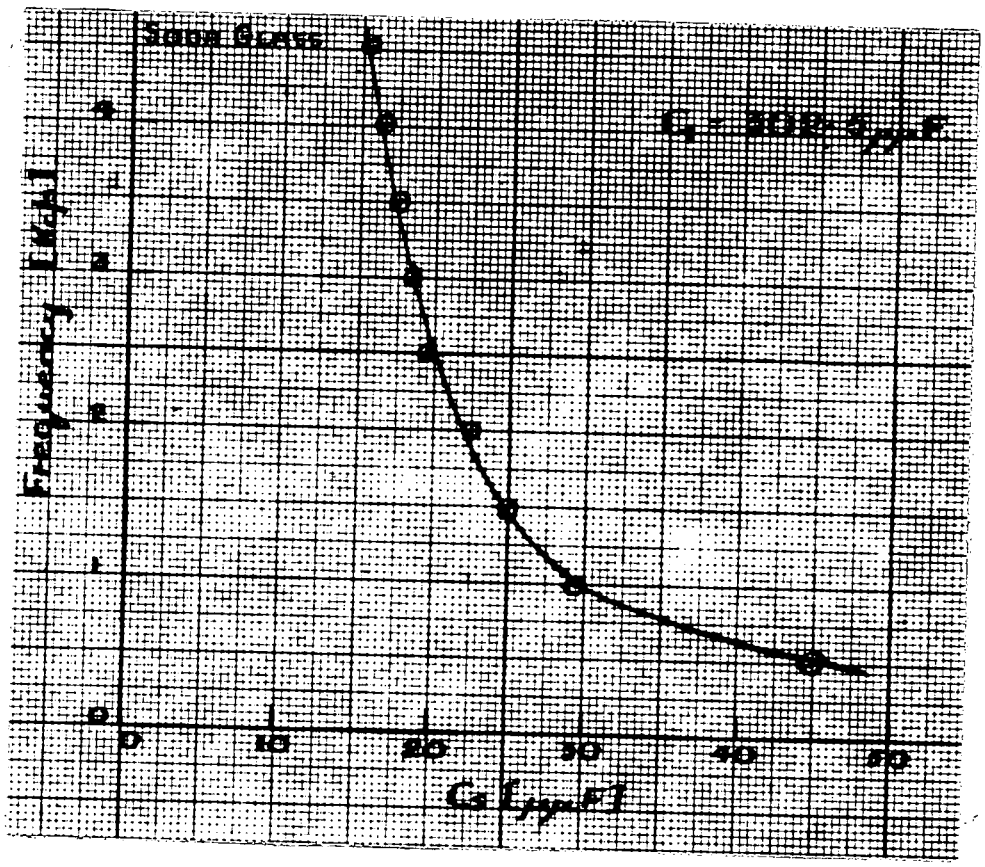

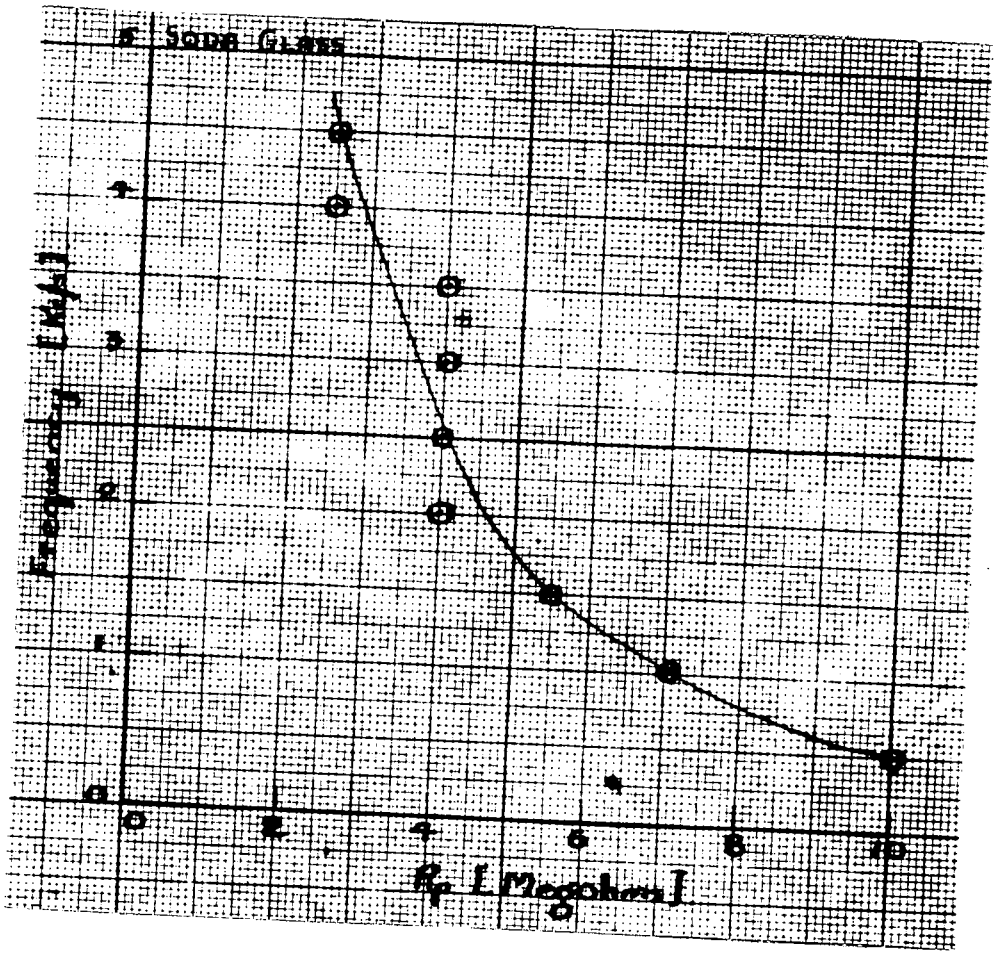
Soda Glass
Energy [kJ]
R_p [Megohm]

3). ICE.

Variation of C_s and R_p with frequency of applied input.

C_1 ($\mu\mu F$)	Frequency (cycles/ sec.)	R_p (M)	$C_1 + C_s$ ($\mu\mu F$)	C_s ($\mu\mu F$)
16.5	11K	0.35	31.5	15.0
	6.0K	0.53	45.0	28.5
	5.5K	0.56	49.0	32.5
	5.0K	0.49	53.0	36.5
	4.5K	0.61	57.5	41.5
	4.0K	0.61	63.5	47.0
	3.5K	0.71	71.5	55.0
	3.0K	0.81	80.5	64.0
	2.5K	0.81	91.0	74.5
	2.0K	0.9	106.0	89.5
	1.5K	0.9	127.0	110.5
	1.0K	2.5	146.5	130.0
	0.75K	2.5	154.0	137.5
	0.5K	4.0	162.0	145.5

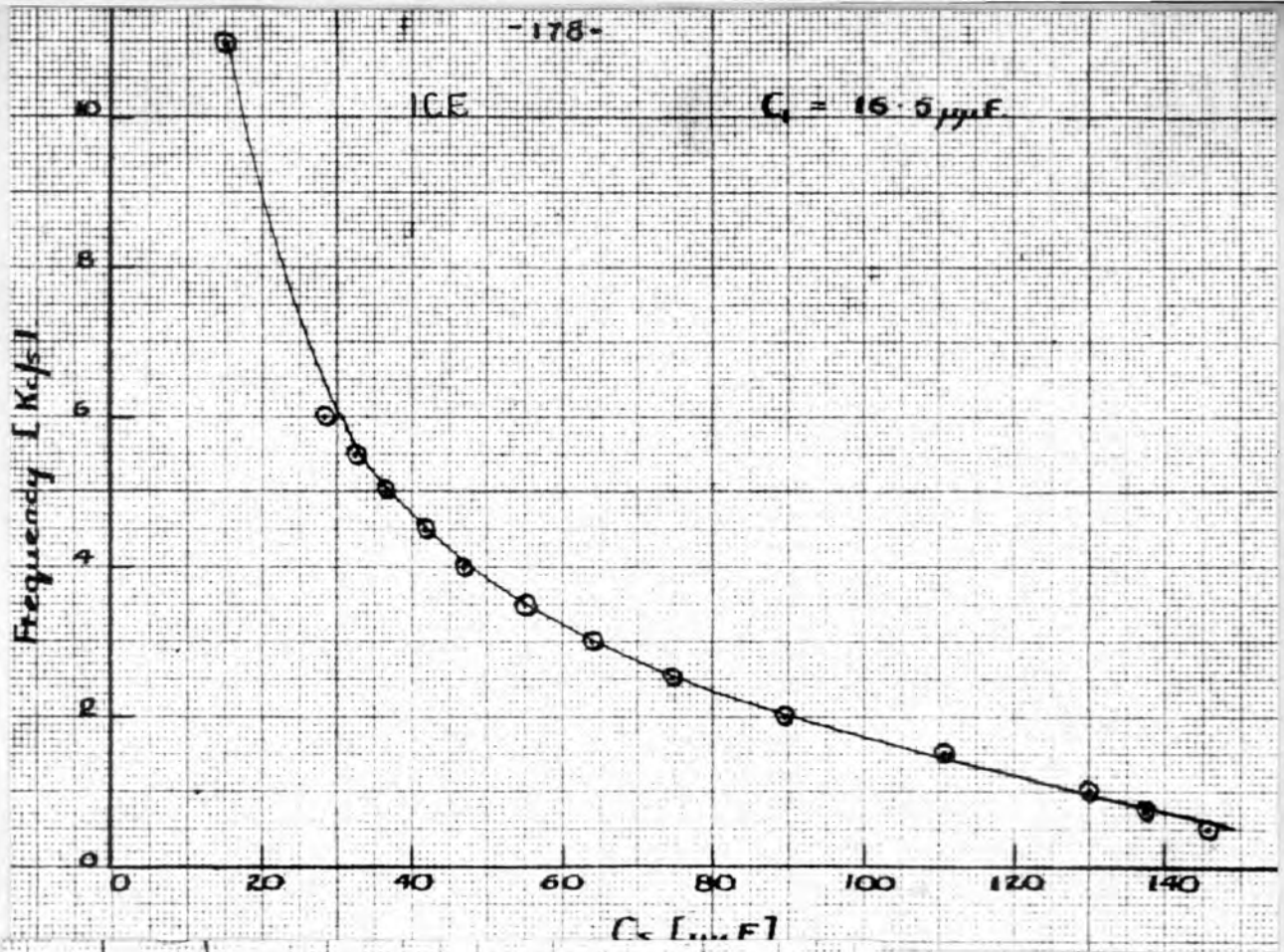
ICE
C_1 = 16·5 μμF.
Frequency [Kc/s]
0
2
4
6
8
10
0
20
40
60
80
100
120
140
C_x [μμF]

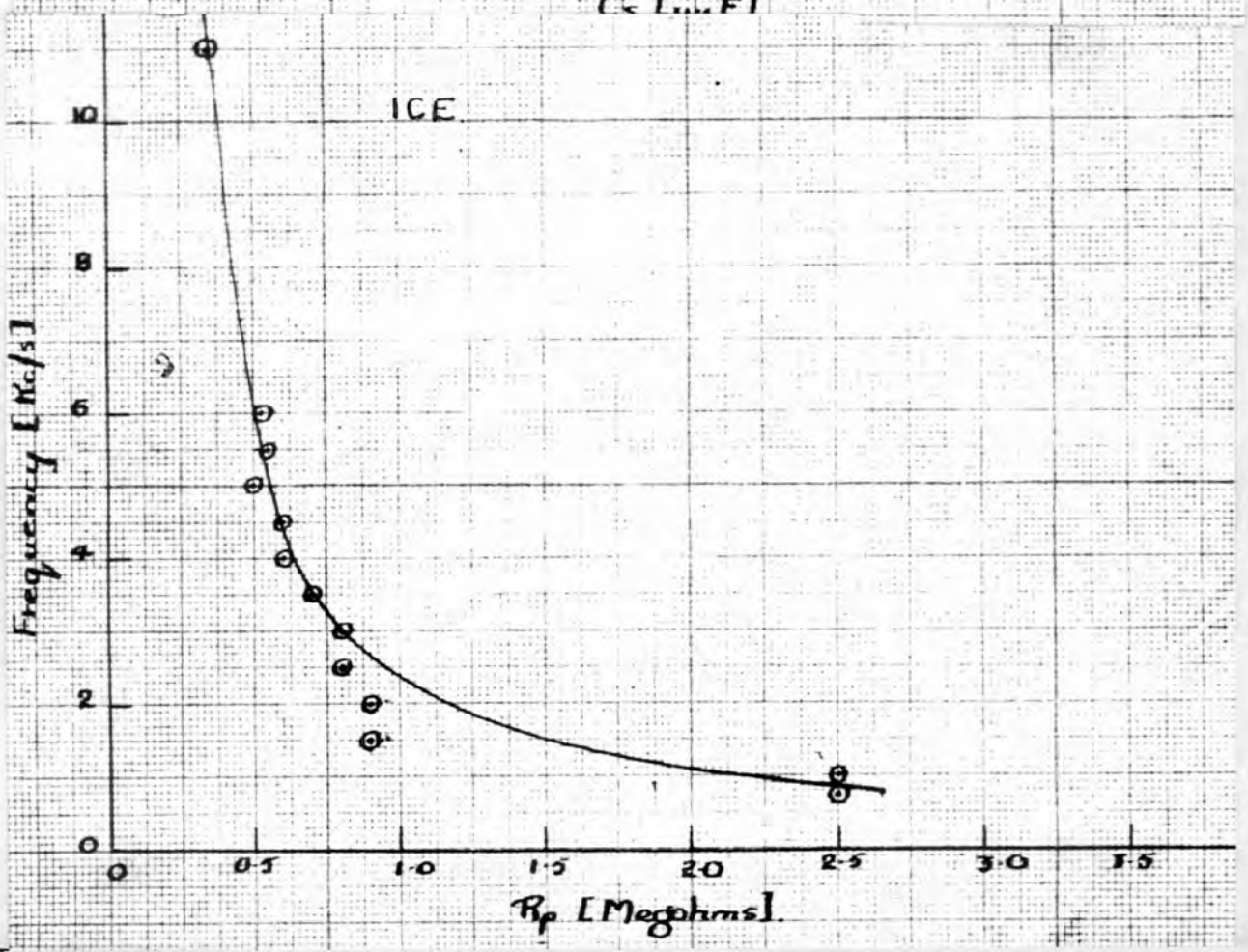
ICE
Frequency [Kc/s]
0
2
4
6
8
10
0
0·5
1·0
1·5
2·0
2·5
3·0
3·5
R_p [Megohms].

BIBLIOGRAPHY.

1).	Yates, J.C.,	Nature,	163,	132,	1949.
	Gledhill, J.A., Patterson, A., Jnr.	Rev. Sci. Inst.	20,	960,	1949.
2).	Brainerd, Koehler, Woodruff, Reich,	" Ultra High Frequency Techniques" Ch.I.			
3).	Arguimbau,	Gen. Rad. Exp.	7,		1939.
	Packard, L.E.	"	"		" .
4).	Morecroft, Turner,	Proc. I.R.E.	13,	487,	1925.
5).	Moody, N.F.	T.R.E. Tech. Mon. No.5A.			
6).	Hague,	"A.C. Bridge Methods", Ch.V.			
	Rosen, A.	J. Sci. Inst.	8,	142,	1931.
	Astbury,	Phil. Mag.	26,	507,	1938.
	Shackleton, Ferguson,	Bell Sys. Tech. Journ.	7,	70,	1928.
	Hartshorn,	"R.F. Measurements", Ch.III.			
7).	Hund,	"H.F. Measurements",			
	Hague,	"A.C. Bridge Methods",			
	Chrystal,	Trans. Roy. Soc. Edin.	39,	609,	1880.
	Prowse, W.A.	Journ. Sci. Inst.	13,	219,	1936.

BIBLIOGRAPHY, (contd.).

8). Clarke, H.A.M., Vanderlyn, P.B., J.I.E.E. (in print).

Yates, Nature, 163, 132, 1949.

Gledhill, J.A. Patterson, A., Jnr. Rev.Sci.Inst. 20, 960, 1949.

9). Jaeger, J.C., "Introduction to the Laplace Transform with engineering applications".

Carslaw, H.S., Jaeger, J.C., "Operational methods in applied mathematics".

10). Frohlich, H. "Theory of Dielectrics".

11). Govers, M. De Pre, F.K. Philips Rec. Rep. 1, 197, 1946.

Stevels, "Physical properties of Glass".

12). Littleton and Morey, "Electrical properties of glass".

13). " "

14). Hartshorn, L. Proc.Phys.Soc. 37, 215, 1924.

Churcher, B.T. Dannat, C. Dalgleish, J.W. J.I.E.E. 67, 271, 1929.

Hartshorn, L. Ward, W.H. Sharpe, B.A. O'Kane, B.J. J.I.E.E. 75, 730, 1934.

15). Cox, S.M. Kirby, P.L. Nature, 159, 162, 1947.

BIBLIOGRAPHY,(contd.).

15).	Lamb,J.	Trans.Far.Soc.	42A,	538,	1946
17).	Gray,	"Absolute measurements in Electricity and Magnetism". Ch.XVIII.			
	Hertz,	"Miscellaneous Papers", No.XIV.			
18).	Sharbaugh,A.H.Jnr. Schmelzer,C. Eckstrom,H.C. Kraus,C.A.	Journ.Chem.Phys.	15,	47,	1947.
19).	"	"	"	"	"
20).	Jackson,W.	Trans.Far.Soc.	42A,	91,	1946
	Jackson,W. Powles,J.G.	Trans.Far.Soc.	42A,	101,	1946
	Hartshorn,L.	Rep.Prog.Physics.			
21)	Hague,	"A.C.Bridge methods". Ch.IV.			
22).	Dye, Jones,	J.I.E.E.	72,	169,	1933.
23).	Cole,K.S. Cole,R.H.	Journ.Chem.Phys.	9,	341,	1933.
24).		Phil.Trans.	166,	489,	1876.
25).	Maxwell,	"Electricity and Magnetism",Vol.I.			
26).	Wagner,	Ann.der Phys.	40,	817,	1913

27). Debye, "Polar Molecules".

28). Onsager, J.Am.Chem.Soc. 58, 1486, 1936

29). Kirkwood,J.G. Trans.Far.Soc. 42A, 7, 1946

30). Frohlich,H. " Theory of dielectrics".

31). " "

32). Whitehead,S. "Dielectric Phenomena".

33). "Radio Designers' Handbook".

ADDENDA, (cf.P.121).

The hypothesis put forward to explain the apparent increase of dielectric loss with temperature of stabilisation for Pyrex glass, is far from rigid. A complete explanation of the results based on the data available is not possible, but some speculations as to the loss mechanism are given here.

The observations made on various glasses, (cf.p.94), indicate that the percentage capacitance associated with series resistance, C_s, is greatest for glasses with the greatest concentration of metallic ions, particularly Sodium ions. This suggests some connection between the losses represented by the series resistance capacitance combination and the presence of the Sodium ions. With this in mind, some possibilities as to the actual loss mechanism will now be considered.

If the loss mechanism in the glass is assumed to arise from the presence of dipoles in the material, the process can be envisaged in terms of the modification of the internal potential field, and hence of the equilibrium positions of the dipoles, upon the application of an external field, (cf.Ch.IX,p.141). This hypothesis however necessitates the presence of an individual negative ion, forming a dipole

with the Sodium positive ion. Also, it would be expected that the time constant associated with this type of loss mechanism would be much smaller than the time constant observed in practice,(about 2μ-secs.).

The relatively large time constants observed in practice may possibly be ascribed to the modification, due to the external applied field, of domains in the glass. This is difficult to envisage for small field strengths such as are involved in the present investigation.

A third possibility is suggested in terms of the picture of ionic conduction resulting from the movement of ions over potential barriers, details of which are given in Ch.VI of this thesis,(cf.p.92). The application of an external field results in a tendency for the ions to jump more in one direction than the other, thus giving rise to a conduction current. The possibility arises of regions occurring in the glass where the potential barriers are above average height. The Sodium ions infiltrate through the glass as much as possible, by way of the potential valleys. But, in the region of the very high potential barriers, a certain proportion of ions will be prevented from infiltrating further. These ions give rise to a static space-charge distortion superposed on the flow of ions. Upon the removal of the field, it is suggested that this space charge distortion

relaxes, and the 'trapped'ions take up a fresh distribution. This relaxation process is represented in the measurements taken, by the series resistance capacitence combination, $C_s R_s$ In the event of there being more than one type of metallic ion present in the silica network, the larger the contribution of the ion to the conductivity, the larger also its contribution to C_s.

The observed imperfections of the final balance of the glass sample against an equivalent electrical network, may well be an indication of the presence of several types of ion contributing to the loss processes, as well as an indication of a distribution of the regions of very high potential barriers

If the hypothesis of space charge inhomogeneities given above is correct, the increase of $C_s/(C_1 + C_s)$ with temperature of stabilisation of Pyrex glass samples suggests that the higher the temperature of stabilisation, the greater the possibility of regions occurring in the glass, whose potential fields are above average height. No evidence has been found in the current literature for or against this.